Synthesis of Artificial Building Blocks for Sortase-Mediated Ligation and Their Enzymatic Linkage

Xiaolin Dai

Univ.-Diss.

zur Erlangung des akademischen Grades
"doctor rerum naturalium"
(Dr. rer. nat.)
in der Wissenschaftsdisziplin "Polymerchemie"

eingereicht an der
Mathematisch-Naturwissenschaftlichen Fakultät
Institut für Chemie
der Universität Potsdam

Potsdam, 19 Okt 2018
Hauptbetreuer: Prof. Dr. Alexander Böker
weitere Gutachter: Prof. Dr. Ulrich Schwaneberg, Prof. Dr. Rainer Haag

Life is like a box of chocolates.

-- «Norwegian Wood» by Haruki Murakami

Published online at the
Institutional Repository of the University of Potsdam:
URN urn:nbn:de:kobv:517-opus4-420060
http://nbn-resolving.de/urn:nbn:de:kobv:517-opus4-420060

Erklärung

Hiermit erkläre ich, dass ich die beigefügte Dissertation selbstständig verfasst und keine anderen als die angegebenen Hilfsmittel genutzt habe. Alle inhaltlich übernommenen Stellen habe ich als solche gekennzeichnet.

Ich versichere außerdem, dass ich die Dissertation nur in diesem und keinem anderen Promotionsverfahren eingereicht habe und, dass diesem Promotionsverfahren keine endgültig gescheiterten Promotionsverfahren vorausgegangen sind.

Potsdam, Xiaolin Dai

Acknowledgements

It is my great honor to thank many people here for their strong support and encouragement, which was invaluable for my scientific work and daily life. Some of them are especially nominated gratefully in the following words. However, I believe that this text cannot express all my feeling of gratitude.

First, I would like to take the opportunity to thank Prof. Dr. Alexander Böker, who allowed me to join his research group, gave me such an interesting topic and, provided the scientific and financial support to make this work possible. I must thank Prof. Dr. Ulrich Schwaneberg, who conceived the initial idea with Prof. Böker as well as the research partners from his group, Dr. Tayebeh Mirzaei Garakani, Dr. Diana M. Mate and Zhi Zou for the harmonious cooperation. My sincere thanks go to many colleagues for scientific discussion and suggestion, among them my former colleague Dr. Walter Tillmann who took me to the secrets of Raman spectroscopy, Dr. Erik Wischerhoff who helped me for the GPC analysis and Dr. Andrea Körner, Sabrina Mallmann, Dr. René Kalbitz, Steffi Grunst for help with analytical measurements.

I'd like to express my further greatest thanks to the other Chinese in our research group: Li Tan, Xiao Cheng, Shuhao Zhang and Xuepu Wang for their scientific advice and help in life. I like to acknowledge my former colleague and roommate Dr. Himanshu Charan, who brought very much happy time to me. And also my friend Carolin Riedel, who showed me so much German culture and took care of me when I came to Germany.

Last but not the least, I want to thank my family and my close relatives for the endless love and support. I am particularly indebted to my husband and my daily supervisor, Dr. Ulrich Glebe, who is always there for me no matter what happens. Very special thanks to my parents and my parents-in-law for the selfless support behind me. I like to remember my cousin Yueqi Pan who takes care of my parents when they need help.

Many thanks to all of you!

Publications

Sortase-mediated ligation of purely artificial building blocks
X. Dai, D. M. Mate, U. Glebe, T. Mirzaei Garakani, A. Körner, U. Schwaneberg, A. Böker,
Polymers, ***2018****, 10, 151.*

Broadening The Scope Of Sortagging
X. Dai, A. Böker, U. Glebe,
in preparation.

Patentanmeldung:
Verfahren zur Herstellung von Block-Polymeren mittels Verknüpfung von Blöcken durch eine Transpeptidase und Block-Polymere erhalten durch Transpeptidase-Verknüpfung
U. Glebe, X. Dai, A. Böker, M. Schmidt, U. Schwaneberg, D. Mate, F. Jakob, T. Mirzaei Garakani
DE 10 2017 115522.8 (Anmeldedatum: 11.07.2017)

Contents

Abbreviations

ABCVA	4,4´-azobis(4-cyanovaleric acid)
ADCs	antibody-drug conjugates
AIBN	azobisisobutyronitrile
AmyA	α-amylase
ATRP	atom-transfer radical polymerization
AUC	analytical ultracentrifugation
BGL	β-glucosidase
BIBA	α-bromoisobutyric acid
CCA	α-cyano-4-hydroxycinnamic acid
CNC	crystalline nanocellulose
CRP	controlled radical polymerization
CTA	chain transfer agent
CtxB	cholera toxin B subunit
CuAAC	Cu^{I}-catalyzed azide-alkyne cycloaddition
CWSS	cell wall sorting signal
DCC	*N,N'*-dicyclohexylcarbodiimide
DCM	dichloromethane
DHB	2,5-dihydroxybenzoic acid
DIC	N,N'-diisopropylcarbodiimide
DLS	Dynamic Light Scattering
DMAP	4-(dimethylamino)pyridine
DMF	dimethylformamide
DMSO	dimethylsulfoxide
DNA	deoxyribonucleic acid
E. coli	*Escherischia coli*
EDC	1-ethyl-3-(3-dimethylaminopropyl)carbodiimid
EGF	epidermal growth factor
eGFP	enhanced green fluorescent protein
EGFR	epidermal growth factor receptor
EK	enterokinase
ESI	electrospray ionization
Fba	fibronectin-binding protein

FESEM	Field Emission Scanning Electron Microscopy
FFF	field flow fractionation
FITC	fluorescein isothiocyanate
Fmoc	fluorenylmethoxycarbonyl
FRI	fluorescence reflectance imaging
GCE	glassy carbon electrode
GDH	glucose dehydrogenase
GMA	glycidyl methacrylate
GOas	galactose oxidase
GPC	gel permeation chromatography
GPI	glycosylphosphatidylinositol
HBTU	N,N,N',N'-tetramethyl-O-(1H-benzotriazol-1-yl)uronium hexafluorophosphate
HPLC	high performance liquid chromatography
IFN-α	human interferon alpha
IR	infrared
kDa	kilo Dalton
LC-MS	liquid chromatography-mass spectrometry
MALDI-ToF	matrix-assisted laser desorption ionization-time of flight
MPS	3-(trimethoxysilyl) propyl methacrylate
MSP	membrane scaffold protein
MT	mushroom tyrosinase
MWCO	molecular weight cut off
NAC	*N*-acetyl-L-cysteine
NHS	N-hydroxysuccinimid
NMI	N-methylimidazole
NMM	4-methylmorpholine
NMP	methylpyrrolidone
NMR	Nuclear Magnetic Resonance
NP	nanoparticle
NTA	nitrilotriacetic acid
PBS	phosphate buffered saline
PDI	polydispersity index
PEG	polyethyleneglycol
PEGMA	poly(ethylene glycol) methyl ether acrylate

PET	positron emission tomography
PNIPAM	poly(*N*-isopropylacrylamide)
POEGMA	poly(oligo(ethyleneglycol)methylethermethacrylate)
PSI	photosystem I
PVCL	poly(*N*-vinylcaprolactam)
RAFT	reversible adition-fragmentation chain transfer
S. aureus	*Staphylococcus aureus*
SDS-PAGE	sodium dodecylsulfate-polyacrylamide gel electrophoresis
SLS	Static Light Scattering
SML	sortase-mediated ligation
SPAAC	strain-promoted azide-alkyne cycloaddition
SPECT	single-photon emission computed tomography
SPPS	solid-phase peptide synthesis
SrtA	sortase A
STEM	Scanning Transmission Electron Microscopy
*t*Boc	*tert*-butyloxycarbonyl
TEM	Transmission Electron Microscopy
TEOS	tetraethyl orthosilicate
TEV	tobacco etch virus
TFA	trifluoroacetic acid
THF	tetrahydrofuran
Tiips	triisopropylsilane
TM	thrombomodulin
TMR	tetramethylrhodamine
UV/Vis	ultraviolet/visible

Peptides

Peptide sequences used in the work:

Peptide 1: H-Cys-Ile-Arg-His-Met-Gly-Phe-Pro-Leu-Arg-Glu-Phe-Leu-Pro-Glu-Thr-Gly-OH

Peptide 2: H-Gly-Gly-Gly-Gly-Gly-Phe-Glu-Arg-Leu-Pro-Trp-Phe-Trp-Gly-Met-His-Arg-Ile-Cys-OH

Peptide 3: H-Gly-Gly-Gly-Gly-Gly-Trp-Phe-Trp-Cys-OH

Peptide 4: H-Cys-Ile-Arg-His-Phe-Leu-Pro-Glu-Thr-Gly-OH

Chain Transfer Agents

The synthesized CTAs in the work:

CTA 1:

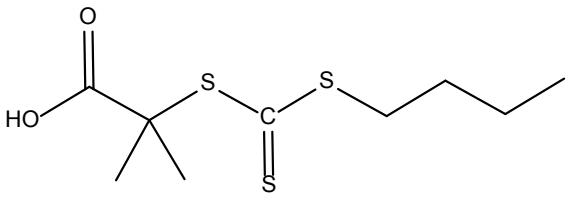

CTA 2:

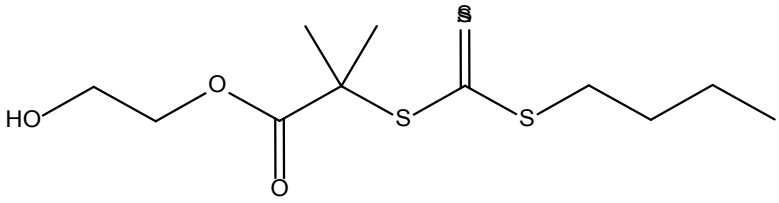

CTA 3:

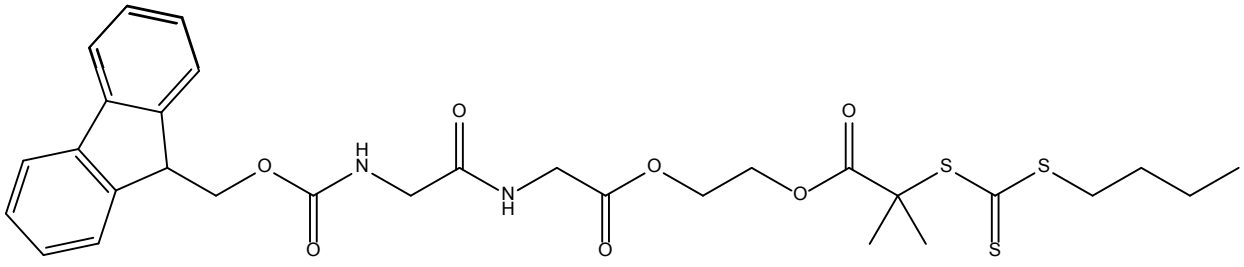

1 Introduction

Nowadays, the collaboration between the research fields of biology and chemistry becomes closer and closer. Science continually develops to be more interdisciplinary. People are always looking for bio-based materials or biological energy sources which are able to replace the traditional chemical materials used in industry. Among such interesting application fields, enzymatically catalyzed reactions play a key role.

The use of enzymes as catalysts for chemical reactions has several advantages. First, the enzymes are functional proteins, which are very economically friendly. Second, enzymes are very efficient and have a very high selectivity. Moreover, the reaction conditions are very mild. Therefore, the application of enzymes has a broad potential not only in the field of biology, but also in chemistry and materials science. Enzymatically catalyzed reactions are seen as strong alternatives to the traditional chemical reactions and are widely used in basic research, chemical and medical industry. However, there is still much more potential that can be used in interdisciplinary research.

Sortases are members of the class of transpeptidases. They are produced by Gram-positive bacteria, and their function is to catalyze the formation of a peptide bond between two specific peptide sequences. This special enzyme was discovered at the end of 1990s. In the last two decades, the sortase family has been intensively studied. Until now, with sortase A, B, C, D, E and F, six species with different functions have been found. Thereof, sortase A is the best known, studied and most applied. In nature, it is responsible for the covalent anchoring of surface proteins with the recognition sequence LPXTG onto oligoglycine functionalities of the cell wall via a two-step transpeptidation. The expression of sortase A can be performed in *Escherichia coli*, which enables its broad application *in vitro*. At present, a wide range of applications have been reported: for instance, the modification of cells with proteins, the ligation between proteins and peptides, the modification of proteins with small molecules like dyes, the immobilization of proteins on planar surfaces as well as particles etc. However, to the best of my knowledge, the linkage between purely artificial blocks has not been reported yet. This work shows for the first time, that two synthetic chemical building blocks can be linked via sortase-mediated ligation. Attractive building blocks for such linkages are nanoparticles and different polymer blocks.

Sortase A is now already commercially available, which demonstrates its values for the mentioned applications. I believe that more and more potential application of SrtA will be discovered in the near future.

2 Fundamentals

2.1 Enzymes and transpeptidases

2.1.1 Introduction to enzymes

Enzymes are biological macromolecules which have catalytic functions. In the system of an enzymatically catalyzed reaction, the enzyme acts on the substrate and converts it into a different molecule, namely the product. In order to enhance the reaction rate, enzymes take part in nearly the whole cellular metabolism[1].

Enzymes are proteins, hence they are also called "biocatalyst". More than 5000 different types of biochemical reactions are catalyzed by enzymes[2]. Equally to the principle of all non-biological catalysts, enzymes accelerate the reaction rate by means of reducing its activation energy. Most of them can increase the rate of a reaction by millions of times. Catalysts are not consumed and don't influence the equilibrium of the reactions. The catalysis takes place on the so called active site of the enzyme, which occupies only a small part of the protein, the remainder acts as "scaffold" in the system. As shown in Fig 2.1, during the catalytic process, the substrate molecule perfectly fits into the active site in order to promote the specific reaction. Different to other catalysts, enzymes have a high specificity[3].

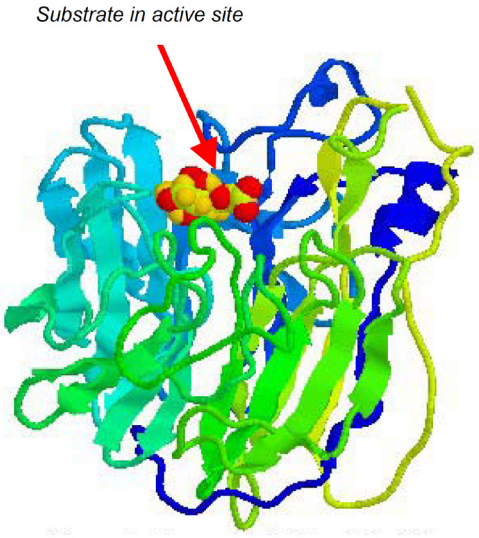

Fig 2.1 General graphic of the structure of the enzyme trypsin with a substrate in the active site. Reprinted from reference [3].

2.1.2 Transpeptidase

Transpeptidase is a superfamily[4] including for example DD-transpeptidase, peptidyl transferase, Gamma-glutamyl transpeptidase, D-glutamyl transpeptidase, sortase etc. The process of the catalysis is a two-step reaction. The first step contains the cleavage of the peptide bond from one substrate, the release of the by-product, and the formation of the intermediate product. The second step involves to resolve the intermediate under the formation of a new peptide bond between the two substrates[5]. Scheme 2.1 shows the mechanism of DD-transpeptidase as an example.

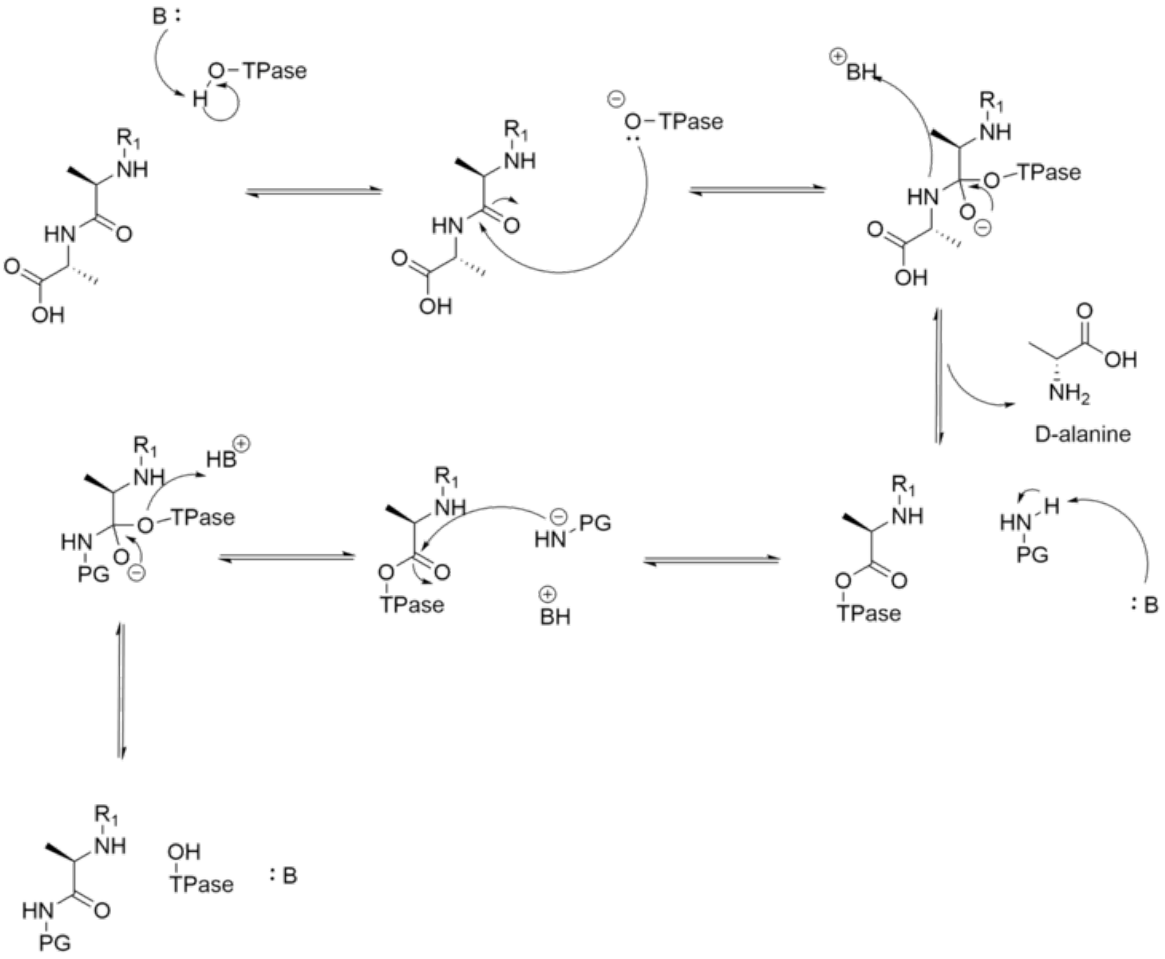

Scheme 2.1 Schematic representation of DD-transpeptidase catalysis mechanism. Reprinted from reference [6].

2.2 Sortase and Sortase A

2.2.1 Sortase

Sortases are the enzymes, which are responsible for attaching specific surface proteins covalently on the peptidoglycan of the cell wall. They are transpeptidases produced by Gram-positive bacteria and have been more and more studied over recent years. It has already been shown that

sortases are very meaningful for some industrial applications[7–10].

Bacterial cell walls have diverse compositions although they are prokaryotic. The cell wall complexes vary for different species. For instance, Gram-negative and Gram-positive are two main categories for bacteria, in spite of holding the elementary structure. Among many distinctions, one assignable point is their peptidoglycan content.

The peptidoglycan consists of a large number of glycan polymer chains which are composed of *N*-acetyl glucosamine and *N*-acetyl muramic acid repeating units. They are normally cross-linked by peptide stems which are usually made up of 5 amino acids. On the position 3 of the 5 amino acids from the peptide stems, there is an inter-peptide branch which varies between Gram-positive and Gram-negative bacteria[11].

Gram-positive bacteria often have a pentaglycine branch in their peptide stem. For instance, the peptide stem in *Staphylococcus aureus* (*S. aureus*) contains L-Ala-D-Glu-L-Lys-D-Ala-D-Ala, which crosslinks the peptidoglycan strands and has a pentaglycine inter-peptide branch on the L-Lys position as shown in Fig 2.2[12]. *S. aureus* is one of the Gram-positive microorganisms, which is to a great extent in charge of human pathologies, for example, *Pneumonia (Lungenentzündung), impetigo (Eiterflechte), osteomyelitis (Knochenmarksentzündung)*[13,14] However, another related important point is the display of virulence and adhesion-associated proteins anchored into the thick peptidoglycan layer, which are the primary contributors to the pathogens[8]. Frequently, in Gram-positive bacteria, the sortase enzymes are responsible for covalently linking these surface proteins to the peptidoglycan cell wall by means of transpeptidation reaction[13–15].

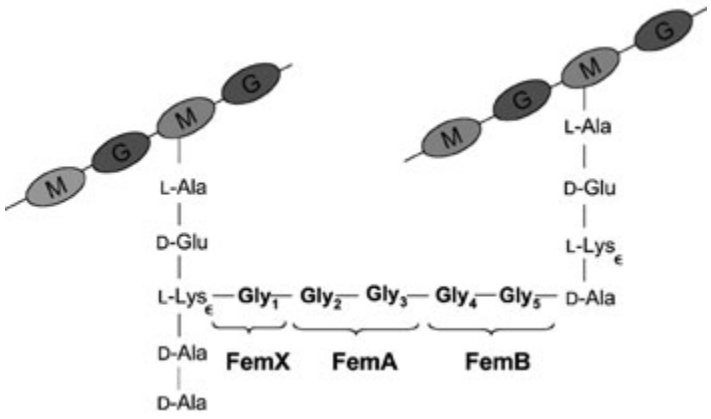

Fig 2.2 Structure of interpeptide branch of *Staphylococcus aureus.* Reprinted from reference [12].

Since their discovery, the sortase family has been deeply studied and is considered to be a powerful molecular biology catalyst to site-specifically immobilize proteins onto various kinds

of biomolecules due to their special role of anchoring cell surface protein virulence factors in pathogens[10,16]. Interestingly, the targeted proteins for the transpeptidation process by sortases are embodied in a common C-terminal cell wall sorting signal (CWSS) located on the cell surface. The CWSSs comprise a pentapeptide recognition sequence (such as LPXTG, NPQTN and so on, Table 2-1) followed by a hydrophobic domain in a basic region, which promotes the localization in a membrane. With different sortase variants having various functions, the pentapeptide sorting signals play an important role in the anchoring processes, which make the covalent attachment to the peptidoglycan thick layer catalyzed by sortases feasible[7,8]

The majority of sortases have been found in conventional Gram-positive bacteria. Based on their primary recognition sequences, sortases are categorized into A-F different classes (Fig 2.3 and 2.4)[10].

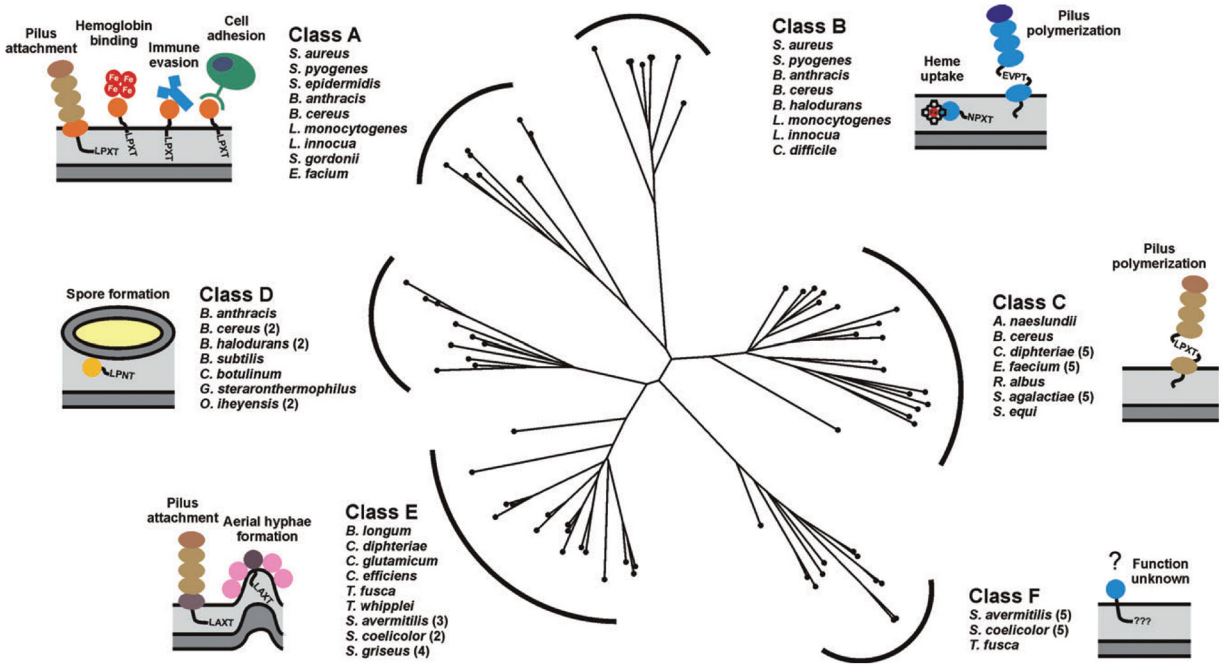

Fig 2.3 Family tree of sortases from Gram-positive bacteria. Reprinted from reference [10].

Table 2-1 Overview of the recognition motives, the substrates and the species in which sortase classes A-F occur. Reprinted from reference [7].

Sortase class	Motif	Substrates	Species
A	LPXTG	Surface proteins	All low GC content Gram-positive bacteria
B	NP(Q/K)TN	Haem acquisititon proteins	Low GC content Gram-positive bacilli and cocci
C	(I/L)(P/A)XTG	Pilin subunits	Both low and high GC content Gram-positive bacteria
D	LPNTA	Endospore envelope proteins	*Bacillus* species
E	LAXTG	Pili	High GC content Gram-positive bacteria
F	–	–	*Actinobacteria*

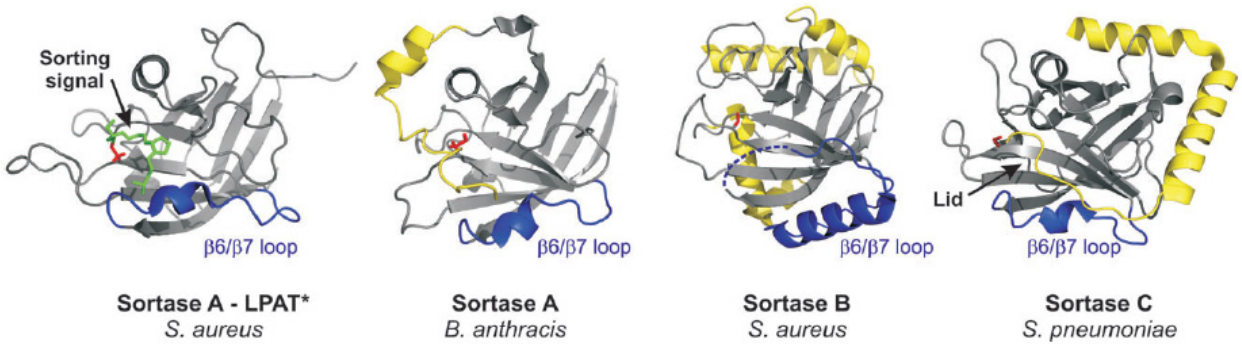

Fig 2.4 The overview of the structures of sortases A, B, and C. Reprinted from reference [10].

Class A sortase enzymes exist in many Gram-positive bacteria. They perform a housekeeping role and covalently link the surface proteins to the cell wall. The Sortase A (SrtA) group enables to attach a variety of distinct proteins such as internalins and is the best studied group. More details of SrtA will be stated in the following section. Class B sortase enzymes present widely in Firmicutes and play a key role in anchoring the iron acquisition protein IsdC to the cell wall. Class C sortase enzymes are also widely distributed in Gram-positive bacteria and have the function to assemble pili. Class D sortase enzymes anchor proteins to the cell envelope that facilitate sporulation and they are not so much investigated. The situation is similar for Class E and Class F sortase enzymes which are mainly discovered in Actinobacteria. Sortases also exist in some Gram-negative bacteria and archabacterial species[8,10].

2.2.2 Sortase A (SrtA)

SrtA from *Staphylococcus aureus* is best studied and characterized among the sortase enzyme family members. Nearly every enzyme anchors quite many of functionally distinct proteins to the cell wall, which results in the idea that they play a housekeeping role to the cell wall[13,17] SrtA is found in many Gram-positive bacteria and responsible for anchoring the CWSS which consists of a pentapeptide recognition motif LPXTG (X denotes all the natural amino acid residues except Cys and Trp which are not tested so far)[10] to the lipid II, which are often involved in pathogenesis. The mechanism of SrtA catalysis has been well researched and extensive applications of SrtA were developed in the last two decades. Fig 2.5A shows the representative scheme of sortase-mediated transpeptidation and Fig 2.5B shows the crystal structure of SrtA. Fig 2.6 shows the two-step reaction, namely the formation of the thioester intermediate, which is then attacked by the amine nucleophile of pentaglycine[8].

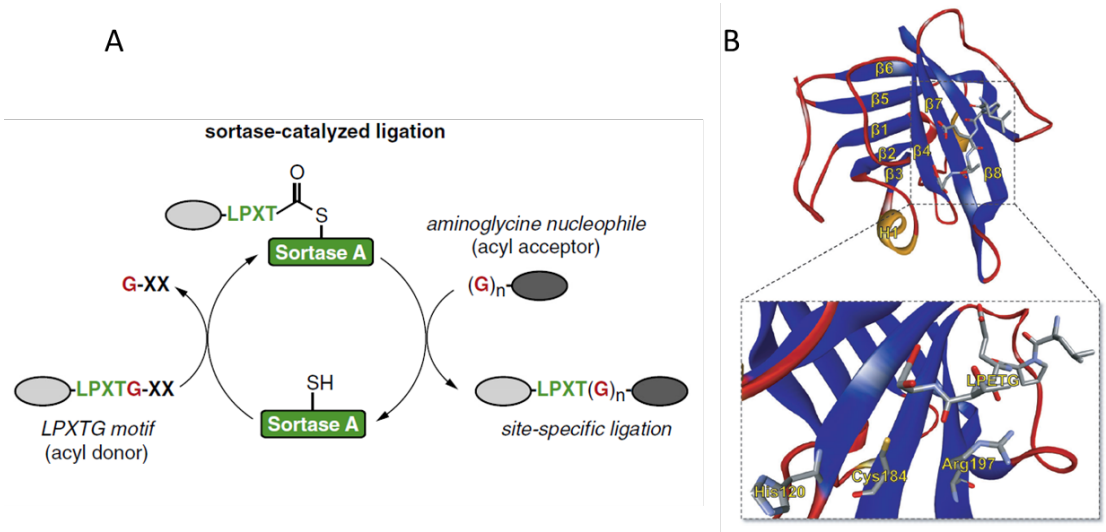

Fig 2.5 Representative scheme of sortase-mediated transpeptidation (A) and the crystal structure of SrtA (B). Reprinted from references [18] and [19].

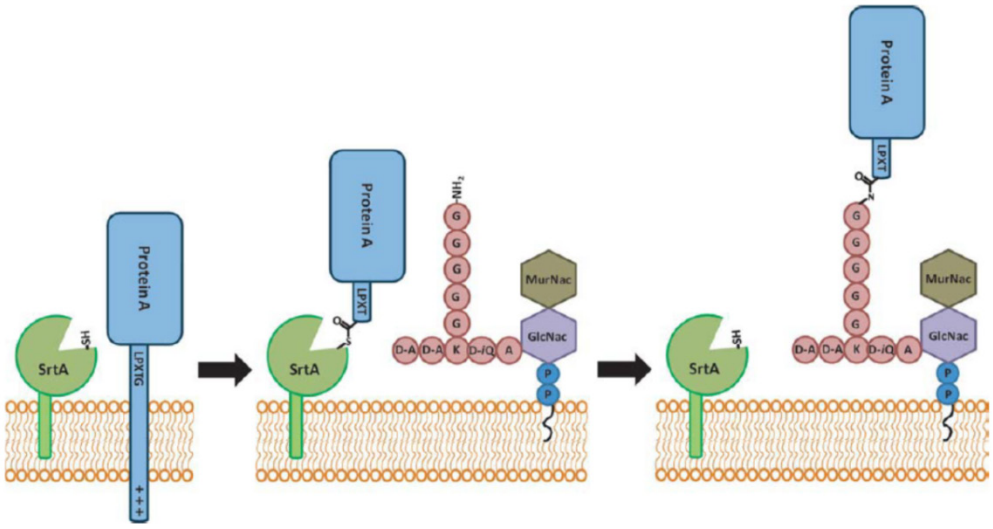

Fig 2.6 Formation of the thioester intermediate and its breakdown within bacterial membranes. Protein A is covalently linked to the peptidoglycan and SrtA is regenerated. Reprinted from reference [8].

The cysteine residue in the active site of SrtA nucleophilically attacks and cleaves the peptide bond between the threonine and the glycine residues in the LPXTG motif, forming a LPXT-SrtA complex in which the two substrates are linked through a thioacyl bond. The thioacyl LPXT-SrtA complex is then resolved by the nucleophilic attack of the amine terminus of a pentaglycine to form an isopeptide protein-lipid product (Scheme 2.2)[19,20].

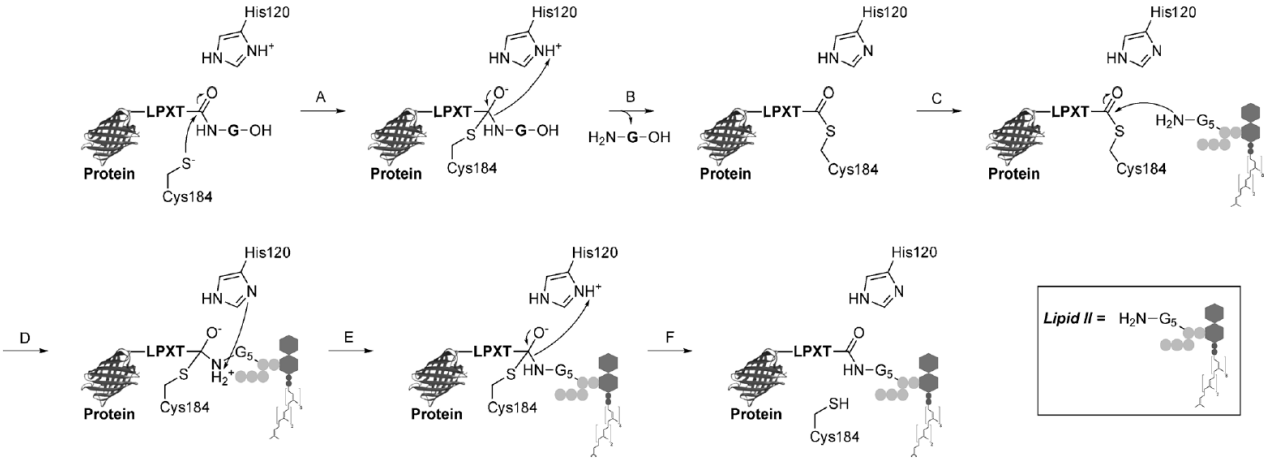

Scheme 2.2 Representative scheme of sortase-mediated transpeptidation. Reprinted from reference [19].

The two-step-reaction of the enzyme catalysis consists of transglycosylation and transpeptidation, which covalently link the cell wall with the cross bridge peptide. Due to its high selectivity SrtA has been considered to be a significant potential drug target. Furthermore, this enables the ligation of two proteins via a specific way, which is a potentially useful and powerful technique. More details about the applications of SrtA in the last years will be reviewed in the next section.

2.3 Previous SrtA studies

SrtA has been well studied on many aspects since its discovery in the last decades. Among the studies, cell modification and protein engineering via sortase-mediated ligation (SML) are the two classic and main functions of SrtA, including cell surface modifications, the ligation of different proteins or of protein and other biomolecules. With the extensive investigation, SrtA has been then widely used to also catalyze the ligation of small chemical molecules such as dyes to proteins. In addition, SrtA also enables the immobilization of proteins onto different surfaces and colloidal substrates.

SML or *sortagging* developed to a frequently used tool in basic research. Within enzymatic approaches, SML is one of the most promising methods for the linkage of building blocks in general because of its high selectivity towards specific peptide motifs, the very robust nature of sortase, synthetic and commercial accessibility of all required compounds (including sortase), the simplicity to perform *sortagging* in a lab and possibilities to reach high yields. Disadvantages of sortagging are the low catalytic efficiency, hence comparably high enzyme concentrations are required. Furthermore, SrtA is Ca^{2+}-dependent and the reaction is reversible. These shortcomings were partially solved by biotechnological methods through the development of Ca^{2+}-independent variants that have, moreover, a up to 140-fold higher activity[18]. Several approaches were developed to shift the equilibrium of the reaction. Often, the yield of the reaction product is increased by using an excess of one of the substrates. In addition, the by-product G-XX can be removed from the equilibrium (formation of unreactive fragments, complexation with metal ions, reaction under dialysis conditions)[18,21]. Furthermore, the addition of the amino acids WTWTW at both peptide motifs leads to the formation of a *β-hairpin* structure which cannot be recognized by SrtA anymore and is therefore removed from the reverse reaction[22,23].

The following chapters give an overview about the different application fields of sortase, starting with the ligation of solely biomolecules and, in more detail, going on to the incorporation of synthetic entities. A special emphasis is put on new developments in recent years.

2.3.1 Cell surface modification

Since SrtA anchors the surface proteins on the cell wall in nature, the latter hence can be modified via SML also in lab scale. In addition to proteins, also small molecules and polymers can be ligated to the cell wall.

Nelson *et al.* reported for the first time that the cell surface from wild-type *S. aureus,* being a dangerous pathogen, can be modified with synthetic small molecules such as fluorescein or biotin[24]. The SrtA enzymes of the bacteria covalently link non-native molecules bearing the LPETG recognition sequence to the peptidoglycan (Scheme 2.3). This research expanded the scope of the applications of SrtA and demonstrated the cell wall engineering of Gram-positive bacteria.

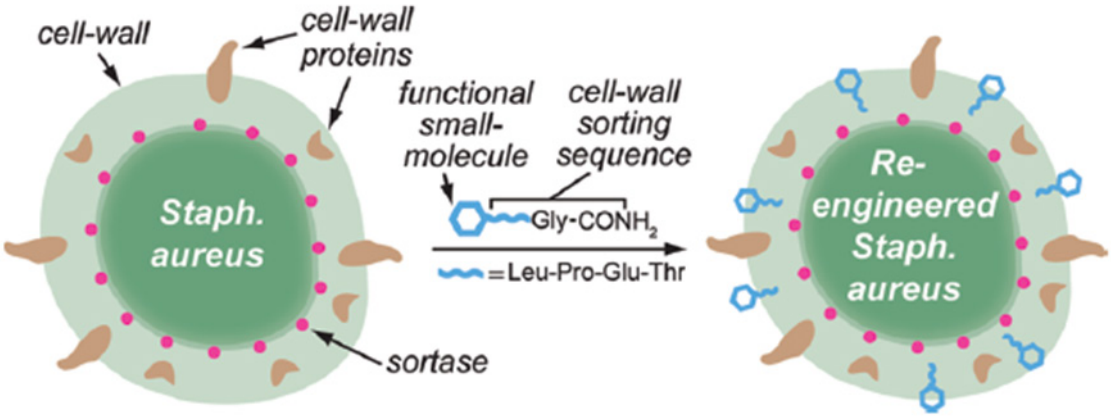

Scheme 2.3 Functional small molecule equipped with the CWSS are recognized by SrtA and covalently linked to the *S. aureus* cell wall. Reprinted from reference [24].

Tomita *et al.* reported the SrtA enzymatic modification of living cells with proteins[25]. A GGGYC peptide-polyethylenglycol (PEG)-lipid conjugate was incorporated into the membrane of living cells with its lipid domain. After incubation, the free PEG-lipid was removed. The presence of PEG can avoid the formation of aggregates in solution without adding any co-solvent or detergent. To demonstrate the principle of the method, enhanced green fluorescent protein (eGFP) was linked to the living cells with a high efficiency. The substrate protein, eGFP-LPETG, and SrtA were both added to perform the SML (Scheme 2.4). The successful ligation was proved by microscopy and sodium dodecylsulfate-polyacrylamide gel electrophoresis (SDS-PAGE). Furthermore, antibodies were displayed on cancer cells using this approach.

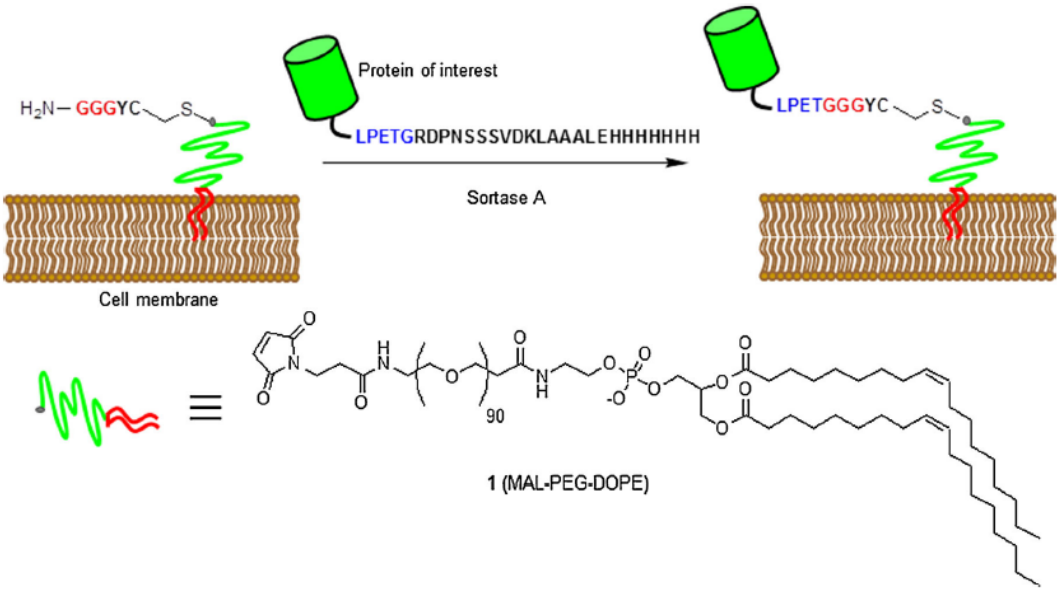

Scheme 2.4 SML of a protein of interest and a GGG-PEG-lipid modified cell membrane. Reprinted from reference [25].

Swee *et al.* reported a simple way of making use of SML for the surface display of engineered proteins or probes on cells. LPETG equipped probes were conjugated onto glycine residues naturally exposed at the cell surface in phosphate buffered saline (PBS) at RT for 1h. The authors demonstrated the conjugation of biotin probes to mouse hematopoietic cells, yeast cells and *Toxoplasma gondii* as well as the installation of antibodies onto different cells via the SrtA enzymatic approach[26].

Much research concerning cell engineering has been done via sortagging in the last years. Nguyen *et al.* displayed surface proteins successfully on the *Bacillus subtilis* cell surface using the sortases of this bacterium[27]. Park and Jung *et al.* reported the labeling of cells, harboring an optimized SrtA variant in its membrane, with different probe-LPETG substrates[28]. Veerman's group studied the influence of variable recognition sequences on the anchoring of peptides on *S. aureus* cells[29]. The sortagging was more efficient when positively charged amino acids follow after the recognition sequence and also when LPMTG was used instead of LPETG.

2.3.2 Modification of proteins or peptides with biomolecules such as DNA, lipids, and sugars

The rapid development of Srt studies influenced the field of protein engineering to a large extent. SML became a very user-friendly method on the modern way of protein engineering also for the modification with various biomolecules.

Koussa *et al.* ligated proteins covalently to deoxyribonucleic acid (DNA) via SML[30]. Oligoglycine units were first linked to DNA fragments by Cu^{I}-catalyzed azide-alkyne cycloaddition (CuAAC) click reaction. Next, protein-LPETG was ligated by sortagging and this enzymatic approach influenced the protein function only slightly. Moreover, different proteins could be sequentially ligated to DNA by using partially masked GGG which was liberated after the first coupling by tobacco etch virus (TEV) protease.

Antos *et al.* developed a general method for the site-specific modification of proteins with lipids (Fig 2.7). Lipid and protein were decorated with oligoglycine or LPETG motif, respectively, and ligated by SrtA. In their work, the purification procedure proposed by Parthasarathy *et al.*[31] was employed to remove the sortase enzyme as well as the excess of the model protein eGFP-LPETG-His_6 by the Ni-affinity resin[32]. The approach was achieved through the addition of a His_6-tag after the recognition sequence which is cleaved during sortagging. The same strategy was adopted by Guo *et al.* on the application for the ligation of protein (eGFP) and liposome (Scheme 2.5)[33], which opened the door for a new method for the modification of liposomes with proteins. The efficiency of the ligation was improved for higher GG concentrations on the liposomes and for larger distances after incorporation of a PEG spacer. Tabata *et al.* then developed the application of peptide-labeled liposome in drug-delivery field[34].

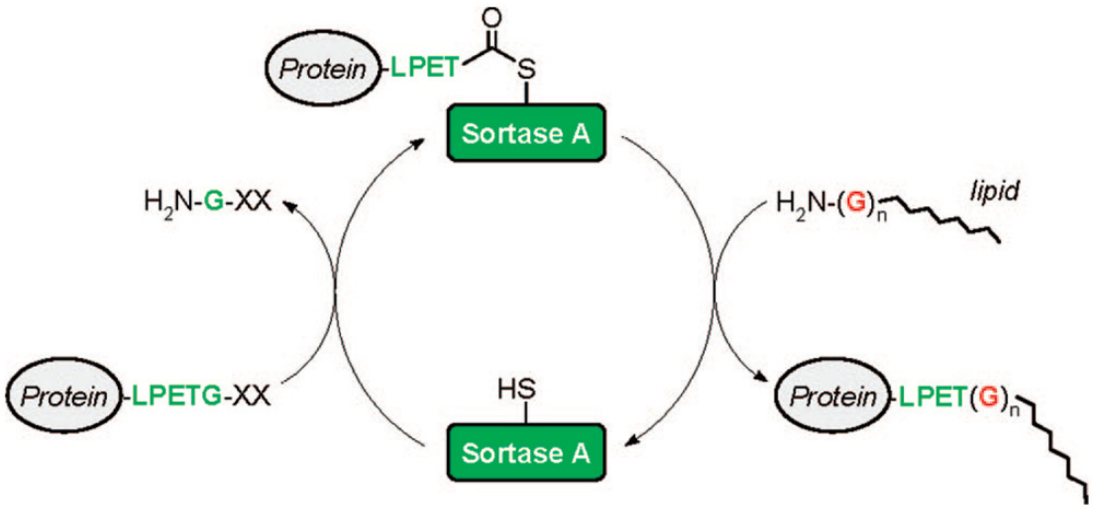

Fig 2.7 Site specific attachment of a lipid on a protein. Reprinted from reference [32].

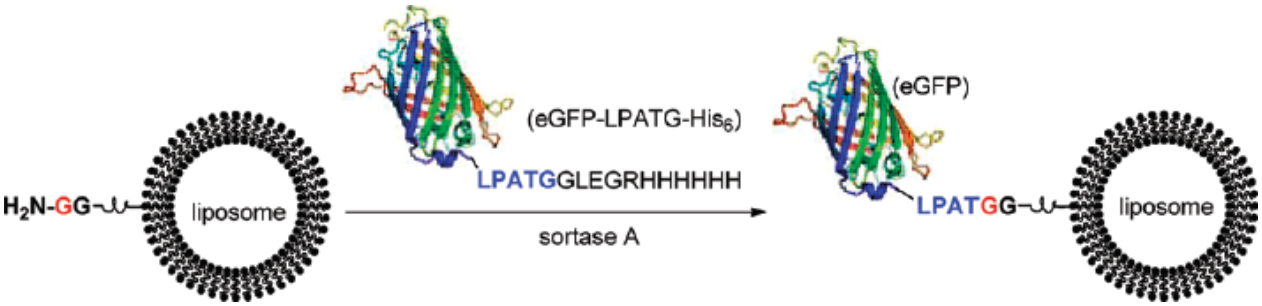

Scheme 2.5 Protein attachment on oligoglycine-functionalized liposomes. Reprinted from reference [33].

Due to the vital function of natural glycopeptides or glycoconjugates, sugar-peptide or sugar-protein conjugates became popular and well researched in the last years[35,36] With the development of sortase research, SML was introduced as a tool for linking sugars with peptides or proteins. Samantaray *et al.* reported that the SrtA transpeptidation enabled the transfer of peptide-LPETG substrates onto oligosaccharides which have amino groups that can act as nucleophile[35]. Therefore, the general approach for the ligation of peptide and sugar was demonstrated. Wu *et al.* presented the strategy of catalyzing the ligation of a glycosylphosphatidylinositol (GPI), which are glycolipids that anchor glycoproteins to the cell surface of eukaryotic cells, and proteins as shown in Scheme 2.6[37]. The authors demonstrated that the SML is successful between large proteins and complex GPI anchors.

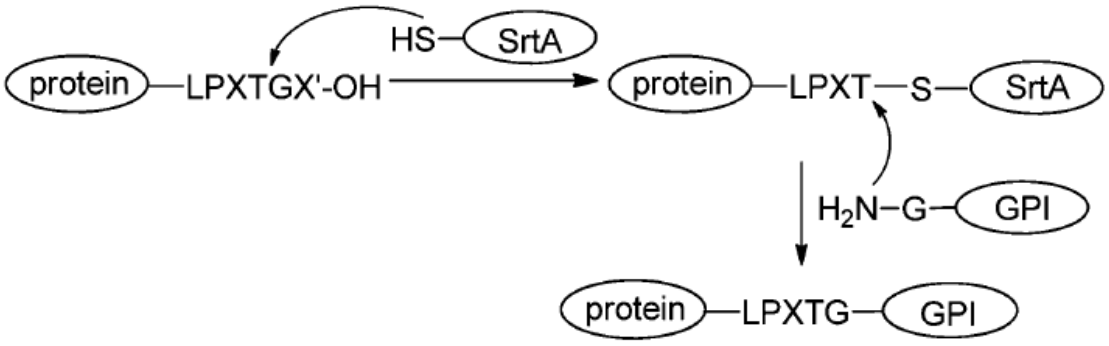

Scheme 2.6 SrtA catalysis applied for the ligation of GPI and protein. Reprinted from reference [37].

2.3.3 Ligation of proteins or peptides

Protein engineering by site-specific incorporation of functionalities in proteins or peptides has been widely used as a modern biochemical tool. The controlled ligation between peptides and proteins became one of the most popular and powerful methods in synthetic biology. Normally two synthetic peptides can be ligated under certain conditions by forming a peptide bond[38,39]. However, this can be difficult for large substrates such as proteins from a technical point of view. In 2004, Mao *et al.* presented for the first time that protein engineering can be realized via

SML[40]. They reported the ligations of protein-protein, protein-peptide and peptide-peptide to demonstrate the utility of SML. After testing various oligoglycine nucleophiles, they concluded that the number of glycines doesn't influence the efficiency of sortagging. This novel approach for protein engineering was extensively expanded in the following years, e.g. for the ligation of fluorescent proteins to a protein of interest[41–43] Many other studies focused on the ligation of two proteins or peptides in order to incorporate functional proteins into hydrogels[44], to facilitate the purification of recombinant fusion proteins[45], to develop immunoassays with the aim of monitoring glucose levels[46], to generate fusion proteins that are inaccessible via direct expression[47], and to form an enzyme cascade within *Escherischia coli* (*E. coli)*[48]. The group of Beck-Sickinger demonstrated that the modification of recombinant proteins by SML is not only possible in analytical lab scale, but also successful in large scale by utilizing sortase immobilized on a solid support. The enzyme is still active after being immobilized on a PEG-based resin by CuAAC and can be easily recycled[49].

In addition to the ligation of two proteins or peptides, the cyclization of a peptide or protein developed as another application field of sortase catalysis. A major aim of such studies is that (therapeutic) proteins have a higher stability in their cyclized than in the native form. Compared with native chemical ligation, cyclic polypeptides can be efficiently formed by SML, which needs only minimal modification on the proteins to be circularized. Antos *et al.* reported the cyclization of different substrates of the structure G_x-protein-LPXTG (Scheme 2.7, right)[50]. It turned out that it depends on the distance of the termini of the protein if cyclization takes place or oligomers are formed. In addition, both cyclization and oligomerization was reversible after addition of an excess of diglycine nucleophile. Hu *et al.* combined protein cyclization by SML with the conjugation of a synthetic polymer. The formed c-GFP-poly(oligo(ethyleneglycol)methylethermethacrylate) (POEGMA) conjugate showed increased thermal stability and improved tumor retention[51]. In the last years, the strategy of peptide or protein cyclization by SML was adopted for a myriad of studies[52–54].

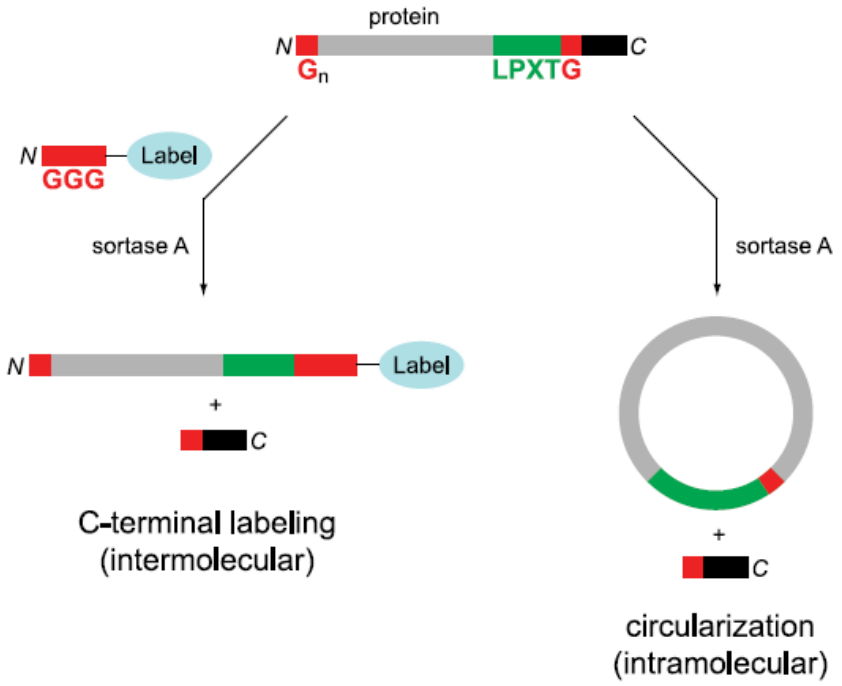

Scheme 2.7. Labeling (left) as well as circularization (right) of a protein with both peptide motifs for SML. Reprinted from reference [50].

In recent years, the binding of functional proteins to virus-like particles (VLP) was facilitated by SML. While the group of Chen used recombinant oligoglycine equipped E2 nanocages to ligate different LPETG functionalized proteins[55,56], Tang *et al.* used the opposed strategy with LPETGG functionalized VLPs to ligate GGG-equipped proteins[57]. The latter pointed out that SML is more efficient than chemical coupling and their strategy is a new approach in the design of vaccines[57]. Further studies in the group of van Hest focused on the encapsulation of cargo and later on the enzyme CalB in virus capsids[58,59] While the activity of the enzyme was unaffected, the enzyme was protected against proteases[59].

SML also proved helpful in the formation of protein samples for NMR spectroscopic studies. Multi-domain proteins with domain-selective isotope labeling could be formed[60][61] as well as a fusion protein of an isotopically labeled protein of interest and a solubility tag in order to facilitate NMR studies of proteins with limited solubility[62].

2.3.4 Ligation of proteins and small synthetic molecules

In addition to ligating a protein and a biomolecule, the scope of SML has been enlarged for the linkage of small synthetic molecules to proteins. It was shown with multiple examples that the ligation of peptide-functionalized small molecules to both C- and N-terminus of a protein is easily achievable exploiting sortase catalysis. In this respect, SML was most widely used for the attachment of dyes - often called probes in a more general sense - and ligands for metal ions as

well as azide or C≡C triple bond functionalities for further click chemical modification of the functionalized proteins. A main advantage of SML is the site specificity of modification which furthermore takes place at the C- or N-terminus of the protein and therefore has less impact on structure and function of the protein. After proof-of-principle, main application fields for SML of proteins with small synthetic compounds have been the formation of antibody conjugates, protein fusions and functional protein assemblies. The next paragraphs summarize the major directions from the last years. A special group of ligated compounds are initiators for a polymerization and will be presented in the following chapter 2.3.5 in the context of forming protein-polymer conjugates aided by SML.

2.3.4.1 Labeling of proteins

The site-specific modification of proteins with labels at both the N- and C-termini was demonstrated by the group of Ploegh[63,64]. The labeling at one terminus is comparably easy and was shown with the model protein cholera toxin B subunit (CtxB) having N-terminal glycines and fluorescein isothiocyanate (FITC) and biotin labels functionalized with the recognition sequence[63]. The installation of two modifications within one protein is much more challenging and required a cumbersome strategy using two different SrtA variants (Scheme 2.8)[63]. eGFP and UCHL3 served as model proteins with C-terminal LPXTG-His_6 recognition sequence and N-terminal MLVPRG sequence, which functioned as masked glycine. $SrtA_{pyogenes}$ (SrtA from *Streptococcus pyogenes*) accepts alanine nucleophiles (in addition to glycine) and was used at first to ligate tetramethylrhodamine-labeled dialanine (AA-TMR) to the C-terminus of the model proteins. The formed LPXTA sequence can't be cleaved by $SrtA_{aureus}$ (SrtA from *Staphylococcus aureus*), which was used for the second modification step. Therefore, after removing $SrtA_{pyogenes}$, the N-terminal sequence was cleaved by thrombin setting the glycine nucleophile available. Finally, FITCs could be installed at the N-terminus forming the site-specific dual-labeled model proteins.

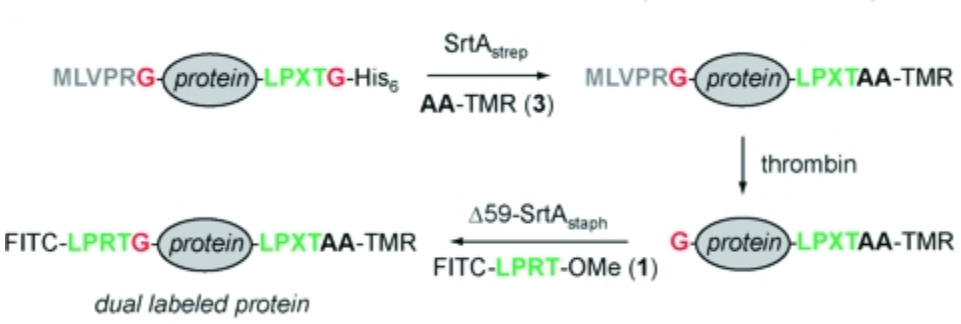

Scheme 2.8 Strategy to equip both termini of one protein with labels using $SrtA_{pyogenes}$ ($SrtA_{strep}$) and $SrtA_{aureus}$ ($\Delta59\text{-}SrtA_{staph}$). Reprinted from reference [63].

Warden-Rothman *et al.* developed a strategy to express a protein followed by modification and purification[65]. A chimeric protein, consisting of protein of interest with C-terminal recognition sequence, spacer, and SrtA with His_6-tag, was expressed and isolated on beads of a nickel column. Upon addition of calcium ions and GGG-label, the protein of interest (called ligand) is cleaved off and modified with the label (Scheme 2.9). It was postulated that any kind of cargo can be ligated to the C-terminus of a protein of interest exploiting this strategy. The proof-of-concept was demonstrated with an azide group that was subsequently utilized for click chemical reaction (compare the paragraphs below). The main advantage compared to SML in solution is omitting an additional step for purification of the desired product from SrtA.

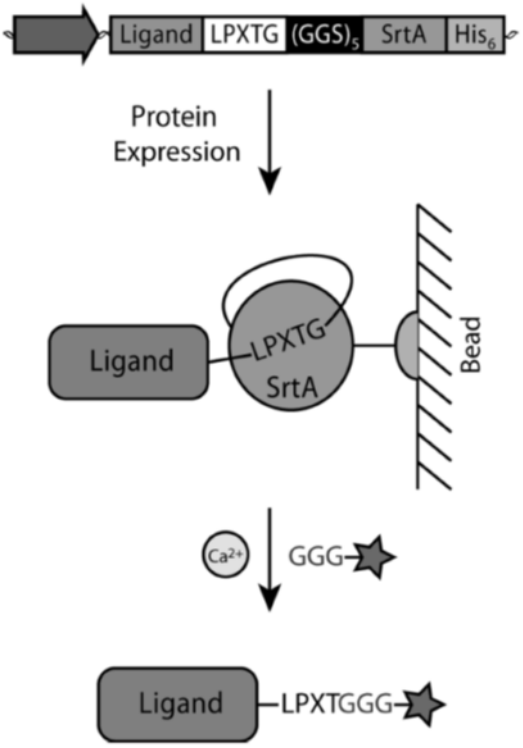

Scheme 2.9 Strategy from Warden-Rothman *et al.* for C-terminal labeling of a protein. Reprinted from reference [65].

For N-terminal protein labeling, Sarpong *et al.* developed a procedure that combines TEV protease cleavage, SML and affinity purification[66]. The protein of interest with TEV recognition motif is cleaved yielding an N-terminal glycine. A label with sortase recognition sequence and affinity tag for isolation of the modified protein is subsequently linked. This strategy was exemplarily shown with the ligation of fluorescent dyes to epidermal growth factor receptor (EGFR) and membrane scaffold protein (MSP).

Furthermore, several examples exist showing the labeling of proteins with fluorescent dyes utilizing SML. The C-terminal modification with oligoglycine-functionalized dyes was performed[67–69] as well as the N-terminal modification with LPETG-functionalized dyes[70–72].

2.3.4.2 Introduction of functional groups for click chemical reactions

In case proteins can't be easily ligated to the compound of interest directly, functional groups need to be introduced that can be addressed by chemical reactions in a subsequent step. The introduction of such functional groups into the proteins can be achieved by SML. The mainly favored chemical reactions for subsequent protein modification are the Cu^{I}-catalyzed azide-alkyne cycloaddition or its metal-free analogue strain-promoted azide-alkyne cycloaddition (SPAAC). These cycloadditions are among the prominent examples of a click reaction, which are reactions that stand out with high yield, negligible side products, mild reaction conditions and ease of execution among others[73,74]. The 1,3-dipolar azide-alkyne Huisgen cycloaddition is a reaction between substituted azides and alkines leading to 1,2,3-triazoles which can be executed at RT under Cu^{I} catalysis[75]. The reaction is bioorthogonal as there are neither azides nor alkynes present in nature, and therefore has been often used for the conjugation of biomolecules[76]. A more recent development is exploiting the ring strain of cyclooctynes to lower the energy barrier of the reaction which omits the use of Cu^{I} as catalyst – a development especially important for metal-free protein conjugation[77].

Gupta *et al.* ligated proteins with LPXTG-His_6 C-terminus with N_3- or C≡C-functionalized oligoglycines in order to construct a dendrimer by CuAAC[78]. A dendritic scaffold with multivalent display of proteins couldn't be formed directly by ligating proteins to a compound exhibiting several oligoglycine units. The reasons for the latter are most probably steric hindrance and the reversibility of the sortase reaction which does not allow to isolate products with several linked proteins in acceptable yields. However, using SML to link a protein to a compound having more than one azide or alkyne group, enabled to form the dendrimer by CuAAC subsequently. Sortase and unlabeled proteins, exhibiting both a His-tag, could be removed using Ni-nitrilotriacetic acid (NTA) beads.

The same approach was used by Wang *et al.* who compared four reactions for site-specific introduction of azide functionalities into proteins[79]. SML between protein-LPETG-His_6 and GG-PEG_3-N_3 resulted in the highest overall yield, compared to recombinant expression with unnatural amino acid, amidation at the N-terminus, and tyrosine selective three-component Mannich reaction. Furthermore, single site modification preserved the highest activity of the used membrane glycoprotein thrombomodulin (TM_{456}).

A strategy was developed in the group of Ploegh in order to form unnatural N-to-N and C-to-C protein-protein fusions[80]. As such fusion proteins are genetically impossible, a chemical

strategy was developed. SML was exploited to ligate the click handles azide and strained cyclooctyne to the N-termini of two different proteins. The subsequent SPAAC yielded N-to-N fusion proteins (Fig 2.8)[80]. The click handles can be likewise ligated to proteins' C-termini to form C-to-C fusions[81].

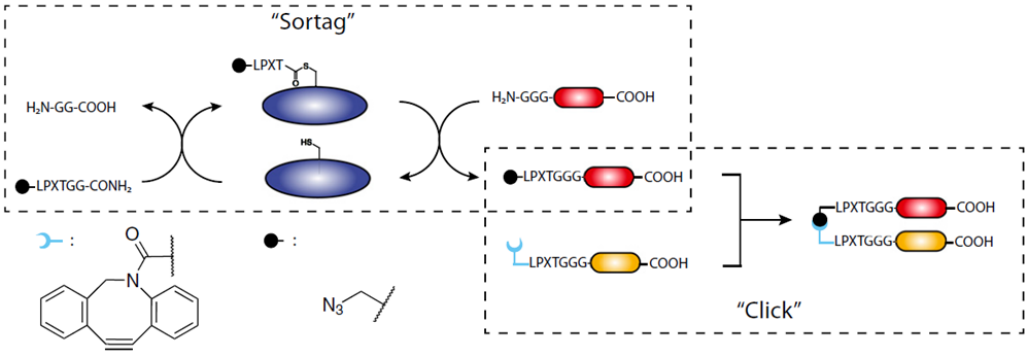

Fig 2.8 Schematic strategy of preparing unnatural N-to-N and C-to-C fusion proteins. Reprinted from reference [80].

Matsumoto *et al.* ligated azide groups to tetrameric streptavidin by SML in order to form a hydrogel with immobilized enzymes[82]. The SPAAC reaction with branched PEG exhibiting multiple alkyne groups yielded the hydrogel to which biotin-modified enzymes could be attached. As an application, the coating of the hydrogel on a glassy carbon electrode (GCE) and oxidation of glucose using glucose dehydrogenase (GDH) was demonstrated.

Click chemical approaches became also popular in recent years for the functionalization of antibodies. Alt *et al.* used the copper-free SPAAC to link an antibody with C-terminal Srt recognition sequence and a glycine-functionalized strained cyclooctyne by SML[83]. The product could be reacted with fluorescent dyes or macrocyclic ligands bearing an azide group. Therefore, this versatile strategy proofed to be well suited for the 2-step ligation of proteins with other biomolecules, labels or any kind of functionalities. Li *et al.* demonstrated that antibodies can be labeled with multiple (identical) fluorophores to improve fluorescent yields[84]. First, a GGG peptide equipped with both a fluorescent dye and an azide was linked to a single-chain antibody fragment by means of SML. Next, a DNA Holliday junction with strained cyclooctyne and three fluorescent dyes was reacted with the functionalized antibody fragment in a SPAAC reaction. The semi-rigid DNA structure of the Holliday junction ensures certain spacing between the dyes to avoid self-quenching of fluorophores.

2.3.4.3 Synthesis of antibody conjugates

In general, the modification of antibodies is an important research field and antibody conjugates can be formed by means of SML. The antibody fragment $scFv_{anti\text{-}LIBS}$ was modified at its C-terminus with a chelate ligand using SML. Through complexation of the isotope ^{64}Cu, the antibody fragment was radiolabeled having diagnostic potential[85]. In a similar fashion, Massa *et al.* linked GGGYK-functionalized chelate ligands and a fluorescent dye to camelid single-domain antibody-fragments. The chelate ligands were meant to bind ^{111}In for use in single-photon emission computed tomography (SPECT) and ^{68}Ga for positron emission tomography (PET), respectively, and the fluorescent dye for fluorescence reflectance imaging (FRI)[86]. Rashidian and Wang *et al.* showed the introduction of different functionalities into antibodies in order to improve their therapeutic properties[87]. GGG-peptides with two functionalities were linked to the C-terminus of single-chain antibody fragments via SML. These functionalities were either a fluorophore or served for introduction of ^{18}F isotopes for imaging on the one side and an azide on the other side. The latter was used for SPAAC with cyclooctynes, for instance for PEGylation of the antibody.

SLM allows the site-specific formation of antibody-drug conjugates (ADCs) which are potentially anti-tumor drugs. ADCs use a specific antibody for targeting of cancer cells in combination with small-molecule toxic payloads. Beerli *et al.* linked small molecule toxins to the C-termini of antibodies[88]. Compared to classical chemical conjugation to lysine or cysteine side chains, SML forms conjugates in site-specific manner and 1:1 ratio. The newly formed antibody-drug conjugates showed similar *in vitro* and *in vivo* tumor killing activities like traditional conjugates used in clinic. In a following study, the authors could show that ADCs based on anthracycline toxin and anti-HER2 antibody exhibited potencies even exceeding those of marketed products[89].

Fang *et al.* used a similar approach to form antibody-dye and antibody-drug conjugates[90]. Rapid tumor targeting could be shown using NIR imaging of the fluorescent dye and therapeutic potency demonstrated with the drug conjugate. Van Lith *et al.* showed the formation of antibody-nanoparticle (NP) structures based on SML and click chemistry[91]. Antibody-LPETG proteins were ligated with click handles for SPAAC. The following click reaction formed bispecific C-to-N as well as C-to-C antibody constructs. Click reaction with functionalized PEG_{2000} enabled to form PEG-based micellar nanoparticles with exposed antibodies. Van der Steen *et al.* developed a new concept for targeting the cancer extracellular matrix with specific antibody-functionalized lyophilisomes[92]. Lyophilisomes are albumin-based biocapsules that

were loaded with the toxin doxorubicin. The antibody was linked to this drug delivery vehicle in a two-step process consisting of first introducing a clickable group by SML and subsequently linking the protein to functionalized lyophilisomes by SPAAC.

The group of Chen developed approaches for the synthesis of ADCs comparable to strategies explained above. First, ADCs were prepared by SML between antibody-LPETG and GGG-toxin[93]. However, a 100-fold excess of toxin is required because of the reversibility of sortase reaction, but still steric hindrance reduces the efficiency for certain combinations of antibody chains and toxin. Consequently, the group developed a two-step procedure to first ligate small click handles to antibodies followed by SPAAC to link the toxic payload (Scheme 2.10)[94]. For the latter, only a two-fold excess of clickable toxin was needed, hence reducing toxic waste.

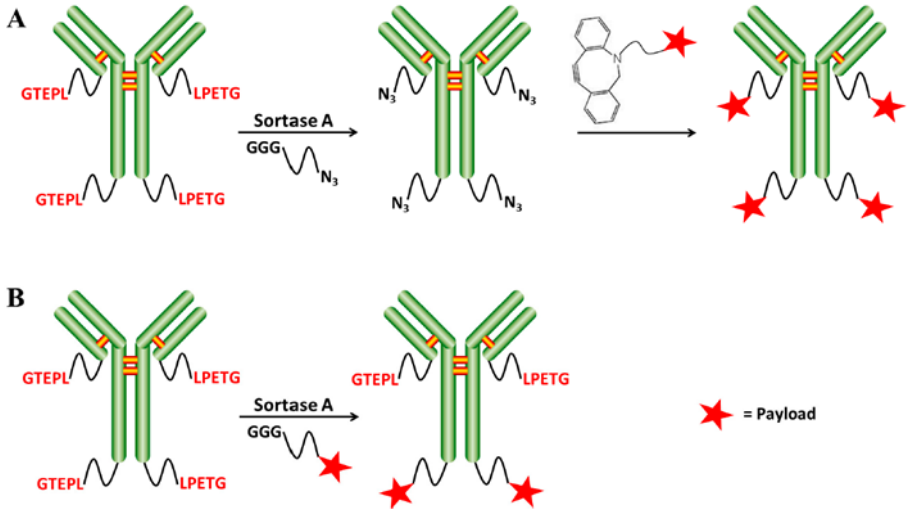

Scheme 2.10 Two strategies for generating antibody-drug conjugates: SML and SPAAC (A), only SML (B). Reprinted from reference [94].

2.3.4.4 Modification of multiphages

The construction of complex virus-type structures with the help of SML was demonstrated by Hess *et al*[95]. In order to attach different dye molecules to capsid proteins of M13 bacteriophage, the sortase variants $SrtA_{pyogenes}$ and $SrtA_{aureus}$ were used subsequently like already described in the beginning of this chapter. At first, $SrtA_{pyogenes}$ ligated a dye to the body of the phage, followed by linkage of dyes to both ends of the phage by $SrtA_{aureus}$. After labeling, SML was utilized to link LPETGG- or GGGK-functionalized DNA oligonucleotides to the ends of the phage structure. DNA hybridization led to multiphage particles in which phage structures are linked by DNA connections. The labeling with different dyes enabled visualization of the multiphage structures.

2.3.4.5 Non-proteinic amines as nucleophiles

In addition to oligoglycines, it was shown that different non-proteinic amines can function as nucleophiles in SML. In a recent study, diverse commercially available amines were tested for their ligation to model proteins with LPETGG recognition sequence mediated by the engineered sortase variant SrtA7M, which has seven mutations leading to higher activity and Ca^{2+} independency[96]. All successful examples – 3-azido-1-propanamine, propargylamine, tetrazine amine, ethylenediamine, aminoethylbenzenesulfonamide, and histamine – were unbranched at the α-carbon, while amines branched at the α-carbon did not show product formation. The latter suggests that SrtA7M prefers unbranched primary amine nucleophiles. Furthermore, the protein modification with diverse amines was not only possible *in vitro*, but also in living *E. coli* cell culture.

2.3.5 Formation of protein-polymer conjugates aided by SML

Two different cases have to be distinguished concerning the formation of protein-polymer conjugates using sortase-mediated ligation. First, initiators for atom-transfer radical polymerization (ATRP) were ligated to proteins by SML and the polymerization carried out afterwards. Hence, sortase is only involved in the first step of the conjugate formation and this has to be classified as the ligation of a protein with a small chemical molecule. Second, amine- or peptide-functionalized polymers were also directly ligated to proteins by sortase catalysis.

In general, two approaches are commonly used to synthesize protein-polymer conjugates, denoted as grafting-to and grafting-from[97–99]. Grafting-to is used since decades to link pre-formed polymers with end-functional groups to proteins. The most prevalent example is PEGylation, the linkage of PEG[100]. The attachment of polymer chains usually stabilizes proteins in non-natural environment and improves both solubility and resistance against unfolding[98,101,102]. The modification of therapeutic proteins is the main application field of protein-polymer conjugates and they were extensively studied for drug delivery[103]. Grafting-to enables the individual synthesis and characterization of polymers without being restricted to reaction conditions that are compatible with proteins. However, the binding of two macromolecules is thermodynamically unfavorable and accompanied by low grafting yields. Furthermore, the purification of the conjugates from unreacted protein and polymer is challenging. In 2005, Maynard and coworkers introduced the grafting-from approach[104,105]. Initiators or mediators of a polymerization are linked to a protein and the polymers directly synthesized from the protein. Main advantages are the higher grafting yield and easy purification

of the conjugates as only small molecules need to be removed (monomer, eventually catalyst). Controlled radical polymerization (CRP) techniques, mainly ATRP and reversible addition-fragmentation chain transfer (RAFT) polymerization (see chapter 2.5 for details), are the methods of choice for grafting-from. Reaction conditions for ATRP and related techniques were shown to be adapted to biologically relevant conditions[105–109].

Although around half of the amino acids can principally be targeted, lysine and cysteine side chains are mainly exploited for protein modification because of their unique reactivity with readily available functional groups[110,111]. However, targeting lysines and cysteines often means a loss of control of stoichiometry and position of modification as there are usually more than one of these amino acids available and solvent exposed in a protein[111,112]. Alternatively, unnatural amino acids and other tags were on occasion used for a site-specific incorporation of an initiator group for polymerization[103,113]. The modification of proteins with polymerization initiators or polymers by sortase-mediated ligation has the advantage over conventional conjugation methods that the functionality is site-specifically and stoichiometrically (1:1) introduced to the protein. Furthermore, modifications at the protein termini have usually negligible influence on activity and folding of a protein.

2.3.5.1 Ligation of initiators for a polymerization

Qi *et al.* ligated an initiator for ATRP to the C-terminus of GFP by SrtA catalysis and conducted the grafting-from polymerization subsequently (Fig 2.9a)[114]. Attachment of the initiator group was performed with 30-fold excess of the GGG-functionalized small molecule and a high yield reached (ca. 95 % from quantification of SDS-PAGE band intensities). For the purification of the product, it was exploited that SrtA and unmodified protein possess a His_6-tag which is cleaved off from the protein of interest during SML. Therefore, the reaction product is the only proteinic species without affinity tag – a strategy often exploited for product purification after SML. ATRP of OEGMA was performed in aqueous buffer conditions with a copper-based catalyst system.

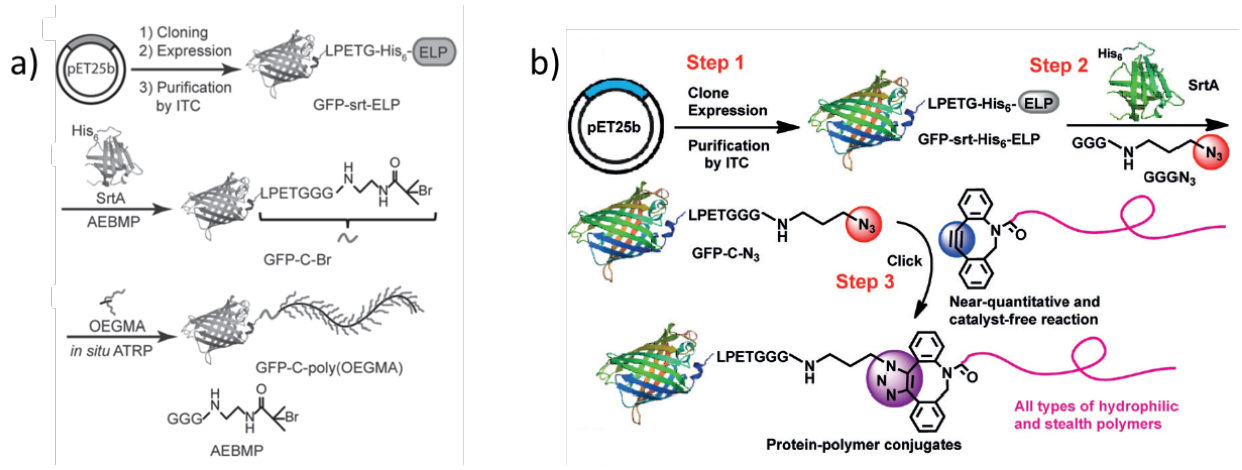

Fig 2.9 a) The synthetic route of the conjugate of GFP and poly(OEGMA) via SML and grafting-from polymerization; b) GFP-polymer was formed by SML and a grafting-to strategy. Reprinted from references [114] and [115].

In an alternative approach of their strategy, the group of Chilkoti published the SML of azide groups to proteins followed by the attachment of alkyne-functionalized polymers through SPAAC reaction (Fig 2.9b)[115]. Instead of ligating a polymerization initiator to the protein and grafting the polymer directly from the protein, the polymer was individually formed, characterized and subsequently linked to the protein. Diverse polymers were synthesized, end-functionalized with suitable cyclooctynes and finally conjugated to GFP-N_3 by SPAAC click reaction. This process was described as a modular approach for the synthesis of defined protein-polymer conjugates and all three steps could be carried out in high yield without catalyst.

Hu *et al.* used SML to link an ATRP initiator to a therapeutically relevant protein and compared the performance of the subsequently formed protein-polymer conjugate with the clinically approved PEGylated protein[116]. The target protein is human interferon alpha (IFN-α), therapeutically used in unmodified and PEGylated form. In order to improve the conjugate formation, SrtA was used to link an ATRP initiator to IFN-LPETGGH_6 and subsequently polymerize OEGMA from the C-terminus of IFN-Br. After purification, an overall yield of 66 % was reached for IFN-POEGMA. For comparison, the authors also performed post-polymerization linkage of GGG-POEGMA to IFN-LPETGH_6 by SML. However, only 1.1 % yield was reached when using a 20-fold excess of the polymer. First studies indicated that IFN-POEGMA, possessing a PEG-like polymer, showed a higher efficiency in tumor therapy than unmodified IFN-α and clinically approved forms that are PEGylated in the traditional way.

2.3.5.2 Ligation of polymer blocks

Although Hu *et al.* could not reach a satisfactory yield for conjugating a polymer directly to a protein[116]– the reason could be the high molecular weight of the polymer (around 66 kDa) –

some examples for this strategy exist. Such an approach refers more to the grafting-to strategy. It has the clear advantage over the classical grafting-to technique that the polymer linkage takes place site-specifically and sortase acts as a kind of catalyst for the reaction. However, shift of the equilibrium of the sortase reaction and purification of the reaction product are most probably even more important for the linkage of two macromolecules.

Parthasarathy *et al.* PEGylated eGFP at the C-terminus utilizing SML[31]. Commercially available PEG of 10 kDa was used and applied with amine as well as GGG end groups. The formation of eGFP-PEG conjugates could be observed with both polymers and no significant difference noticed for H_2N-PEG and GGG-PEG. However, SDS-PAGE indicated low efficiency for the conjugate formation in both cases. This is not surprising when taking into account the low 1.5-fold excess of polymer compared to protein during one of the first reports for SML with one artificial substrate which was published in 2007. Popp *et al.* used a similar approach and PEGylated proteins at the C-terminus with 10 and 20 kDa PEG[117]. The polymers were functionalized with GGGK peptides and ligated to IFN-LPETGGH_6 among others using 40-fold excess. Quantitative conversion was not reached, however, after purification by ion exchange chromatography, pure conjugates could be shown by SDS-PAGE.

Qu *et al.* demonstrated the C-terminal PEGylation of thrombomodulin[118]. Therefore, commercially available 5 kDa PEG with amine end group was used. While WT SrtA showed unsatisfactorily performance, a SrtA pentamutant (eSrtA) with greatly enhanced activity significantly improved the PEGylation efficiency. Nearly 80 % yield could be reached for the reaction between TM-LPETG and H_2N-PEG after 2 h when using a 100-fold excess of the nucleophile. It is worth noting that 10-fold excess of H_2N-PEG led only to minimal product formation. In a subsequent work, the groups of Liu and Chaikof developed new sortase variants having different peptide recognition sequences (LPXSG, LAXTG)[119]. Orthogonality of these variants enables the introduction of two substrates into one protein, for instance, fluorophore-protein-PEG conjugates were formed. Hence, some of the shown ligations involve protein PEGylation with 10 kDa GGG-PEG which was synthesized from commercially acquired H_2N-PEG. PEGylated conjugates could be isolated after purification with Ni-NTA filtration and concentration using 10 kDa molecular weight cut off (MWCO) membranes in yields of up to 20 %.

Hou *et al.* synthesized different kinds of protein-poly(amino acid) conjugates with unnatural amino acids[120]. Among their conjugates are further examples for PEGylation of eGFP and IFNα

by SML. Glycine-functionalized commercially available PEG of 2 kDa was reacted with protein-LPETGGLEH$_6$ and about 90 % conversion reached (Fig 2.10). After purification by Ni-NTA affinity chromatography, conjugates with a yield in the range of approximately 45-55 % could be isolated. Optimized conditions for the formation of eGFP-PEG were 30 min reaction time, 0.1 equiv. SrtA and, remarkably, only 5 equiv. G$_5$-PEG.

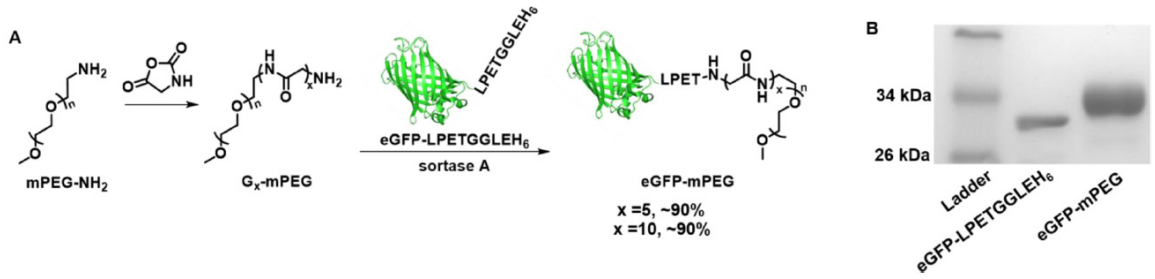

Fig 2.10 A) Synthesis of eGFP-PEG conjugate via SML; B) SDS-PAGE of the product. Reprinted from reference [120].

However, the successful direct ligation of a polymer synthesized by oneself was not reported yet. This would enable that any desired polymer could be synthesized by a CRP method and then ligated to a protein in one step. The presented studies so far are limited to commercially available polymers with a suitable end group and only include PEG and derivatives.

2.3.6 Immobilization of proteins on surfaces by SML

An interesting application of SML is seen in the immobilization of proteins on surfaces. It was shown with many examples that such surfaces can be planar as well as curved particle surfaces. Furthermore, the proteins` immobilization in micro- and hydrogels could be achieved as well. All approaches will be presented one after the other in the following paragraphs.

The immobilization of proteins on surfaces is always accompanied by the search for a suitable linking chemistry so that the structure and activity of the protein is preserved to a high degree. Nonspecific adsorption or nonspecific covalent binding usually lead to random orientations and reduced activity. Thus, the focus of recent years moved to techniques for site-specific attachment that favor an oriented immobilization of the biomolecule and a homogeneously covered surface[121]. Sortase-mediated ligation is such a technique which provides the possibility to immobilize recombinant proteins via their termini on surfaces. In contrast to some chemical methods, such an enzymatic approach goes along with reaction conditions that do not disturb protein functionality. Furthermore, design of the peptide sequences allows the incorporation of a short spacer. Hence, SML was studied for immobilization of proteins on various peptide- or amine-functionalized surfaces. The ligation via C-terminus is much more prevalent among the

examples for the immobilization of proteins on solid surfaces. To the best of my knowledge, N-terminal immobilization on planar or particle surfaces was not reported yet and the only examples for this type of oriented attachment are within gels.

2.3.6.1 Immobilization on planar surfaces

The functionalization of biacore sensor chips with proteins was demonstrated by Clow *et al.*[122]. Therefore, a peptide with N-terminal GGG was attached to the dextran surface of the chip via a cysteine at the C-terminus. While the SML with LPETG-tagged protein was not successful during flow over the chip surface, incubation overnight at 37 °C yielded in immobilized proteins. Recombinant fibronectin-binding protein (Fba) from the streptococcal cell wall was exemplarily used and ligand-analyte interaction demonstrated with human factor H (FH).

Jiang *et al.* immobilized thrombomodulin on glass surfaces and published two approaches (Fig 2.11)[123]. On the one side, TM-LPETGH$_6$ was directly immobilized on glycine-functionalized glass surfaces via SML. On the other side, the protein was first ligated with biotin via sortase catalysis and the immobilization conducted on streptavidin-functionalized glass slides. Enhanced bioactivity could be observed through the site-specific immobilization of thrombomodulin. The activity measurements indicated that the immobilization via biotin-streptavidin interaction was slightly more efficient. As TM is a membrane protein involved in natural anticoagulant system, the demonstrated approach was postulated as promising for antithrombogenic surfaces for cardiovascular biomaterials to minimize incompatibility and thrombosis.

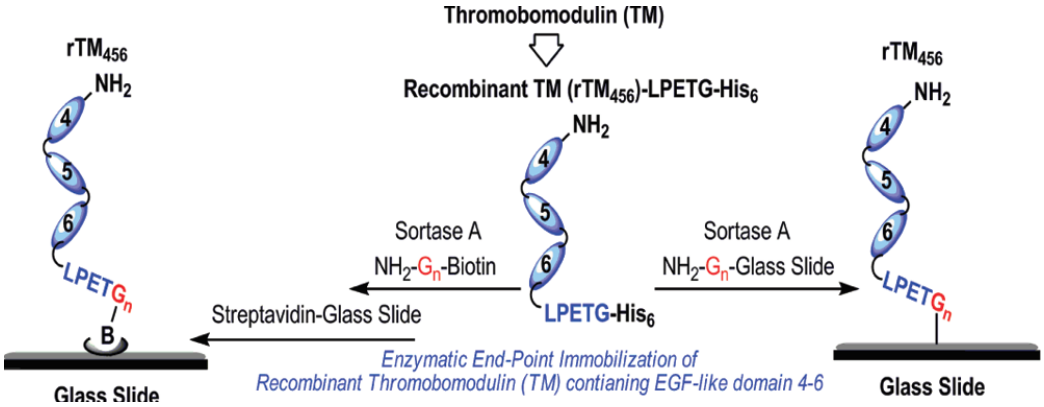

Fig 2.11 Immobilization of recombinant human thrombomodulin on glass slides via SML. Reprinted from reference [123].

Sinisi *et al.* ligated LPETG-tagged proteins to GGG-functionalized glass surfaces[124]. The authors showed with several Influenza virus proteins that the ligation is possible directly from a cellular extract without purification of the extracted protein. Antigens from Influenza A were

used as proof of concept, but such a protein array was postulated to be used for early detection of seasonal flu on the one side and in general for high-throughput screening on the other side.

Dorr *et al.* demonstrated the simultaneous dual surface modification using two orthogonal SrtA variants[119]. GGG-PEG-functionalized 96-well plates were incubated with two newly evolved sortase variants with preference for LPESG and LAETG recognition sequences and two fluorophores equipped with the respective peptide sequences. Hence, two distinct compounds could be simultaneously ligated to a surface.

The immobilization of proteins on crystalline nanocellulose (CNC) was studied by Uth *et al*.[125]. CNC has a large surface area, is easily prepared from renewable source cellulose and the introduction of orthogonally addressable aldehyde groups is possible. The authors could show that SML leads to a higher activity of immobilized proteins compared to traditional coupling between protein amino groups and surface carboxylic groups. Peptide sequences bearing a pentaglycine motif for sortase catalysis were introduced by linkage to the mentioned aldehyde groups. Three different recombinant proteins – GFP, the antibody-like domain Lys-vNAR and the enzyme galactose oxidase (GOas) were expressed with LPETG recognition sequence and ligated to CNC using an evolved SrtA variant.

The attachment of photosystem I (PSI) complex on a conductive gold surface is interesting for biophotovoltaics. In order to overcome limitations from non-uniform and undesired orientations, Le *et al.* ligated PSI-LPETGH$_6$ to a GGGC-functionalized Au surface (thiol-gold bond utilizing cysteine)[126]. Through immobilization by SML, 94 % PSI could be oriented in the desired manner which is mainly important for the photoinduced electron transfer to the gold surface. Thus, an enhanced electron transfer could be reached compared to other reported immobilization techniques.

The group of Boder continued their work by studying the immobilization of protein layers on gold surfaces using orthogonal SrtA variants[127]. SrtA$_{aureus}$ ligating LPETG / GGG and SrtA$_{pyogenes}$ ligating LPETA / AAA (and less efficiently also LPETG / GGG) were already introduced in chapter 2.3.4. Two fluorescent model proteins, eGFP-LPETG and mCherry-LPETA, were at first independently ligated to gold-coated microscope slides with the mentioned thiol-gold linkage to bind GGGC or AAAC peptides, respectively (Fig 2.12 left). Next, protein oligomers were formed on gold by using either AAA-mCherry-LPETA or GGG-GFP-LPETG. AFM analysis of the surfaces suggested that at least dimers should have been formed. Finally, the controlled formation of two protein layers was performed. Therefore, GGG-mCherry-LPETA

was first ligated to AAA-tagged gold by $SrtA_{pyogenes}$. The formed LPETAAA peptide is not a substrate for $SrtA_{aureus}$, hence the first protein layer will not be cleaved by $SrtA_{aureus}$. Consequently, eGFP-LPETG could be attached as a second layer catalyzed by $SrtA_{aureus}$ (Fig 2.12 right). The disadvantage of the used orthogonal sortase variants is the possibility of partially forming immobilized protein oligomers of mCherry in the first step as GGG is a weak nucleophile for $SrtA_{pyogenes}$.

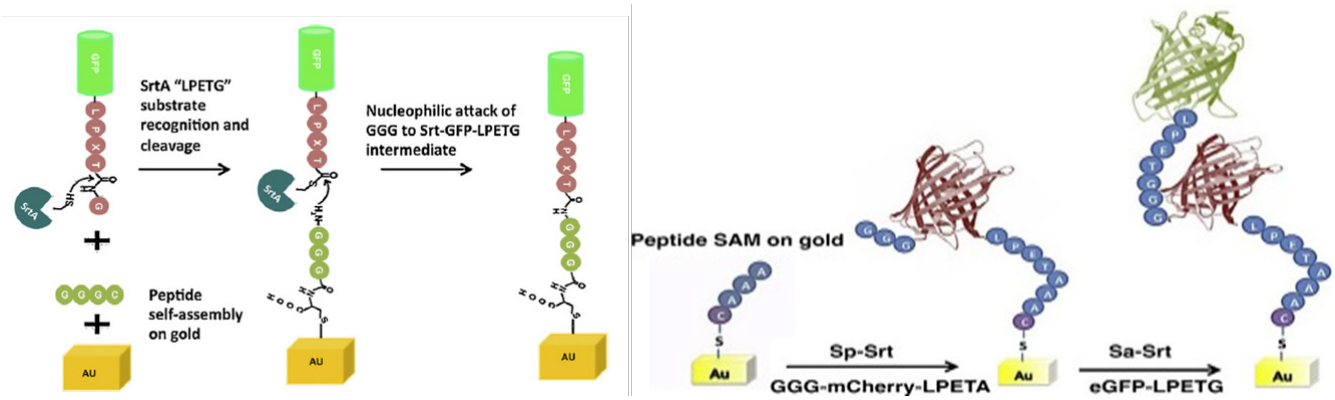

Fig 2.12 Immobilization of LPETG-equipped-GFP onto GGG-functionalized gold surface via SML (left). Strategy of immobilization two protein layers onto a gold surface by using the two different variants $SrtA_{pyogenes}$ (Sp-Srt) and $SrtA_{aureus}$ (Sa-Srt) (right). Reprinted from reference [127].

As an alternative strategy that avoids the use of two different sortase variants, the same group published the protein layer-by-layer immobilization using a protection group for the GGG nucleophilic sequence[128]. The peptide sequence DDDDKGGG can be cleaved by enterokinase (EK) after lysine to set the oligoglycine free. At first, eGFP oligomers were formed in solution and up to pentamers reached. On GGG-functionalized polystyrene bead and gold surfaces, protein layers were formed by first ligating DDDDKGGG-eGFP-LPETG, second cleavage of the protecting sequence and third ligation of mCherry-LPETG using the same sortase A variant. However, dimer formation in solution even when the protection group should be present and unequal ratio of the proteins on gold surface suggest an improvement of biotechnological techniques before the strategy can be broadly established.

Ham *et al.* showed that the reversibility of the sortase reaction can be used to repeatedly regenerate immobilized protein films on surfaces[129]. GGGGGK-biotin was assembled on streptavidin-functionalized surfaces and thrombomodulin-LPETG ligated. Adding GGG excess together with sortase removed the protein film nearly completely (Fig 2.13). The charge / strip cycles could be repeated 10-times in vitro. Evolved sortase A (eSrtA) was significantly more efficient for both immobilization and removal compared to SrtA WT. Moreover, as LPETG and GGG motifs exist rarely in nature, the charge / strip cycles could be likewise performed in 50 %

v/v whole blood at 37 °C. As the described regeneration of bioactive coatings is interesting for blood-contacting surfaces and TM is known to reduce thrombosis, the process was further conducted on implanted polyurethane catheter in living mice with intravenous administration of eSrtA and either biotin-LPETG or GGG.

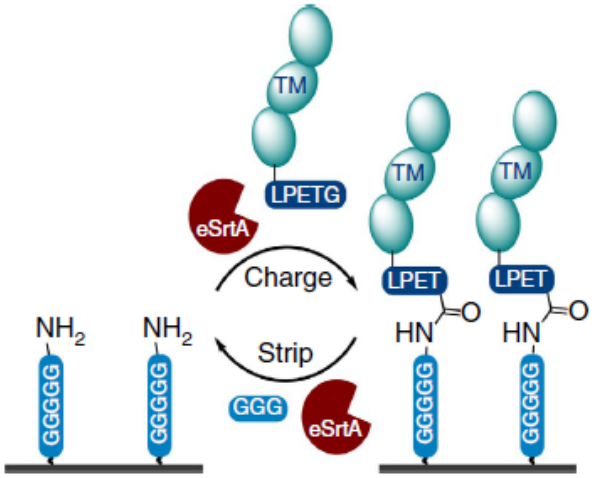

Fig 2.13 Reaction cycle of immobilizing LPETG-Biomolecules on a pentaglycine-equipped surface and its removal by adding eSrtA together with an excess GGG. Reprinted from reference [129].

Srinivasan *et al.* made use of sortagging for the purification and presentation of recombinant proteins on surfaces for single-molecule studies[130]. After thorough surface cleaning and functionalization with a tetraglycine unit, LPETG-tagged proteins could be immobilized by SML both from purified samples as well as whole cell lysate. The oriented attachment of proteins under maintaining functionality is especially important for single-molecule studies and was demonstrated with single-molecule force spectroscopy.

2.3.6.2 Immobilization on particle surfaces

The ligation of proteins to either planar or curved surfaces from particles showed no obvious difference. Hence, particle surfaces were targeted through SML in parallel and the most important examples will be introduced in the following paragraphs.

In addition to eGFP-PEG conjugates (see chapter 2.3.5.2), Parthasarathy *et al.* also reported the ligation of eGFP-LPETG to polystyrene beads[31]. The beads with a diameter of 3 µm were used with either amine groups on the surface or functionalized with GGG peptides. Fluorescence intensity after SML indicated that efficiency of immobilizing eGFP is higher for GGG-functionalized than NH_2-terminated beads.

Chan *et al.* published one of the first universal studies for the sortase-mediated immobilization of proteins on surfaces and demonstrated the ligation on crosslinked glycidyl methacrylate polymer beads, agarose affinity resins and planar glass surfaces[131]. All support materials were functionalized with oligoglycine motifs followed by the immobilization of different fluorescent proteins and the DNA binding protein Tus of which the functionality on polymer beads could be verified.

Ito *et al.* used SML to find a suitable immobilization technique for the class of extremely unstable glycosyltransferases[132]. Two recombinant enzymes, rhGalT and rhFucT, were ligated via their C-termini on alkylamine-functionalized sepharose. This site-specific covalent attachment enabled an immobilization without loss of activity and stability. Furthermore, reuse of the immobilized enzymes with sugar transfer activity was demonstrated.

Adhesive proteins were ligated to microbeads in the group of Proft[133]. Adhesins are proteins on the cell wall of bacteria that are responsible for the adhesive properties of bacteria to host cell tissue. While many proteins are possible adhesins, their interaction with cells can be studied after immobilization on microbeads. The *in vitro* immobilization by sortase has the advantage that the orientation of the proteins on the beads is identical as in nature where sortase enzymes are responsible for the ligation to the bacterial cell wall. Cell binding studies showed that the microspheres with adhesins bound specifically stronger to cells than the negative control samples.

Matsumoto *et al.* identified a sortase variant from *Lactobacillus plantarum* with the recognition sequence LPQTSEQ[134]. eGFP-LPQTSEQ was ligated to primary amine-modified microbeads by both *S. aureus* SrtA and SrtLp. Fluorescence microscopy showed that the immobilization was more efficient using SrtLp.

The formation of antibody-drug conjugates by SML was presented in chapter 2.3.4.3. In addition, the ligation of antibodies to particles enables the targeted delivery of imaging agents, drug carrier capsules and therapeutic proteins exposed on micelles. Ta *et al.* demonstrated the ligation of scFv antibodies to a model protein, particles and cells[135]. The single chain antibodies (scFv) expressed with LPETG recognition sequence were ligated to eGFP (Fig 2.14a) and iron oxide beads (Fig 2.14b), both functionalized with triglycine motifs. The magnetic particles can be used as contrast agents for magnetic resonance imaging (MRI) and the site-specific immobilization of antibodies is crucial for targeted delivery. In case of cells, the antibodies were ligated directly to amino groups on the surface; however, the efficiency was significantly higher

for GGG-functionalized cells (Fig 2.14c). Bioactivity of antibodies and successful targeting could be demonstrated. The groups of Caruso and Peter expanded their work with the site-specific attachment of antibodies on polymer carrier vehicles that are promising for targeting applications in the medical field[136][137]. Low fouling capsules were prepared by layer-by-layer assembly of polymers around silica particles followed by subsequent removal of silica by hydrofluoric acid (HF). Peptides with N-terminal triglycine were linked to the polymer capsules by CuAAC and finally scFv-LPETG antibodies ligated by sortagging. Site-specific immobilization via their C-terminus leaves the antigen-binding sites available for targeting. Furthermore, protein micelles bearing both targeting and therapeutic proteins were formed (Fig 2.14d)[138]. The micelles composed of elastin-like polypeptide (ELP) with a diameter of ca. 50 nm were generated with multiple triglycine units. scFv antibodies for targeting and the catalytically active domain of thrombomodulin for inhibition of thrombus formation were ligated using evolved SrtA. The multifunctional protein micelles could be formed in a one-pot transpeptidation and targeted delivery as well as formation of an inhibitor of the coagulation cascade shown.

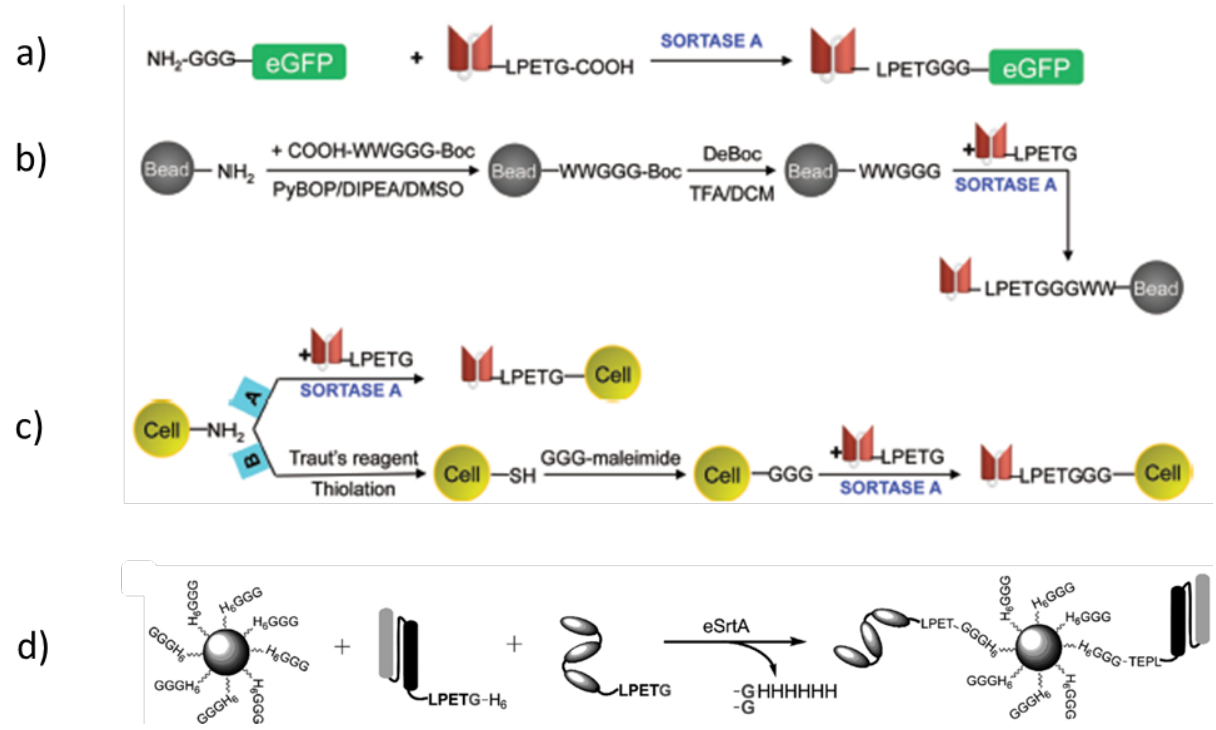

Fig 2.14 Scheme of the ligation process of scFv-LPETG antibodies to eGFP (a), magnetic iron oxide particles (b), cells (c) and protein micelles (d). Reprinted from references [135] and [138].

The group of Richter used the exemplarily chosen immobilization of eGFP-LPETGGH$_6$ on GGG-polystyrene microbeads for a continuous monitoring of reactions using different sortase variants[139]. The real-time flow cytometry assay followed the covalent attachment of the proteins on the surface by an increase of the microbead fluorescence. Interestingly, H$_6$-SrtA$_{\Delta59}$, H$_6$-

$SrtA_{\Delta 25}$, $SrtA_{\Delta 59}$-H_6 as well as triple-, tetra- and penta-mutated $SrtA_{\Delta 59}$-H_6 showed distinct differences in their performance for the investigated reaction.

Hata *et al.* exploited sortagging for the oriented immobilization of enzymes on particles[140]. β-glucosidase (BGL) and α-amylase (AmyA) were ligated to GGG-tagged polystyrene particles of 500 nm in diameter. In parallel, the enzymes were also linked to COOH-functionalized particles through chemical crosslinking using 1-ethyl-3-(3-dimethylaminopropyl)carbodiimid (EDC) and N-hydroxysuccinimid (NHS). While the same amount of enzymes was attached through both methods, the oriented immobilization by SML provided a higher activity of the enzymes along with better reusability performance.

Qafari *et al.* published the C-terminal immobilization of protein A on silica and graphene oxide nanoparticles[141]. While the amount of immobilized protein was higher for G_5-SiO_2 NPs than for H_2N-SiO_2 NPs, the situation was opposite for graphene oxide NPs suggesting that the nature of the nanoparticles influences the immobilization efficiency in addition to the type of amine nucleophile.

2.3.6.3 Immobilization in gels and formation of gels

In recent years, it was also demonstrated that sortase is successful in modifying hydrogels and microgels. Moreover, even the formation of a hydrogel network itself could be catalyzed by sortase.

The functionalization of PEG-based hydrogels with epidermal growth factor (EGF) was performed by Cambria and Renggli *et al.*[142]. The sortase recognition sequence LPRTG was linked with an N-terminal cysteine to acrylate groups in the hydrogel. The amount of ligated GGG-EGF was dependent on the amount of incorporated LPRTG motifs and the concentration of the model protein. Although EGF appeared to be enriched at the surface of the hydrogel, diffusion of the relatively small sortase enzyme into the hydrogel could be concluded. Reversibility of the sortase reaction was exploited to cleave the protein from the hydrogel by adding the used evolved sortase A variant again together with excess GGG nucleophile. Bioactivity of the immobilized proteins could be demonstrated and the shown protein cleavage opens up possibilities for a controlled release.

Gau and Mate *et al.* functionalized stimuli-responsive microgels with the model protein eGFP (Scheme 2.11)[143]. Poly(*N*-vinylcaprolactam) (PVCL) microgels are temperature-responsive and, due to their biocompatibility, interesting candidates for biomedical applications. Microgels were

synthesized containing glycidyl methacrylate (GMA) in order to bind peptides with the recognition sequence LPETG via an N-terminal cysteine to the epoxy groups. The reaction kinetics of sortase-mediated ligation of GGG-eGFP could be determined through the fluorescence intensity of ligated protein at different reaction times. After 7 h, no more protein seems to be ligated. The amount of immobilized protein could be further controlled in a linear fashion by the concentration of GGG-eGFP in solution.

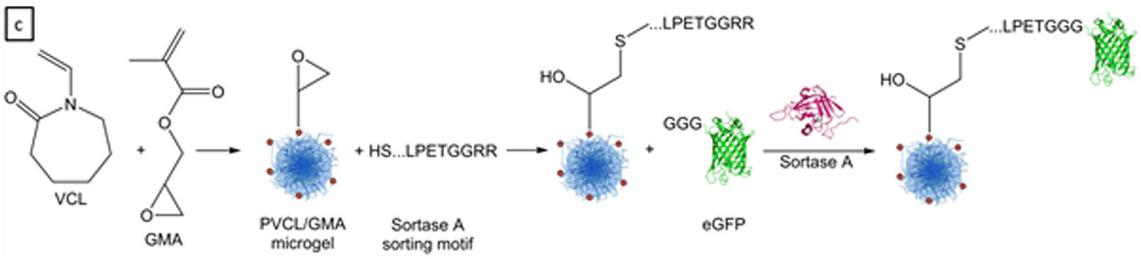

Scheme 3.11 Synthesis of a PNVCL microgel followed by a sortase-mediated immobilization of eGFP. Reprinted from reference [143].

Arkenberg *et al.* demonstrated that sortase is also capable to form a hydrogel network by crosslinking the peptide-functionalized precursors[144]. Therefore, 8-arm PEG-OH (8 OH-groups in the polymer) was first reacted with 5-norbornene-2-carboxylic acid, followed by reaction of the introduced double bonds with cysteine residues of the used peptides. Crosslinking of LPRTG- or GGGG-functionalized PEGs was performed by addition of SrtA7M for 10 min. The speed of the gelation scaled with enzyme concentration. An additional mushroom tyrosinase (MT)-triggered secondary crosslinking through dityrosine formation between incorporated tyrosine residues could be performed in order to tune the hydrogel properties. Finally, *in situ* cell encapsulation was demonstrated under mild conditions.

2.4 Peptide synthesis

Monodisperse polypeptides are important biological activities, which have a defined sequence of amino acids. They have a broad range of interesting functions, and can be obtained via solid-phase peptide synthesis (SPPS) - the most important and often used modern synthetic method.

The original chemical ligation approach for peptide synthesis coupling was quite efficient, but the peptide formed after each step must be washed and purified, which is very inefficient for long peptide sequences[145].

In 1963, R. B. Merrifield introduced a new approach for SPPS[146], which developed to a manifold exploited method for peptide synthesis in the following years. In this approach, the

peptide is synthesized from the C-terminus through the stepwise addition of N-protected amino acids. After cleavage of the protection group and washing, the next amino acid can be coupled. The attachment of the peptides' C-terminus to a solid support (resin) facilitates the purification of the growing peptide after every coupling step. The final peptide can be liberated from the resin. While *tert*-butyloxycarbonyl (tBoc) protection groups were commonly used in the early decades of peptide synthesis, fluorenylmethoxycarbonyl (Fmoc) groups developed to be currently the most popular protection groups because of the milder conditions for cleavage. Nowadays, SPPS can be performed in an automatic fashion in a commercial peptide synthesizer.

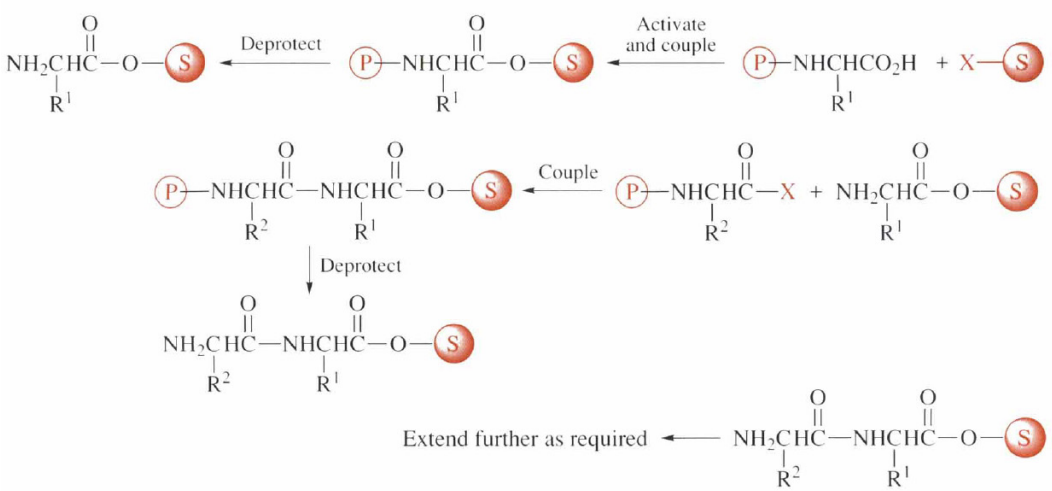

Scheme 2.12 Solid-phase peptide synthesis from a support (S) with stepwise coupling of activated amino acid units, followed by cleavage of the protection group (P). Reprinted from reference [145].

2.5 Polymer-peptide or polymer-protein conjugates via controlled radical polymerizations (CRP)

Polymers can be obtained from different polymerization methods. Among them, controlled radical polymerization (or living radical polymerization) provides big benefit to construct biochemical nanostructures[147]. Controlled radical polymerizations include atom-transfer radical polymerization (ATRP), reversible addition-fragmentation chain transfer (RAFT) polymerization and nitroxide-mediated polymerization (NMP)[148]. In the recent years, ATRP and RAFT technique were widely used for the conjugation of polymers to biomolecules.

In the polymerization process via ATRP, the generation of a radical involves an alkyl halide, which undertakes a reversible redox transformation catalyed by transition metal complexes (normally copper compounds with halogen atoms)[147,148]. The process contains an electron transfer and activates the halide initiator. The reaction can be well performed in aqueous media, therefore, being compatible biomolecules which require buffer systems. In addition, initiators and catalysts required for ATRP polymerization are normally commercially available. Usually,

the initiator is attached on the biomolecule and the polymer chain can be then polymerized from the initiator, which is called 'grafting from'.

Differs from ATRP, dithioester or similar compounds (chain transfer agent, CTA) are needed in the RAFT process to generate an intermediate radical at the carbon-center as shown in Scheme 2.13[149].

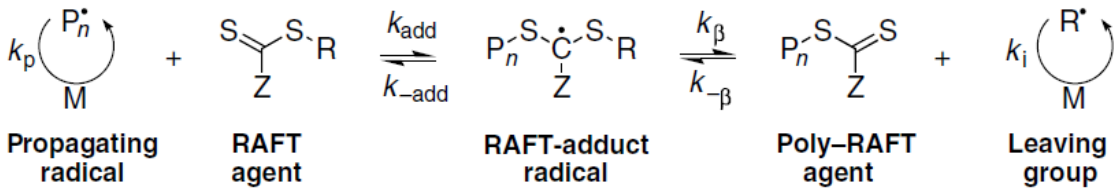

Scheme 2.13 RAFT polymerization process. Reprinted from reference [149].

The CTAs contain Z-group and R-group, which are the two substituents next to the C=S group. the Z-group activates the carbon-center towards radical addition and then stabilises the generated radical. In the meanwhile, the R-group performs as a leaving group and reinitiates the radical polymerization. RAFT polymerization shows a nice tolerance towards functional groups and can be performed under mild conditions. In addition, it avoids the usage of a metal catalyst, which is bio-friendly. Therefore, RAFT has been shown great interest over the last decades. Although the CTAs are only to some extent commercially available, the polymer product with a removable or alterable end group makes RAFT attractive[148,150].

2.6 References

[1] J. M. Berg, J. L. Tymoczko, L. Stryer, *Biochemistry*, 5th Edition, *W H Freeman,* **2002**, *New York*, 320–323.

[2] I. Schomburg, A. Chang, S. Placzek, C. Söhngen, M. Rother, M. Lang, C. Munaretto, S. Ulas, M. Stelzer, A. Grote, *et al.*, *Nucleic Acids Res.* **2013**, *41*, D764–D772.

[3] biologymad.com/resources/Ch 4 - Enzymes.pdf

[4] W. Wencewicz, C. Wencewicz, T. Wencewicz, in *Antibiot. Challenges, Mech. Oppor.*, **2016**, pp. 5–31.

[5] E. Fonzeť, M. Vermeire, M. Nguyen-Distèche, R. Brasseur, P. Charlier, *J. Biol. Chem.* **1999**, *274*, 21853–21860.

[6] https://en.wikipedia.org/wiki/DD-transpeptidase

[7] W. J. Bradshaw, A. H. Davies, C. J. Chambers, A. K. Roberts, C. C. Shone, K. R. Acharya, *FEBS J.* **2015**, *282*, 2097–2114.

[8] K. W. Clancy, J. A. Melvin, D. G. McCafferty, *Biopolymers* **2010**, *94*, 385–396.

[9] T. Proft, *Biotechnol. Lett.* **2009**, *32*, 1–10.

[10] T. Spirig, E. M. Weiner, R. T. Clubb, *Mol. Microbiol.* **2011**, *82*, 1044–1059.

[11] W. Vollmer, D. Blanot, M. A. De Pedro, *FEMS Microbiol. Rev.* **2008**, *32*, 149–167.

[12] T. Schneider, M. M. Senn, B. Berger-Bächi, A. Tossi, H. G. Sahl, I. Wiedemann, *Mol. Microbiol.* **2004**, *53*, 675–685.

[13] L. A. Marraffini, A. C. DeDent, O. Schneewind, *Microbiol. Mol. Biol. Rev.* **2006**, *70*, 192–221.

[14] S. K. Mazmanian, H. Ton-That, O. Schneewind, *Mol. Microbiol.* **2001**, *40*, 1049–1057.

[15] S. K. Mazmanian, G. Liu, H. Ton-That, O. Schneewind, *Science* **1999**, *285*, 760–763.

[16] A. W. Maresso, O. Schneewind, *Pharmacol. Rev.* **2008**, *60*, 128–141.

[17] D. Comfort, *Infect. Immun.* **2004**, *72*, 2710–2722.

[18] J. M. Antos, M. C. Truttmann, H. L. Ploegh, *Curr. Opin. Struct. Biol.* **2016**, *38*, 111–118.

[19] M. Ritzefeld, *Chem. Eur. J.* **2014**, *20*, 8516–8529.

[20] M. W. Popp, J. M. Antos, G. M. Grotenbreg, E. Spooner, H. L. Ploegh, *Nat. Chem. Biol.* **2007**, *3*, 707–8.

[21] L. Schmohl, D. Schwarzer, *Curr. Opin. Chem. Biol.* **2014**, *22*, 122–128.

[22] Y. Yamamura, H. Hirakawa, S. Yamaguchi, T. Nagamune, *Chem. Commun.* **2011**, *47*, 4742.

[23] H. Hirakawa, S. Ishikawa, T. Nagamune, *Biotechnol. J.* **2015**, *10*, 1487–1492.

[24] J. W. Nelson, A. G. Chamessian, P. J. McEnaney, R. P. Murelli, B. I. Kazmiercak, D. A. Spiegel, *ACS Chem. Biol.* **2010**, *5*, 1147–1155.

[25] U. Tomita, S. Yamaguchi, Y. Maeda, K. Chujo, K. Minamihata, T. Nagamune, *Biotechnol. Bioeng.* **2013**, *110*, 2785–2789.

[26] L. K. Swee, S. Lourido, G. W. Bell, J. R. Ingram, H. L. Ploegh, *ACS Chem. Biol.* **2015**, *10*, 460–465.

[27] H. D. Nguyen, T. T. Phan, W. Schumann, *AMB Express* **2011**, *1*, 22.

[28] K. Park, J. Jung, J. Son, S. H. Kim, B. H. Chung, *Chem. Commun. (Camb).* **2013**, *49*, 9585–9587.

[29] S. H. Maòásková, K. Nazmi, W. Van'T Hof, A. Van Belkum, N. I. Martin, F. J. Bikker, W. J. B. Van Wamel, E. C. I. Veerman, *PLoS One* **2016**, *11*, 1–14.

[30] M. A. Koussa, M. Sotomayor, W. P. Wong, *Methods* **2014**, *67*, 134–141.

[31] R. Parthasarathy, S. Subramanian, E. T. Boder, *Bioconjug. Chem.* **2007**, *18*, 469–476.

[32] J. M. Antos, G. M. Miller, G. M. Grotenbreg, H. L. Ploegh, *J. Am. Chem. Soc.* **2008**, *130*, 16338–16343.

[33] X. Guo, Z. Wu, Z. Guo, *Bioconjug. Chem.* **2012**, *23*, 650–655.

[34] A. Tabata, Y. Ohkubo, N. Anyoji, K. Hojo, T. Tomoyasu, Y. Tatematsu, K. Ohkura, H. Nagamune, *Anticancer Res.* **2015**, *35*, 4411–4418.

[35] S. Samantaray, U. Marathe, S. Dasgupta, V. K. Nandicoori, R. P. Roy, *J. Am. Chem. Soc.* **2008**, *130*, 2132–2133.

[36] M. R. Pratt, C. R. Bertozzi, *Chem. Soc. Rev.* **2005**, *34*, 58–68.

[37] Z. Wu, X. Guo, J. Gao, Z. Guo, *Chem. Commun. (Camb).* **2013**, *49*, 11689–11691.

[38] J. P. Tam, J. Xu, K. D. Eom, *Biopolym. - Pept. Sci. Sect.* **2001**, *60*, 194–205.

[39] P. E. Dawson, S. B. H. Kent, *Annu. Rev. Biochem.* **2000**, *69*, 923–960.

[40] H. Mao, S. A. Hart, A. Schink, B. A. Pollok, *J. Am. Chem. Soc.* **2004**, *126*, 2670–2671.

[41] T. Matsumoto, T. Tanaka, A. Kondo, *Langmuir* **2012**, *28*, 3553–3557.

[42] W. Ott, T. Nicolaus, H. E. Gaub, M. A. Nash, *Biomacromolecules* **2016**, *17*, 1330–1338.

[43] T. Matsumoto, Y. Isogawa, K. Minamihata, T. Tanaka, A. Kondo, *J. Biotechnol.* **2016**, *225*, 61–66.

[44] S. Piluso, H. C. Cassell, J. L. Gibbons, T. E. Waller, N. J. Plant, A. F. Miller, G. Cavalli, *Soft Matter* **2013**, *9*, 6752.

[45] J. J. Bellucci, M. Amiram, J. Bhattacharyya, D. McCafferty, A. Chilkoti, *Angew. Chemie - Int. Ed.* **2013**, *52*, 3703–3708.

[46] N. F. Ismail, T. S. Lim, *Sci. Rep.* **2016**, *6*, 19338.

[47] V. Ulrich, M. J. Cryle, *J. Pept. Sci.* **2017**, *23*, 16–27.

[48] T. Matsumoto, K. Furuta, T. Tanaka, A. Kondo, *ACS Synth. Biol.* **2016**, *5*, 1284–1289.

[49] M. Steinhagen, K. Zunker, K. Nordsieck, A. G. Beck-Sickinger, *Bioorganic Med. Chem.* **2013**, *21*, 3504–3510.

[50] J. M. Antos, M. W. L. Popp, R. Ernst, G. L. Chew, E. Spooner, H. L. Ploegh, *J. Biol. Chem.* **2009**, *284*, 16028–16036.

[51] J. Hu, W. Zhao, Y. Gao, M. Sun, Y. Wei, H. Deng, W. Gao, *Biomaterials* **2015**, *47*, 13–19.

[52] J. Zhang, S. Yamaguchi, T. Nagamune, *Biotechnol. J.* **2015**, *10*, 1499–1505.

[53] N. Rasche, J. Tonillo, M. Rieker, S. Becker, B. Dorr, D. Ter-Ovanesyan, U. A. K. Betz, B. Hock, H. Kolmar, *Bioconjug. Chem.* **2016**, *27*, 1341–1347.

[54] Z. M. Wu, S. Z. Liu, X. Z. Cheng, X. R. Zhao, H. F. Hong, *Chinese Chem. Lett.* **2017**, *28*, 553–557.

[55] Q. Chen, Q. Sun, N. M. Molino, S.-W. Wang, E. T. Boder, W. Chen, *Chem. Commun.* **2015**, *51*, 12107–12110.

[56] Q. Sun, Q. Chen, D. Blackstock, W. Chen, *ACS Nano* **2015**, *9*, 8554–8561.

[57] S. Tang, B. Xuan, X. Ye, Z. Huang, Z. Qian, *Sci. Rep.* **2016**, *6*, 25741.

[58] L. Schoonen, J. Pille, A. Borrmann, R. J. M. Nolte, J. C. M. Van Hest, *Bioconjug. Chem.* **2015**, *26*, 2429–2434.

[59] L. Schoonen, R. J. M. Nolte, J. C. M. van Hest, *Nanoscale* **2016**, 14467–14472.

[60] L. Freiburger, M. Sonntag, J. Hennig, J. Li, P. Zou, M. Sattler, *J. Biomol. NMR* **2015**, *63*, 1–8.

[61] F. P. Williams, A. G. Milbradt, K. J. Embrey, R. Bobby, *PLoS One* **2016**, *11*, 1–16.

[62] B. R. Amer, R. MacDonald, A. W. Jacobitz, B. Liauw, R. T. Clubb, *J. Biomol. NMR* **2016**, *64*, 197–205.

[63] J. M. Antos, G. L. Chew, C. P. Guimaraes, N. C. Yoder, G. M. Grotenbreg, M. W. L. Popp, H. L. Ploegh, *J. Am. Chem. Soc.* **2009**, *131*, 10800–10801.

[64] C. P. Guimaraes, M. D. Witte, C. S. Theile, G. Bozkurt, L. Kundrat, A. E. M. Blom, H. L. Ploegh, *Nat. Protoc.* **2013**, *8*, 1787–1799.

[65] R. Warden-Rothman, I. Caturegli, V. Popik, A. Tsourkas, *Anal. Chem.* **2013**, *85*, 11090–11097.

[66] K. Sarpong, R. Bose, *Anal. Biochem.* **2017**, *521*, 55–58.

[67] R. Jiang, L. Wang, J. Weingart, X. L. Sun, *ChemBioChem* **2014**, *15*, 42–46.

[68] P. N. Atterberry, T. J. Roark, S. Y. Severt, M. L. Schiller, J. M. Antos, A. R. Murphy, *Biomacromolecules* **2015**, *16*, 1582–1589.

[69] G. Y. Chen, Z. Li, J. N. Duarte, A. Esteban, R. W. Cheloha, C. S. Theile, G. R. Fink, H. L. Ploegh, *Biosens. Bioelectron.* **2017**, *89*, 789–794.

[70] P. M. Morrison, M. R. Balmforth, S. W. Ness, D. J. Williamson, M. D. Rugen, W. B. Turnbull, M. E. Webb, *ChemBioChem* **2016**, *17*, 753–758.

[71] S. O. Crowe, G. H. Pham, J. C. Ziegler, K. K. Deol, R. G. Guenette, Y. Ge, E. R. Strieter, *ChemBioChem* **2016**, 1525–1531.

[72] A. I. Petrache, D. C. Machin, D. J. Williamson, M. E. Webb, P. A. Beales, *Mol. Biosyst.* **2016**, *12*, 1760–1763.

[73] H. C. Kolb, M. G. Finn, K. B. Sharpless, *Angew. Chemie - Int. Ed.* **2001**, *40*, 2004–2021.

[74] R. K. Iha, K. L. Wooley, A. M. Nystrom, D. J. Burke, M. J. Kade, C. J. Hawker, *Chem. Rev.* **2009**, *109*, 5620–5686.

[75] J. E. Hein, V. V. Fokin, *Chem. Soc. Rev.* **2010**, *39*, 1302–1315.

[76] E. Lallana, R. Riguera, E. Fernandez-Megia, *Angew. Chemie - Int. Ed.* **2011**, *50*, 8794–8804.

[77] J. C. M. Van Hest, F. L. Van Delft, *ChemBioChem* **2011**, *12*, 1309–1312.

[78] K. Gupta, S. Singh, K. Gupta, N. Khan, D. Sehgal, V. Haridas, R. P. Roy, *ChemBioChem* **2012**, *13*, 2489–2494.

[79] L. Wang, R. Jiang, L. Wang, Y. Liu, X. L. Sun, *Bioorg. Chem.* **2016**, *65*, 159–166.

[80] M. D. Witte, J. J. Cragnolini, S. K. Dougan, N. C. Yoder, M. W. Popp, H. L. Ploegh, *Proc. Natl. Acad. Sci. U. S. A.* **2012**, *109*, 11993–11998.

[81] M. D. Witte, C. S. Theile, T. Wu, C. P. Guimaraes, A. E. M. Blom, H. L. Ploegh, *Nat. Protoc.* **2013**, *8*, 1808–1819.

[82] R. Gui, H. Jin, H. Guo, Z. Wang, *Biosens. Bioelectron.* **2018**, *100*, 56–70.

[83] K. Alt, B. M. Paterson, E. Westein, S. E. Rudd, S. S. Poniger, S. Jagdale, K. Ardipradja, T. U. Connell, G. Y. Krippner, A. K. N. Nair, et al., *Angew. Chemie - Int. Ed.* **2015**, *54*, 7515–7519.

[84] Z. Li, C. S. Theile, G. Y. Chen, A. M. Bilate, J. N. Duarte, A. M. Avalos, T. Fang, R. Barberena, S. Sato, H. L. Ploegh, *Angew. Chemie - Int. Ed.* **2015**, *54*, 11706–11710.

[85] B. M. Paterson, K. Alt, C. M. Jeffery, R. I. Price, S. Jagdale, S. Rigby, C. C. Williams, K. Peter, C. E. Hagemeyer, P. S. Donnelly, *Angew. Chemie - Int. Ed.* **2014**, *53*, 6115–6119.

[86] S. Massa, N. Vikani, C. Betti, S. Ballet, S. Vanderhaegen, J. Steyaert, B. Descamps, C. Vanhove, A. Bunschoten, F. W. B. van Leeuwen, et al., *Contrast Media Mol. Imaging* **2016**, *11*, 328–339.

[87] M. Rashidian, L. Wang, J. G. Edens, J. T. Jacobsen, I. Hossain, Q. Wang, G. D. Victora, N. Vasdev, H. Ploegh, S. H. Liang, *Angew. Chemie - Int. Ed.* **2016**, *55*, 528–533.

[88] R. R. Beerli, T. Hell, A. S. Merkel, U. Grawunder, *PLoS One* **2015**, *10*, 1–17.

[89] N. Stefan, R. Gébleux, L. Waldmeier, T. Hell, M. Escher, F. I. Wolter, U. Grawunder, R. R. Beerli, *Mol. Cancer Ther.* **2017**, *16*, 879–892.

[90] T. Fang, J. N. Duarte, J. Ling, Z. Li, J. S. Guzman, H. L. Ploegh, *Angew. Chemie - Int. Ed.* **2016**, *55*, 2416–2420.

[91] S. A. M. Van Lith, S. M. J. Van Duijnhoven, A. C. Navis, W. P. J. Leenders, E. Dolk, J. W. H. Wennink, C. F. Van Nostrum, J. C. M. Van Hest, *Bioconjug. Chem.* **2017**, *28*, 539–548.

[92] S. C. H. A. van der Steen, R. Raavé, S. Langerak, L. van Houdt, S. M. J. van Duijnhoven, S. A. M. van Lith, L. F. A. G. Massuger, W. F. Daamen, W. P. Leenders, T. H. van Kuppevelt, *Eur. J. Pharm. Biopharm.* **2017**, *113*, 229–239.

[93] L. Pan, W. Zhao, J. Lai, D. Ding, Q. Zhang, X. Yang, M. Huang, S. Jin, Y. Xu, S. Zeng *et al.*, *Small* **2017**, *13*, 1–12.

[94] Y. Xu, S. Jin, W. Zhao, W. Liu, D. Ding, J. Zhou, S. Chen, *Int. J. Mol. Sci.* **2017**, *18,* 2284.

[95] G. T. Hess, C. P. Guimaraes, E. Spooner, H. L. Ploegh, A. M. Belcher, *ACS Synth. Biol.* **2013**, *2*, 490–496.

[96] J. E. Glasgow, M. L. Salit, J. R. Cochran, *J. Am. Chem. Soc.* **2016**, *138*, 7496–7499.

[97] R. M. Broyer, G. N. Grover, H. D. Maynard, *Chem. Commun. (Camb).* **2011**, *47*, 2212–2226.

[98] L. A. Canalle, D. W. P. M. Löwik, J. C. M. van Hest, *Chem. Soc. Rev.* **2010**, *39*, 329–353.

[99] U. Glebe, B. Santos de Miranda, P. van Rijn, A. Böker, in *Bio-Synthetic Hybrid Materials and Bionanoparticles: A Biological Chemical Approach Towards Material Science*, RSC Smart Materials No. 16, **2015**, 1–29.

[100] E. M. Pelegri-Oday, E. W. Lin, H. D. Maynard, *J. Am. Chem. Soc.* **2014**, *136*, 14323–14332.

[101] Y. Qi, A. Chilkoti, *Polym. Chem.* **2014**, *5*, 266.

[102] P. van Rijn, A. Böker, *J. Mater. Chem.* **2011**, *21*, 16735.

[103] W. Zhao, F. Liu, Y. Chen, J. Bai, W. Gao, *Polym. (United Kingdom)* **2015**, *66*, A1–A10.

[104] D. Bontempo, H. D. Maynard, *J. Am. Chem. Soc.* **2005**, *127*, 6508–6509.

[105] K. L. Heredia, D. Bontempo, T. Ly, J. T. Byers, S. Halstenberg, H. D. Maynard, *J. Am. Chem. Soc.* **2005**, *127*, 16955–16960.

[106] Q. Zhang, Z. Li, P. Wilson, D. M. Haddleton, *Chem. Commun.* **2013**, *49*, 6608–6610.

[107] B. S. Sumerlin, *ACS Macro Lett.* **2012**, *1*, 141–145.

[108] B. Zhao, J. Deng, J. Deng, *ACS Macro Lett.* **2017**, *6*, 6–10.

[109] A. Simakova, S. E. Averick, D. Konkolewicz, K. Matyjaszewski, *Macromolecules* **2012**, *45*, 6371–6379.

[110] J. D. Wallat, K. A. Rose, J. K. Pokorski, *Polym. Chem.* **2014**, *5*, 1545–1558.

[111] B. Jung, P. Theato, *Adv. Polym. Sci.* **2012**, 1–34.

[112] S. Moelbert, E. Emberly, C. Tang, *Protein Sci.* **2004**, *13*, 752–62.

[113] R. M. Broyer, G. M. Quaker, H. D. Maynard, *J. Am. Chem. Soc.* **2008**, *130*, 1041–1047.

[114] Y. Qi, M. Amiram, W. Gao, D. G. McCafferty, A. Chilkoti, *Macromol. Rapid Commun.* **2013**, *34*, 1256–1260.

[115] Y. Pang, J. Liu, Y. Qi, X. Li, A. Chilkoti, *Angew. Chemie - Int. Ed.* **2016**, *55*, 10296–10300.

[116] J. Hu, G. Wang, W. Zhao, X. Liu, L. Zhang, W. Gao, *Biomaterials* **2016**, *96*, 84–92.

[117] M. W. Popp, S. K. Dougan, T.-Y. Chuang, E. Spooner, H. L. Ploegh, *Proc. Natl. Acad. Sci. U. S. A.* **2011**, *108*, 3169–3174.

[118] Z. Qu, V. Krishnamurthy, C. A. Haller, B. M. Dorr, U. M. Marzec, S. Hurst, M. T. Hinds, S. R. Hanson, D. R. Liu, E. L. Chaikof, *Adv. Healthc. Mater.* **2014**, *3*, 30–35.

[119] B. M. Dorr, H. O. Ham, C. An, E. L. Chaikof, D. R. Liu, *Proc. Natl. Acad. Sci. U. S. A.*

2014, *111*, 13343–13348.

[120] Y. Hou, J. Yuan, Y. Zhou, J. Yu, H. Lu, *J. Am. Chem. Soc.* **2016**, *138*, 10995–11000.

[121] E. Steen Redeker, D. T. Ta, D. Cortens, B. Billen, W. Guedens, P. Adriaensens, *Bioconjug. Chem.* **2013**, *24*, 1761–1777.

[122] F. Clow, J. D. Fraser, T. Proft, *Biotechnol. Lett.* **2008**, *30*, 1603–1607.

[123] R. Jiang, J. Weingart, H. Zhang, Y. Ma, X. L. Sun, *Bioconjug. Chem.* **2012**, *23*, 643–649.

[124] A. Sinisi, M. W.-L. Popp, J. M. Antos, W. Pansegrau, S. Savino, M. Nissum, R. Rappuoli, H. L. Ploegh, L. Buti, *Bioconjug. Chem.* **2012**, *23*, 1119–1126.

[125] C. Uth, S. Zielonka, S. Hörner, N. Rasche, A. Plog, H. Orelma, O. Avrutina, K. Zhang, H. Kolmar, *Angew. Chemie - Int. Ed.* **2014**, *53*, 12618–12623.

[126] R. K. Le, M. Raeeszadeh-Sarmazdeh, E. T. Boder, P. D. Frymier, *Langmuir* **2015**, *31*, 1180–1188.

[127] M. Raeeszadeh-Sarmazdeh, R. Parthasarathy, E. T. Boder, *Colloids Surfaces B Biointerfaces* **2015**, *128*, 457–463.

[128] M. Raeeszadeh-Sarmazdeh, R. Parthasarathy, E. T. Boder, *Biotechnol. Prog.* **2017**, *33*, 824–831.

[129] H. O. Ham, Z. Qu, C. A. Haller, B. M. Dorr, E. Dai, W. Kim, D. R. Liu, E. L. Chaikof, *Nat. Commun.* **2016**, *7*, 11140.

[130] S. Srinivasan, J. P. Hazra, G. S. Singaraju, D. Deb, S. Rakshit, *Anal. Biochem.* **2017**, *535*, 35–42.

[131] L. Chan, H. F. Cross, J. K. She, G. Cavalli, H. F. P. Martins, C. Neylon, *PLoS One* **2007**, *2*, 1–5.

[132] T. Ito, R. Sadamoto, K. Naruchi, H. Togame, H. Takemoto, H. Kondo, S. I. Nishimura, *Biochemistry* **2010**, *49*, 2604–2614.

[133] S. Wu, T. Proft, *Biotechnol. Lett.* **2010**, *32*, 1713–1718.

[134] T. Matsumoto, R. Takase, T. Tanaka, H. Fukuda, A. Kondo, *Biotechnol. J.* **2012**, *7*, 642–648.

[135] H. T. Ta, S. Prabhu, E. Leitner, F. Jia, D. Von Elverfeldt, K. E. Jackson, T. Heidt, A. K. N. Nair, H. Pearce, C. Von Zur Muhlen, et al., *Circ. Res.* **2011**, *109*, 365–373.

[136] M. K. M. Leung, C. E. Hagemeyer, A. P. R. Johnston, C. Gonzales, M. M. J. Kamphuis, K. Ardipradja, G. K. Such, K. Peter, F. Caruso, *Angew. Chemie - Int. Ed.* **2012**, *51*, 7132–7136.

[137] C. E. Hagemeyer, K. Alt, A. P. R. Johnston, G. K. Such, H. T. Ta, M. K. M. Leung, S. Prabhu, X. Wang, F. Caruso, K. Peter, *Nat. Protoc.* **2014**, *10*, 90–105.

[138] W. Kim, C. Haller, E. Dai, X. Wang, C. E. Hagemeyer, D. R. Liu, K. Peter, E. L. Chaikof, *Angew. Chemie - Int. Ed.* **2015**, *54*, 1461–1465.

[139] T. Heck, P. H. Pham, F. Hammes, L. Thöny-Meyer, M. Richter, *Bioconjug. Chem.* **2014**, *25*, 1492–1500.

[140] Y. Hata, T. Matsumoto, T. Tanaka, A. Kondo, *Macromol. Biosci.* **2015**, *15*, 1375–1380.

[141] S. M. Qafari, G. Ahmadian, M. Mohammadi, *RSC Adv.* **2017**, *7*, 56006–56015.

[142] E. Cambria, K. Renggli, C. C. Ahrens, C. D. Cook, C. Kroll, A. T. Krueger, B. Imperiali, L. G. Griffith, *Biomacromolecules* **2015**, *16*, 2316–2326.

[143] E. Gau, D. M. Mate, Z. Zou, A. Oppermann, A. Töpel, F. Jakob, D. Wöll, U. Schwaneberg, A. Pich, *Biomacromolecules* **2017**, *18*, 2789–2798.

[144] M. R. Arkenberg, C.-C. Lin, *Biomater. Sci.* **2017**, *5*, 2231–2240.

[145] P. G. Katsoyannis, J. Z. Ginos, *Annu. Rev. Biochem.* **1969**, *38*, 881–912.

[146] R. B. Merrifield, *J. Am. Chem. Soc.* **1963**, *85*, 2149–2154.

[147] G. Odian, *Principles of Polymerization*, **2004**.

[148] L. Wu, U. Glebe, A. Böker, *Polym. Chem.* **2015**, *6*, 5143–5184.

[149] C. Barner-Kowollik, *Handbook of RAFT Polymerization*, **2008**.

[150] H. Willcock, R. K. O'Reilly, *Polym. Chem.* **2010**, *1*, 149–157.

3 Sortase-catalyzed linkage of nanoparticles and polymers

3.1 Introduction

The aim of this chapter is to prove the concept, that SrtA can catalyze the linkage between nanoparticles and polymers. Generally speaking, nanoparticles and polymers are important chemical units. Nowadays most drug release or biomedical materials are based on polymers and / or nanoparticles[1,2]. Silica nanoparticles are a classical template and often used as substrate for many kinds of bio-conjugations[3]. However, bare nanoparticles usually tend to aggregate, are neither dispersable in aqueous media nor biocompatible; therefore conjugation of polymers around NPs is the most preferred method to enhance stability and dispersability[4]. Poly(ethyleneglycol) (PEG) is the most often used polymer for conjugations due to its high biocompatibility[5]. In this study, the two substrates, silica nanoparticle and PEG, were designed in the manner that the nanoparticles are equipped with the SrtA recognition motif, namely LPETG (C-terminus is free for SrtA reaction), and the polymers with the nucleophilic sequence, GGGGG (N-terminus is free for SrtA reaction), respectively. The nanoparticle-peptide hybrid and peptide-polymer hybrid were then linked with each other under the catalysis of SrtA (Scheme 3.1).

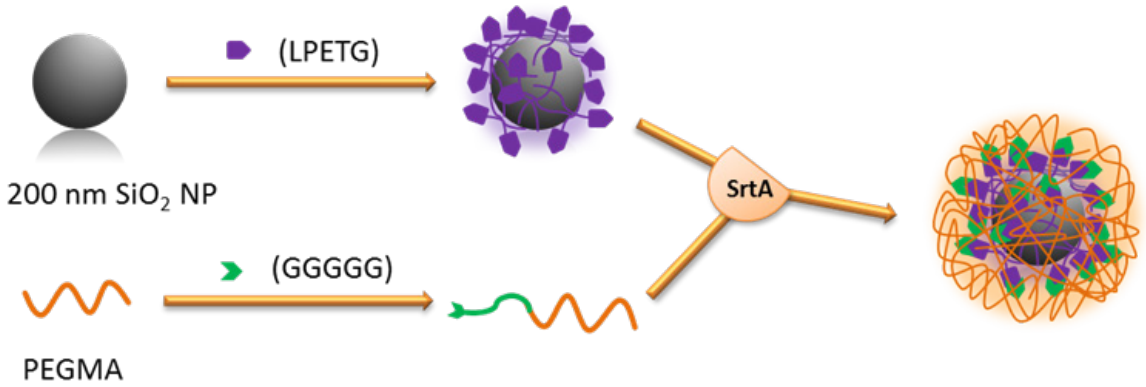

Scheme 3.1 Image illustrating Srt-catalyzed linkage between silica NPs and PEG. Each building block is functionalized with a peptide motif needed for SrtA catalysis.

First, silica nanoparticles were synthesized via sol-gel method and functionalized with 3-(trimethoxysilyl) propyl methacrylate (MPS), to obtain a C=C coating around the particles. A cysteine terminated peptide which has LPETG recognition sequence at its C-terminus was chosen to modify the functionalized silica NPs via thiol-ene reaction between C=C and –SH of

the cysteine residue. Next, a commercially available derivative of PEG, poly(ethyleneglycol) methyl ether acrylate (PEGMA) which possesses a C=C end group, was chosen to react with the peptide which also contains a cysteine and the other SrtA-reaction-required motif GGGGG as terminals. Finally, the two modified building blocks were linked via SrtA catalysis.

Before being applied for the modification of the two peptides, they were replaced by *N*-acetyl-L-cysteine (NAC) as a model cysteine compound to explore the reaction conditions for the modifications of silica NPs and PEG due to the high costs of the peptides.

For the characterization of NP and polymer starting materials and its reaction products, Field Emission Scanning Electron Microscopy (FESEM), Dynamic Light Scattering (DLS; Zetasizer), Transmission Electron Microscopy (TEM), ultraviolet/visible (UV/Vis) and Raman spectroscopy as well as matrix-assisted laser desorption ionization-time of flight (MALDI-ToF) mass spectrometry were used.

3.2 Preparation and characterization methods

3.2.1 Materials

Chemicals: Tetraethyl orthosilicate (TEOS), ammonia solution 28-30%, poly(ethyleneglycol) methyl ether acrylate (PEGMA), 4,4´-azobis(4-cyanovaleric acid) (ABCVA), triethylamine, 3-(trimethoxysilyl) propyl methacrylate (MPS), triethylamine and *N*-acetyl-L-cysteine were purchased from Sigma-Aldrich. SrtA was provided from our cooperation partner, Dr. Diana Mate in Prof. Schwaneberg's group at RWTH Aachen. Peptide 1 – peptide 4 were bought from Biotrend. Millipore pure water with an electrical resistance of 18.2 MΩ·cm was used.

3.2.2 Characterization methods

Field Emission Scanning Electron Microscopy: FESEM measurements were performed on a Hitachi S4800 Field Emission SEM operated at 1-2 kV with a 10 mA current. The samples were prepared by placing a drop on a silicon wafer. The samples were air-dried first, before being placed into the specimen holder.

Raman spectroscopy: Raman spectra were measured with a Bruker RFS 100/S instrument (Bruker, Bremen, Germany) equipped with a 1064 nm Nd:YAG laser. The laser power was between 150-1000 mW and typically 1000 scans with spectral resolution of 4 cm^{-1} used. The solid samples were measured in alumina pans under 180° reflection geometry.

MALDI-ToF mass spectrometry: Spectra were acquired using a 337 nm laser Bruker microflex MALDI-ToF mass spectrometer (Bruker, Bremen, Germany) with pulsed ion extraction. The masses were determined in positive ion linear mode. The sample solutions were applied on a ground steel target using the dried droplet technique. Mass calibration was performed with external calibration. Polymer samples were prepared as follows: α-cyano-4-hydroxycinnamic acid (CCA) was used as matrix substance in a 10 mg/ml solution in Millipore water:acetonitrile 7:3 with 0.1 % trifluoroacetic acid. Sodium trifluoroacetate was used as salt in 0.1 mol/l solution in the same solvent mixture. Sample (5 mg/ml), matrix and salt solutions were mixed in 5:20:1 ratio and 2 µl of the mixture applied on the target. The SrtA sample was prepared as follows: Super-DHB, a 9:1 mixture of 2,5-dihydroxybenzoic acid (DHB) and 2-hydroxy-5-methoxybenzoic acid, was used as matrix substance in a 50 mg/ml solution in Millipore water:acetonitrile 1:1 with 0.1 % trifluoroacetic acid. The sample was applied on the target using $ZipTip_{C18}$ pipette tips (Millipore, Darmstadt, Germany).

Scanning Transmission Electron Microscopy (STEM): STEM images were obtained through Hitachi UHR FE-SEM SU9000 electron microscopy. The sample was dropped on a 0.5 cm × 1.0 cm silicon wafer and spincoated.

Nuclear magnetic resonance (NMR) spectroscopy: ^{1}H-NMR spectra were recorded on an INOVA 500 spectrometer from Varian Inc. at 500 MHz. $CDCl_3$ and D_2O were used as solvents. Measurements were performed at room temperature. The signal of non-deuterated solvent was used as internal standard.

Dynamic Light Scattering: DLS measurements were performed on a Malvern (Worcestershire, England) Zetasizer Nano ZS device at 20 °C. Assuming Mark-Houwink parameters to be A = 0.428 and B = $7.67 \cdot 10^{-5}$, 173° backscattering was analyzed with equilibration time of 120 s. Multi-parameter analysis was performed on an average of three runs for every data point.

Transmission Electron Microscopy: TEM was performed on a Philips CM-200 device operating at 120 kV. The samples were deposited on nitrogen glow discharged carbon film coated grids, which were subsequently washed 3-times with Millipore water.

UV/Vis spectroscopy: The measurements were performed using SPECORD 210 UV-Vis spectrometer from Analytik Jena.

3.2.3 Preparation

Preparation of SiO_2 nanoparticles and surface modification to obtain a C=C coating[6]:

For the preparation of 200 nm NPs, molar concentrations of Millipore water, NH_3 (28–30% aqueous solution) and tetraethyl orthosilicate (TEOS) of 5, 0.2, and 0.2 mol/L, respectively, were used. First, a mixture of ethanol, Millipore water, and ammonia was prepared to achieve the mentioned concentrations. After 30 min equilibration, TEOS was added. The experiments were conducted with 50 mL ethanol at room temperature for 24 h. For surface modification, 3-(trimethoxysilyl) propyl methacrylate (MPS) was directly added to the dispersion at room temperature. After 12 h stirring, the mixture was refluxed for 1 h to ensure the covalent bonding. The silica nanoparticles were then washed with ethanol by centrifugation and ultrasonication several times, until the supernatant did not show UV absorption from MPS anymore.

Modification of silica NPs with NAC or peptide 1: Functionalization of NPs with peptides. 200 nm NPs were reacted with peptide 1 (H-Cys-Ile-Arg-His-Met-Gly-Phe-Pro-Leu-Arg-Glu-Phe-Leu-Pro-Glu-Thr-Gly-OH). C=C-functionalized NPs and peptide were mixed in 1.1:1 molar ratio (peptide: C=C group) with 3 mol % 4,4′-azobis(4-cyanovaleric acid) (ABCVA) in water. The mixture was stirred in N_2 atmosphere for 24 h under exposure to UV light (365 nm). Afterwards, the NPs were washed with Millipore water by centrifugation and ultrasonication.

Modification of PEGMA with NAC, peptide 2 and 3: PEGMA was reacted with peptide 2 (H-Gly-Gly-Gly-Gly-Gly-Phe-Glu-Arg-Leu-Pro-Trp-Phe-Trp-Gly-Met-His-Arg-Ile-Cys-OH) or peptide 3 (H-Gly-Gly-Gly-Gly-Gly-Trp-Phe-Trp-Cys-OH). Polymer and peptide were mixed in equivalence ratio of 1.1:1 in PBS buffer (pH = 7.4) and stirred under N_2 atmosphere for 24 h at RT. The obtained products were dialyzed 2-times against Millipore water using dialysis membrane with a MWCO of 1 kDa for 24 h.

SrtA reaction: The SrtA reaction between functionalized NPs and polymer was conducted by the following procedure. A typical reaction mixture of 100 µL consisted of 30 µL aqueous solution of the two substrates with approximately 50-times excess of GGG substrate with respect to LPETG substrate, 20 µL SrtA (7.95 mg/mL), 20 µL 250 mM Tris-HCl and 750 mM NaCl (pH 7.5), 20 µL 25 mM $CaCl_2$, 10 µL Millipore water, and was conducted at 37 °C in thermomixer for 24 h. NP–polymer samples were washed 3-times with Millipore water by centrifugation and ultrasonication.

3.3 Synthesis and functionalization of NP with C=C coating

SiO_2 nanoparticles were synthesized by sol-gel method, and further functionalized by 3-(trimethoxysilyl) propyl methacrylate which provides a C=C coating on the surface of the nanoparticles[7]. This functionalization was chosen to be able to link the sulfhydryl group of the amino acid cysteine to the NPs in a click chemistry step.

3.3.1 Synthesis of SiO_2 NPs

Hydrolysis reaction of TEOS:

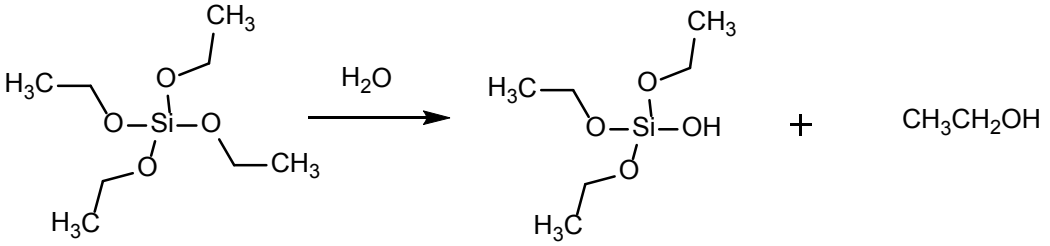

Condensation reaction:

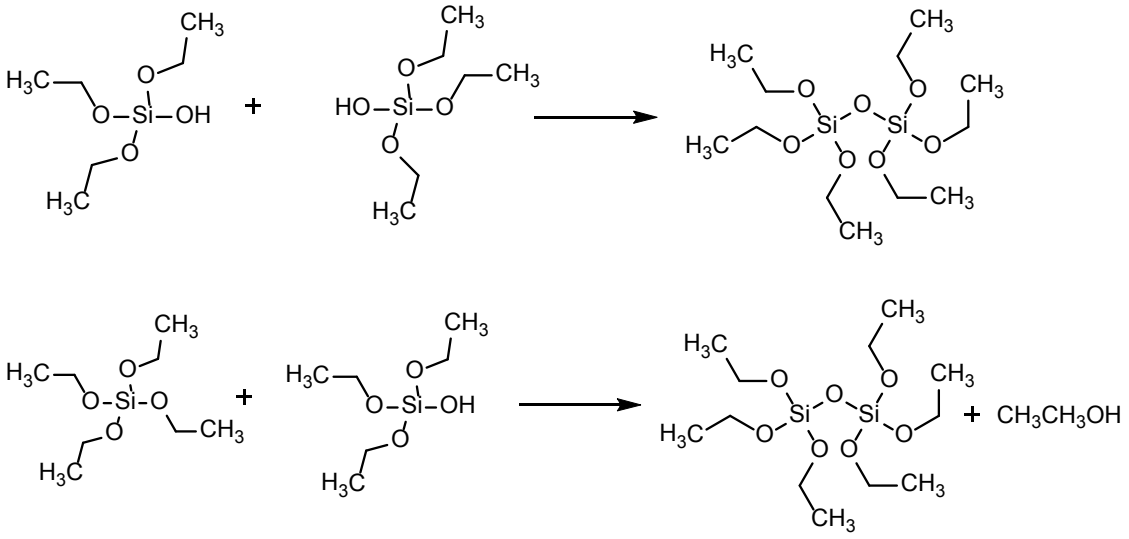

Catalyzed by ammonia, silica NPs were synthesized in ethanol medium through the hydrolysis reaction and condensation reaction of TEOS. Through the hydrolysis reaction of TEOS (reaction 1), cores in the range of several nanometers are formed, which grow and become bigger NPs due to the high surface energy[8]. The final size of the NPs is depending on the concentrations of TEOS and water in the system. They were chosen in order to synthesize NPs of around 200 nm in diameter. FESEM images (Fig 3.1) and Zetasizer DLS and zeta potential analysis (Fig 3.2) clearly show that silica NPs around 200 nm were successfully synthesized.

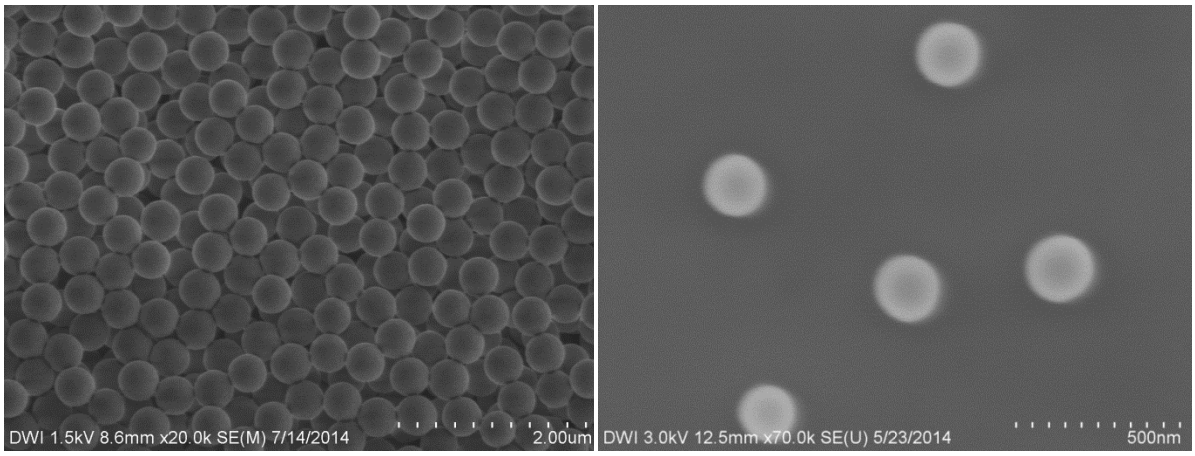

Fig 3.1 FESEM pictures of SiO_2 NPs with diameter around 200 nm.

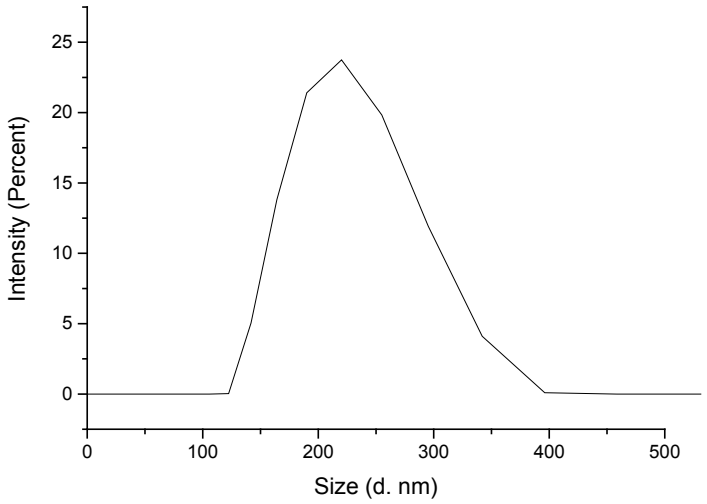

Fig 3.2 Zetasizer size (diameter: 213.4 nm ± 49.8 nm) distribution of SiO_2 NPs with zeta potential (-45.7 nm ± 7.0 mV).

3.3.2 Functionalization of NPs with MPS

To synthesize silica NPs with C=C coating on the surface, they were functionalized with MPS (Scheme 3.2). After silica NPs were formed, in the presence of ammonia, MPS was directly added to the system. The NPs were stirred at room temperature followed by reflux, which ensures the covalent functionalization. Since MPS has a strong UV absorption band between 200 nm and 400 nm, the functionalized SiO_2 NPs were washed with ethanol for several times, until no UV absorption band from the supernatant was detectable between 200 nm and 400 nm. Raman spectroscopy and Zetasizer measurements can be used to analyze the successful functionalization.

The UV spectra in Fig 3.3 show that there was no UV detectable MPS in the supernatant left. No obvious difference was observable between 5-times washing (Fig 3.3, red) and 7-times washing (Fig 3.3 blue), which implies that excess MPS was completely washed away. The Raman spectrum of the functionalized nanoparticles shows obviously the band of the unsaturated C–H stretching vibration at 3110 cm^{-1}, the C=C vibration at 1640 cm^{-1}, and the stretching vibration of C=O at 1720 cm^{-1} (Fig 3.4). These vibrations can only be caused by attached MPS. Hence, the successful functionalization could be proven by Raman spectroscopy. Raman spectroscopy was used instead of infrared (IR) *spectroscopy* due to the strong Si IR signal which overwhelms the other signals[9].

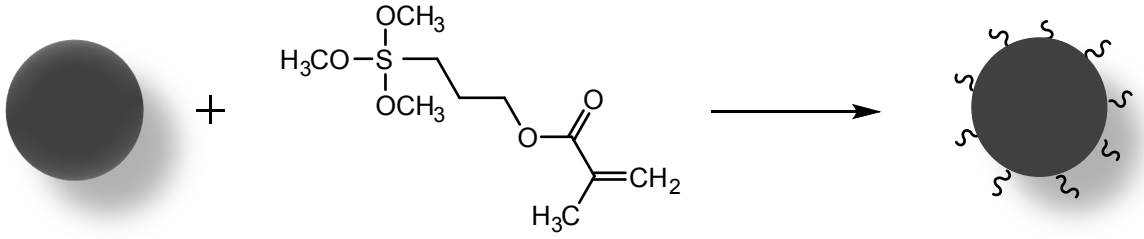

Scheme 3.2 Functionalization of SiO_2 NPs with MPS.

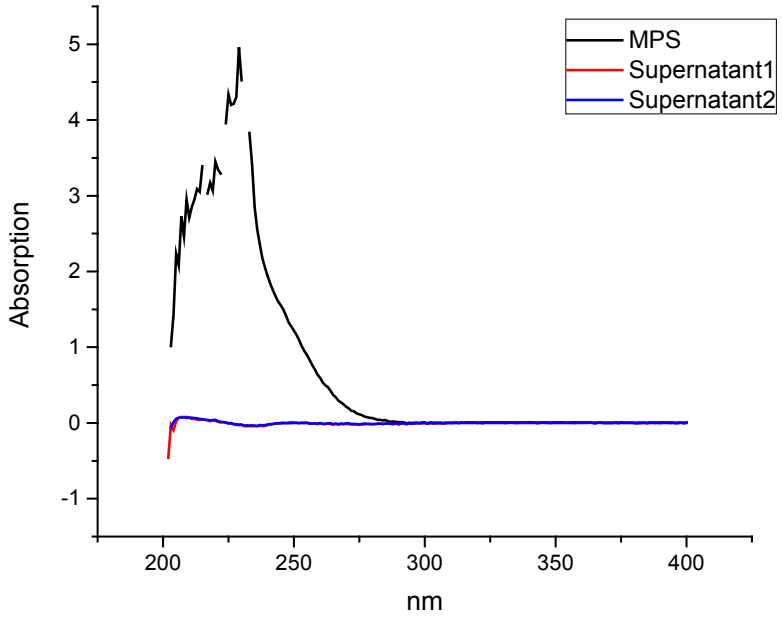

Fig 3.3 UV/Vis spectra of MPS (black) and supernatants from washing solutions after 5-times washing (red) and 7-times washing (blue).

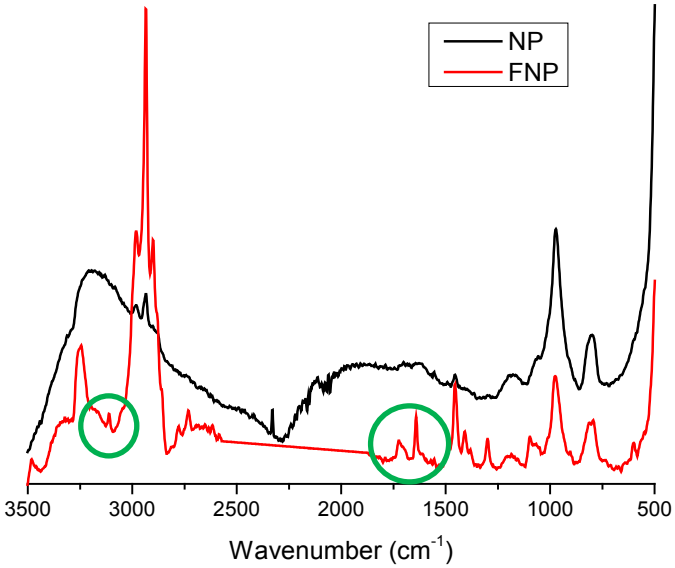

Fig 3.4 Raman spectra of unfunctionalized (black) and MPS-functionalized (red) SiO_2 nanoparticles. The green circles mark the C−H vibration from unsaturated hydrocarbon, C=C and C=O stretching vibration bands that show the successful modification with MPS.

After functionalization, the size and the zeta potential of the nanoparticles changed (comparison: Fig 3.2), but the difference is not that distinct to be a clear proof of the functionalization.

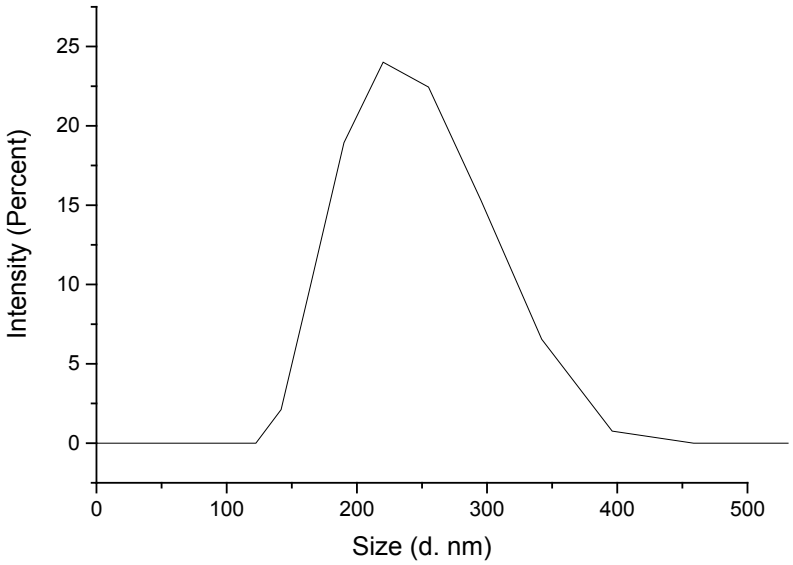

Fig 3.5 Zetasizer size (diameter: 226.0 nm ± 52.1 nm) distribution of MPS-functionalized SiO_2 nanoparticles with zeta potential (-44.9 mV ± 6.2 mV).

3.4 Modification of functionalized NPs with Peptide

A thiol-ene reaction is a possible way to covalently link a peptide which contains a cysteine as well as a sequence that can be recognized by Sortase to the NPs. As a substitute for the peptide, *N*-acetyl-L-cysteine (NAC) was used for the first test experiments due to its low cost.

3.4.1 Modification of functionalized NPs with small amino acid NAC

NAC was used as a test substance to link a sulfhydryl group to the C=C double bonds on the surface of the silica NPs (Scheme 3.3). The water-soluble photoinitiator 4,4'-azobis(4-cyanovaleric acid) was used for this thiol-ene reaction that belongs to the "click chemistry" pool[10]. The success of the reaction can be followed by Raman spectroscopy (Fig 3.6) and Zetasizer measurements (Fig 3.7).

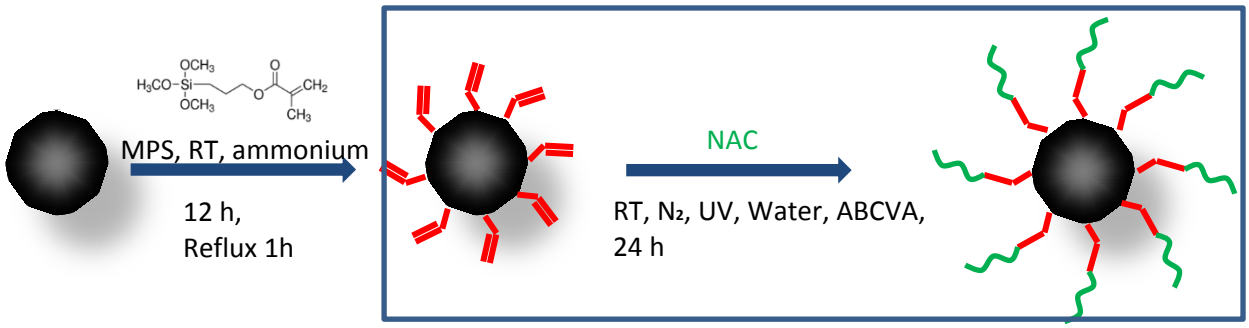

Scheme 3.3 Scheme of the thiol-ene reaction between MPS-functionalized SiO_2 NPs and NAC.

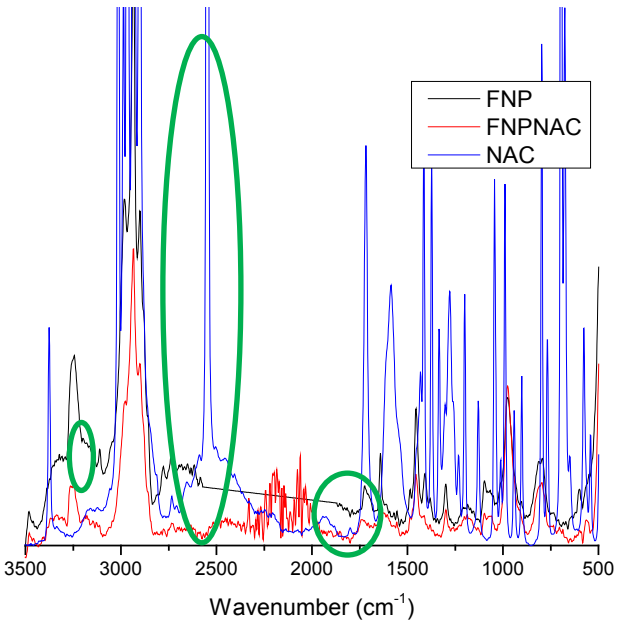

Fig 3.6 Raman spectra of MPS-functionalized NPs (black), NAC (blue) and the reaction product of both (red).

The Raman spectrum of the reaction product shows that the stretching vibration of S–H (from NAC) at 2550 cm^{-1} disappeared as well as the band of unsaturated C–H at 3110 cm^{-1} and C=C at 1650 cm^{-1} (from functionalized NPs). Instead, a wider band at 1615 cm^{-1} appeared which belongs to the amide bond in NAC.

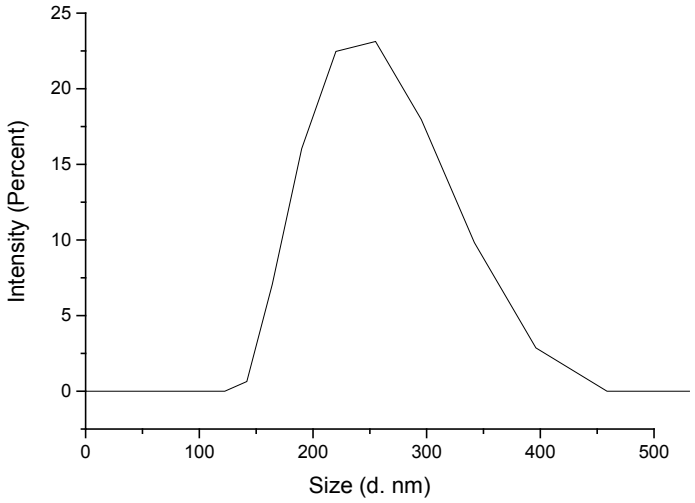

Fig 3.7 Zetasizer size (diameter: 237.7 nm ± 56.5 nm) distribution of the product modified with NAC, potential (-43.5 nm ± 6.6 mV).

The Zetasizer measurements show little difference before and after modification with NAC. Due to the high standard deviation, it is not possible to get an evidence for a successful reaction by these measurements.

3.4.2 Modification of functionalized NPs with peptide

After the exploration of the thiol-ene reaction between functionalized NPs and NAC, the reaction between NPs and peptide 1 (H-Cys-Ile-Arg-His-Met-Gly-Trp-Phe-Trp-Pro-Leu-Arg-Glu-Phe-Leu-Pro-Glu-Thr-Gly-OH) was performed with the same conditions: at room temperature, under N_2 atmosphere and UV light (245 nm), excess peptide and functionalized NPs were added, ABCVA was added as catalyst in amount of 3 wt% of the total weight from peptide and silica NPs (Scheme 3.4). Due to the negative charge on the surface of nanoparticles after the modification, a peptide chain with cysteine (N-terminal, positively charged from NH_3^+) which provides a free thiol group residue on one end and LPETG recognition sequence (C-terminal, negatively charged via COO^-) on the other end was designed. It is assumed that there is a repulsive interaction between the nanoparticle and the negatively charged C-terminus from the peptide, which creates less steric hindrance.

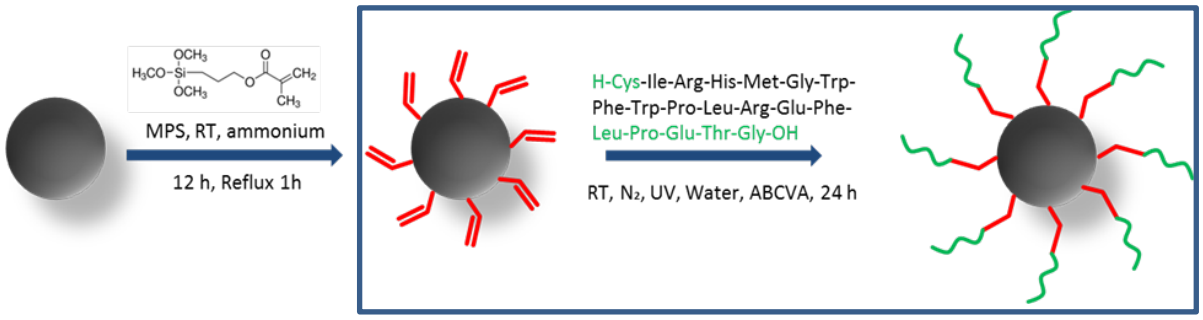

Scheme 3.4 Scheme of the thiol-ene reaction between functionalized silica NPs and peptide 1.

Calculation of the mass of functionalized NP:

From the structure of MPS (Scheme 3.2), it can be derived that for each C=C double bond, three equivalents Si-OH are linked to the surface of NP. With a surface density of Si-OH $\rho_{surface}$ of 8 µmol/m^2[6] and a density of silica NP ρ_{NP} of 1.8 g/cm^3[11], for a reaction of 1 mol (248.35 g) MPS with 3 mol Si-OH, the total nanoparticle surface should be $\frac{3\ mol}{8\ \mu mol/m^2}$. With the assumption of absolutely round particles (particle surface S = $4\pi r^2$, volume per particle $V_{NP} = 4\pi r^3/3$, r = 100 nm). From the calculation, 1 gram nanoparticle requires 11 mg MPS. A 200-times excess of MPS was used to ensure a complete reaction.

$$\frac{3\ mol}{8\ \mu mol/m^2} \times \frac{1}{4\pi r^2} \times \frac{4\pi r^3}{3} \times 1.8\ g/cm^3 = 22500\ g$$

$S_{NP} = 4\pi r^2$

$V_{NP} = 4\pi r^3/3$

r=100 nm

$\rho_{NP} = 1.8\ g/cm^3$

The synthesis of silica NPs and the surface modification with MPS have been reported by many research groups[4,7,12,13], the technique is quite mature. After the reaction, the product was washed with water and then centrifuged for 3-times. The modified SiO_2 NPs were characterized via Raman spectroscopy, DLS and confocal microscopy.

The Raman spectra show that the stretching vibration of the −SH group at 2570 cm^{-1}, the vibration of the aliphatic C−H group (from functionalized NPs) at 3110 cm^{-1} and the C=C band at 1640 cm^{-1} disappeared, while the C−H band of the aromatic groups in the peptide at 3060 cm^{-1} and the characteristic aromatic absorption band between 1500-1600 cm^{-1} appeared (Fig. 3.8). Another mentionable strong and sharp band at 1003 cm^{-1} from phenylalanine appeared

in the product spectrum. Altogether, these findings demonstrate the successful linkage of the peptide to the NPs.

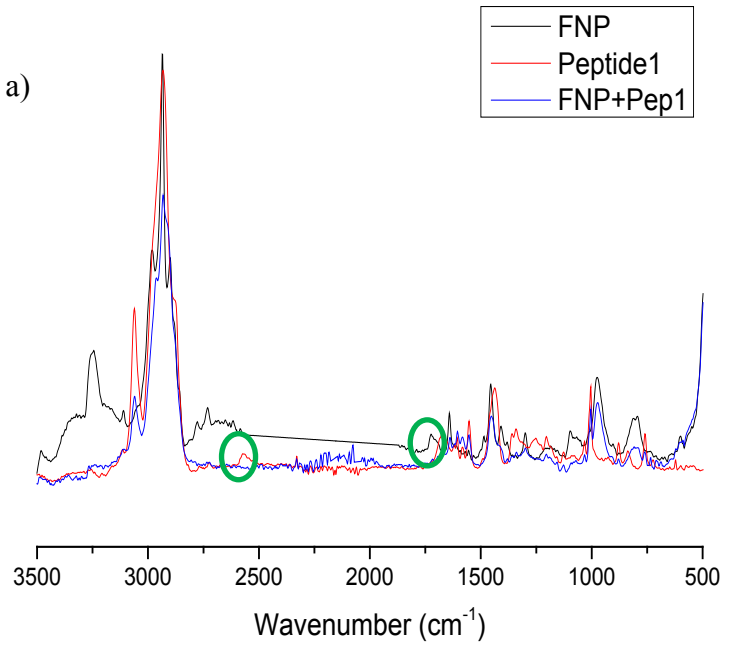

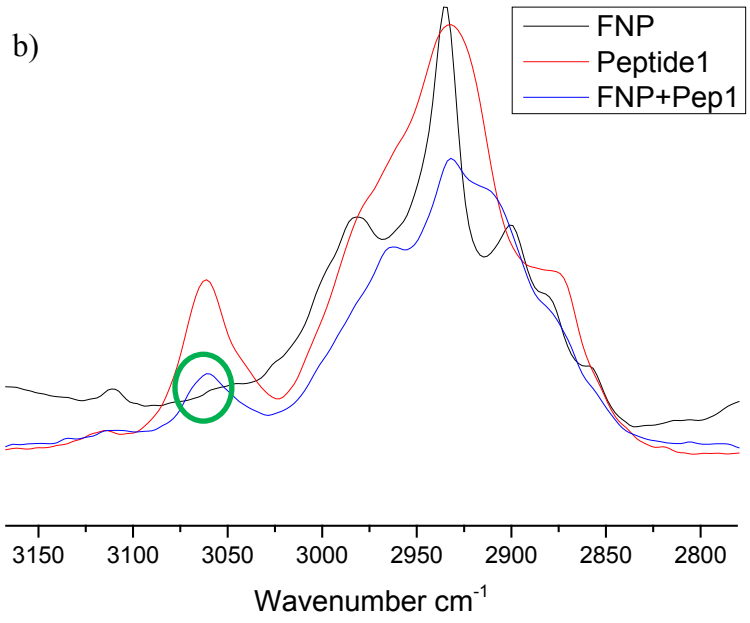

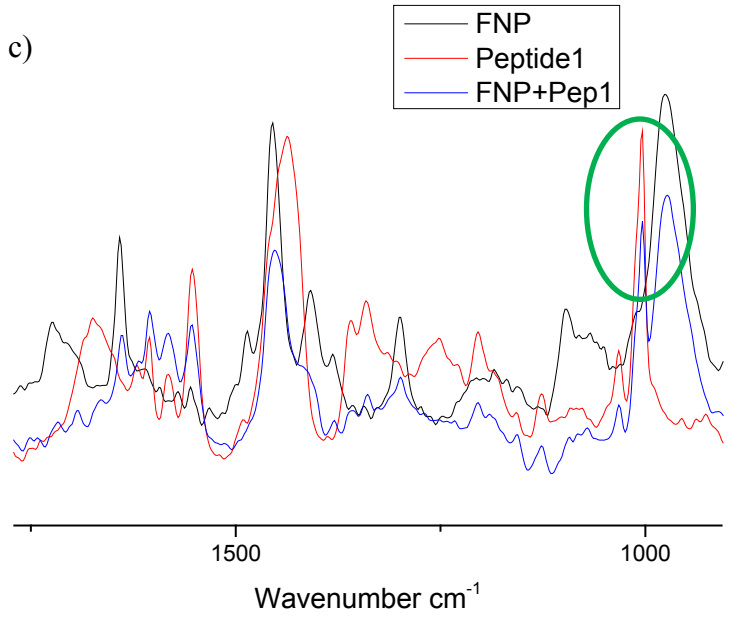

Fig 3.8 Raman spectra of functionalized NPs (black), peptide 1 (red) and the reaction product (blue).

Compared with pure SiO_2 NPs (size: 213.4 nm ± 49.8 nm , zeta potential -45.7 mV ± 7.0 mV, the diameter of NPs increased and the size distribution became broader after functionalization and modification (Fig 3.9).The change in size and zeta potential becomes especially obvious for direct comparison with unfunctionalized and MPS-functionalized NPs (Fig 3.10). However, this cannot be taken as proof for successful modification because of the high standard deviation.

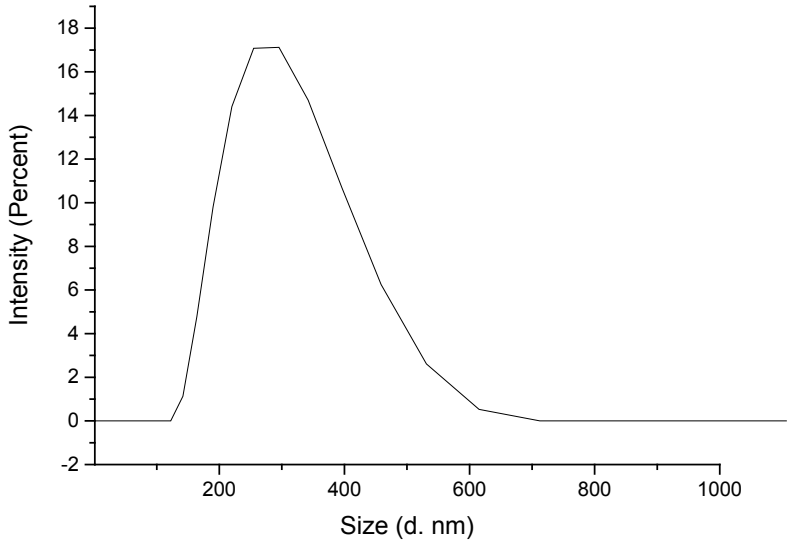

Fig 3.9 Zetasizer size (diameter: 281.1 nm ± 91.7 nm) distribution of the NP-peptide 1 conjugate with zeta potential (-35.7 nm ± 4.8 mV).

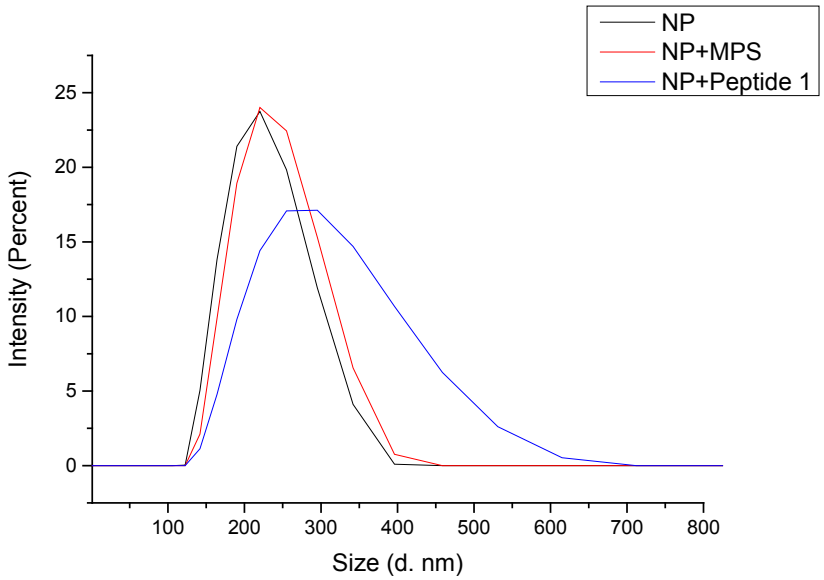

Fig 3.10 Comparison of diameter distribution of unfunctionalized NPs (green), MPS-functionalized NPs (blue) and NP-peptide1 conjugates (red).

The fluorescent amino acid Trp (tryptophan) is present two times in peptide 1. The fluorescence is not detectable for free peptides in solution by confocal microscopy. However, after the linkage of peptide and NPs, a weak fluorescence was detected demonstrating that several peptide units should be linked to most NPs, although large aggregates can be seen in the image (Fig. 3.11).

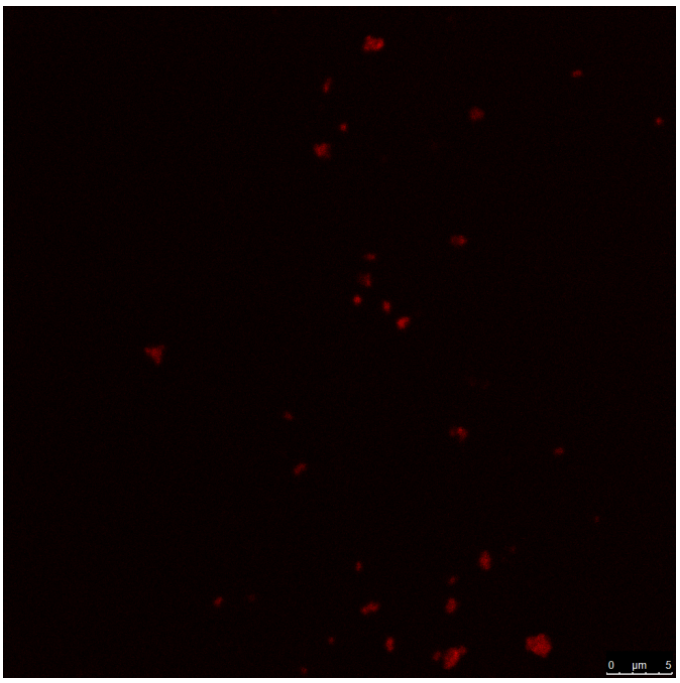

Fig 3.11 Confocal microscopy image of NPs after the linkage with peptide 1.

In summary, silica NPs were successfully modified with LPETG recognition sequence for SML. The synthesis of a corresponding building block, a polymer modified with nucleophilic peptide sequence for sortase A, will be shown in the next subchapter.

3.5 Modification of PEGMA with Peptide

To catalyze the linkage of a polymer to the NPs presented in the last subchapter by sortase, a Gly-Gly-Gly-Gly-Gly motif as the nucleophilic sequence for sortase has to be bound to a polymer. The water-soluble poly(ethylene glycol) methyl ether acrylate (PEGMA) was chosen to use the same thiol-ene chemistry to link a cysteine amino acid to the C=C end functionality of the polymer. Therefore, peptide 2 consists of one Cys at the carboxy terminus and the Gly motif at the amino terminus. Peptide 1 (NP) and 2 should be linked by sortase and hence, a polymer shell formed around the NPs. Due to the low price, NAC was used as a test compound instead of peptide 2 in the beginning to optimize the reaction conditions for the linkage of a Cys amino acid / peptide to the polymer. After the successful modification with peptide 2, a shorter peptide 3 was applied for the reaction to reduce the cost, with which the reaction was also successful.

3.5.1 Modification of PEGMA with small amino acid NAC

Two different thiol-ene reaction mechanisms were tested for the reaction between PEGMA and NAC (Scheme 3.5), namely anionic and free radical reaction mechanisms (Scheme 3.6).

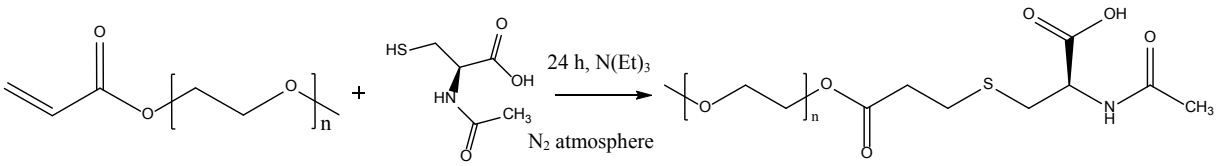

Scheme 3.5 Reaction between PEGMA and NAC.

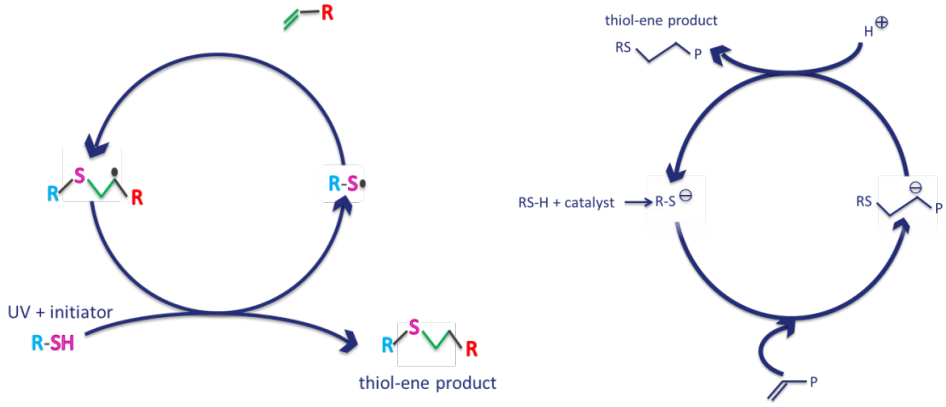

Scheme 3.6 Diagrams of free radical thiol-ene reaction mechanism (left) and anionic reaction mechanism (right). Reprinted from references [10,14].

The reaction via free radical pathway was performed in buffer (pH = 7.6) under N_2 atmosphere and UV light, ABCVA as photoinitiator, while the ionic reaction mechanism was carried out under N_2 atmosphere, triethylamine as catalyst[15–18]. The products were first dialyzed against water for 48 h in order to get rid of small molecules and then characterized via NMR and Raman spectroscopy as well as MALDI-ToF mass spectrometry.

The NMR spectra of NAC and PEGMA show that the signals of the methyl groups are located at 1.96 ppm and 3.27 ppm, respectively (Fig. 3.12). From the NMR spectra of the two products, it can be obviously seen that the desired product is formed via both mechanisms of the thiol-ene reaction (Fig 3.13). However, the yield differs for the two pathways and neither reaches a quantitative conversion. Theoretically, the integral ratio of the two terminal methyl groups from PEG and NAC should be 1:1, the anionic pathway gives the higher ratio with 1:0.71 and hence, will be used for the upcoming functionalization of PEG with a peptide sequence. The non-quantitative yield will be further discussed below with the MALDI-ToF mass analysis.

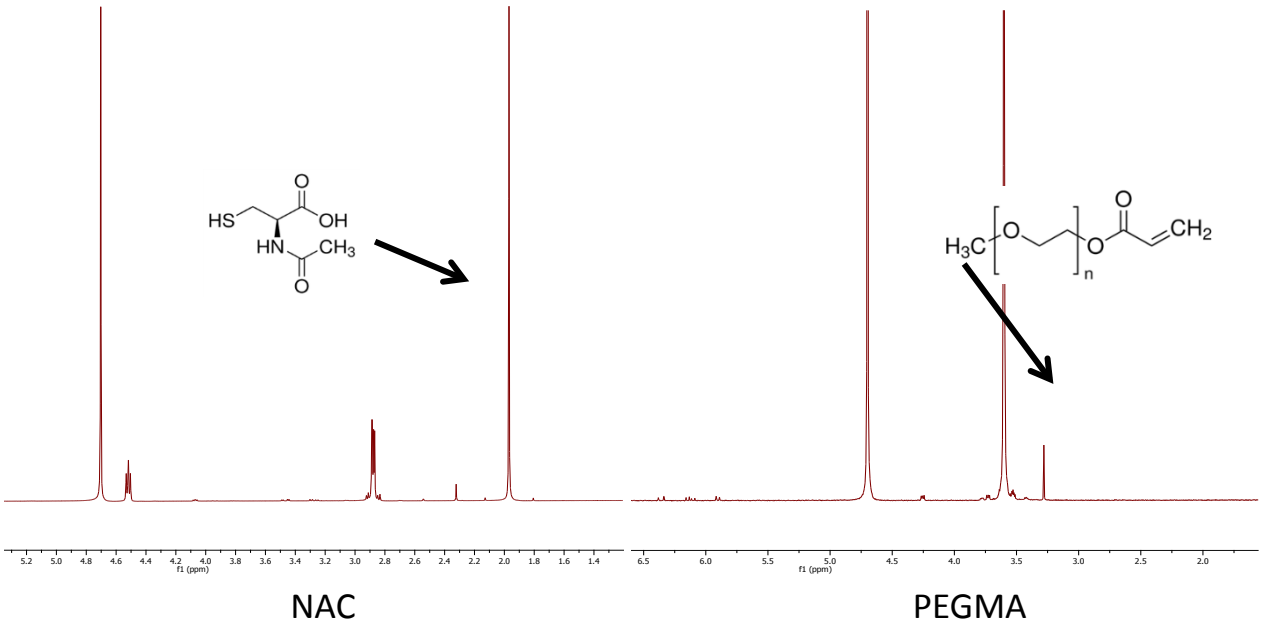

Fig 3.12 ^{1}H-NMR spectra of NAC (left) and PEGMA (right), measured in D_2O.

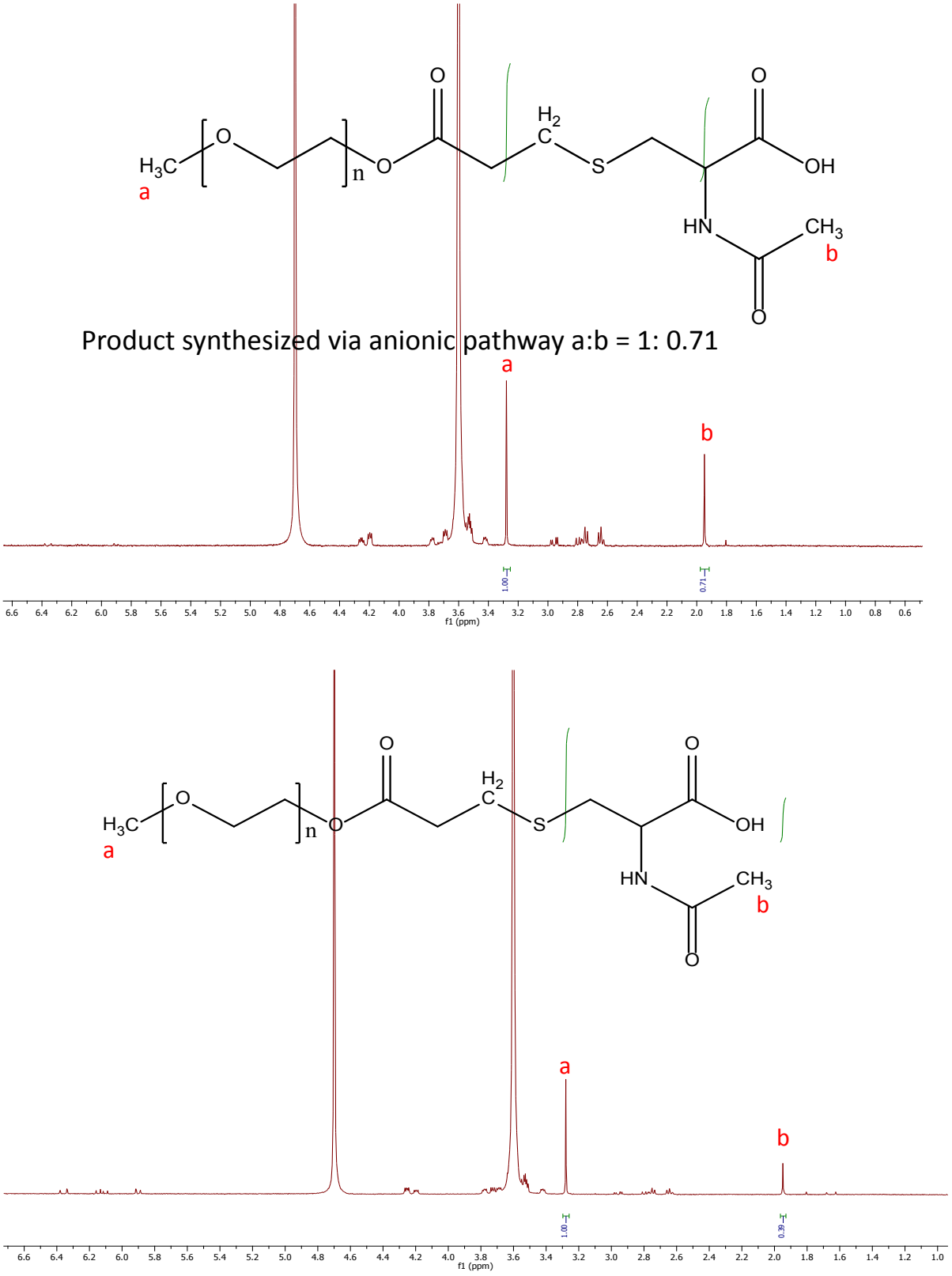

Fig 3.13 NMR spectra of PEG-NAC formed via anionic (above) and radical (below) pathway.

The NMR spectra show that the two singlets (CH_3) of the product (Fig 3.14, green) below 3.5 ppm come from the CH_3-group of the two reactors. The signal of the CH_2-group at 3.6 ppm comes from PEGMA (Fig 3.14, red). The three multiplett-signals around 6 ppm, originally from the C=C group in PEGMA, are not visible anymore in the spectrum of the product after reaction with the thiol group. Therefore, the NMR spectra demonstrate the successful modification of PEGMA.

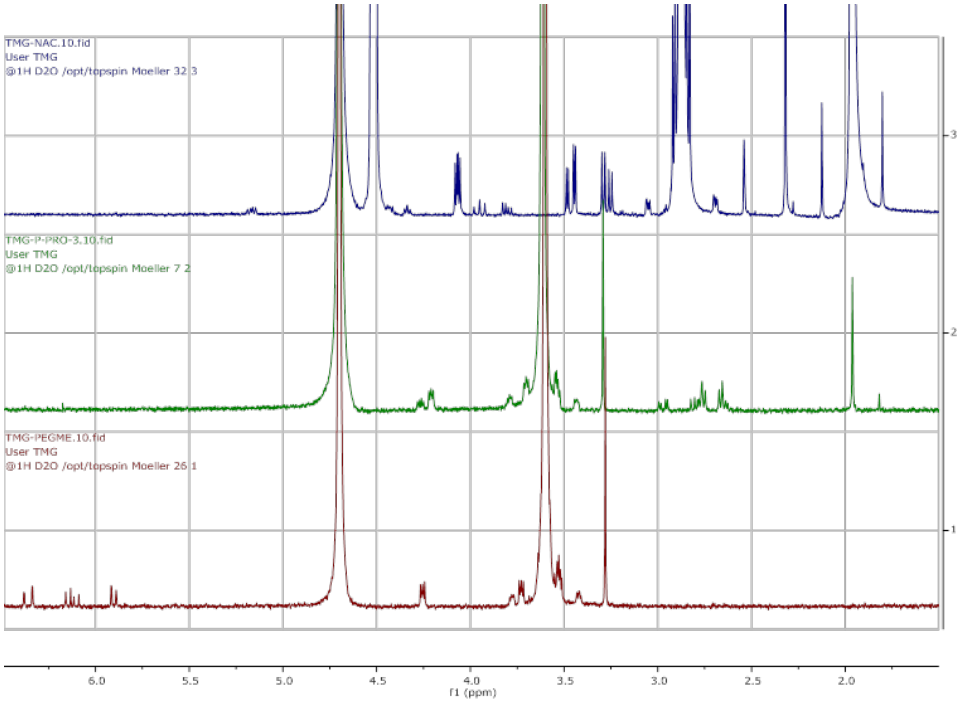

Fig 3.14 ^{1}H-NMR spectra of NAC (blue), PEGMA (red), and their respective reaction product after zooming-in (green) in one picture for comparison.

From the Raman spectra, it can be seen that the strong S−H stretching vibration band from NAC between 2500-2600 cm^{-1} was sharply decreased as well as the bending vibration band of C=C at around 1600 cm^{-1} (Fig. 3.15 and 3.16). In agreement with the NMR results, it means that, in principle, the reaction is successful via both of the mechanisms. Since the anionic way gives a higher yield according to the NMR spectra, this mechanism is exploited later for the reaction between PEGMA and peptide.

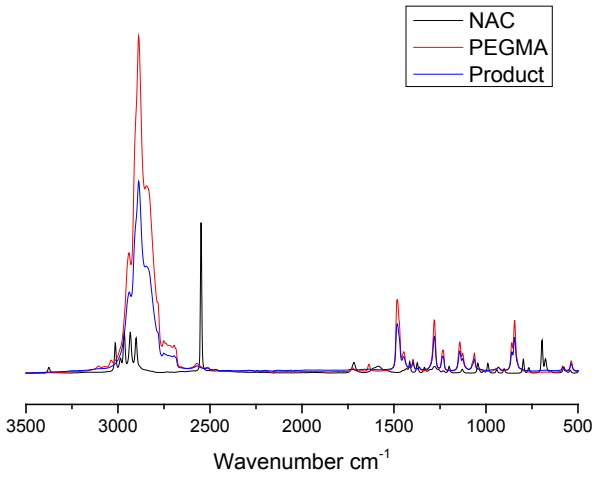

Fig 3.15 Raman spectra of NAC (black), PEGMA (red), the reaction product via anionic mechanism (blue).

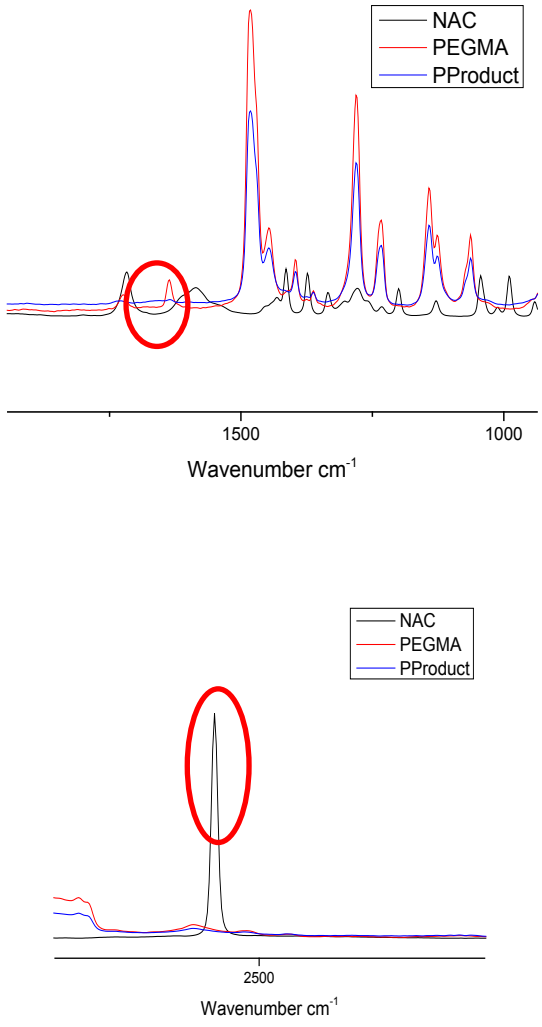

Fig 3.16 Raman spectra of NAC (black), PEGMA (red) and the reaction product anionic mechanism (blue) in overview and zoom-in.

The MALDI-ToF mass spectrum of PEGMA shows that there seem to be different PEG series, probably with different end groups (Fig. 3.17). It implies that the commercial PEGMA is not pure with acrylic end group, which leads to the fact, that the part without acrylic end group cannot be modified. This observation is in agreement with the NMR spectra, which showed that the ratio between two methyl groups from different reactors could not reach 1:1. A detailed analysis of polymers' MALDI spectrum will be shown in chapter 5 that confirms the assumption. However, the mass of the main series in the MALDI spectrum is shifted by 164 g/mol after modification. This difference is exactly the molecular weight of NAC, which shows that the modification of the polymer series with expected end group was successful.

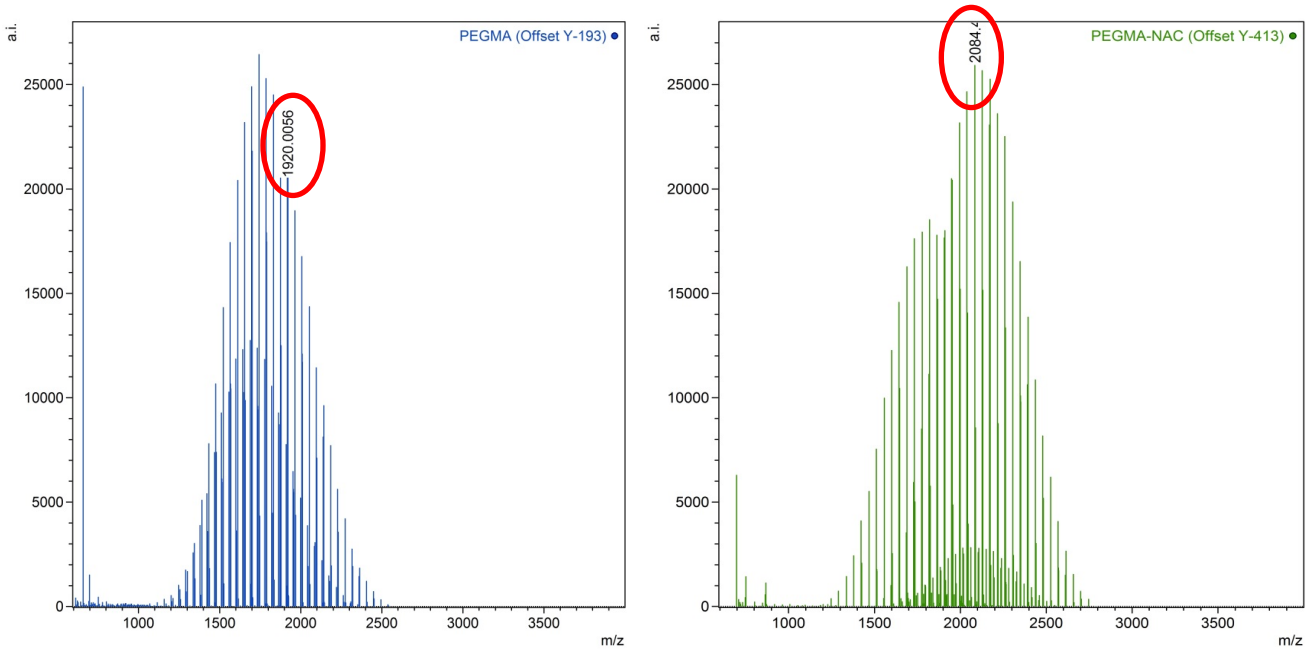

Fig 3.17 MALDI-ToF mass spectra of PEGMA (blue) and the modification product (green).

3.5.2 Modification of PEGMA with peptide

After the successful modification of PEGMA with NAC, the same conditions were taken to perform the modification with peptide 2: H-Cys-Ile-Arg-His-Met-Gly-Trp-Phe-Trp-Pro-Leu-Arg-Glu-Phe-Gly-Gly-Gly-Gly-Gly-OH.

The aromatic C−H vibration band above 3000 cm^{-1} from the peptide appears also in the Raman spectrum of the product (Fig 3.18 b, red and black). However, the stretching vibration of C−H from C=C (PEGMA, blue) does not appear in the product spectrum. Both indicate the successful conversion. The middle wavenumber region of the product spectrum resembles much the spectrum of peptide 2 which consists mainly of aromatic C−H stretching bands. Hence, the Raman spectra show that the modification of the polymer with peptide 2 was successful.

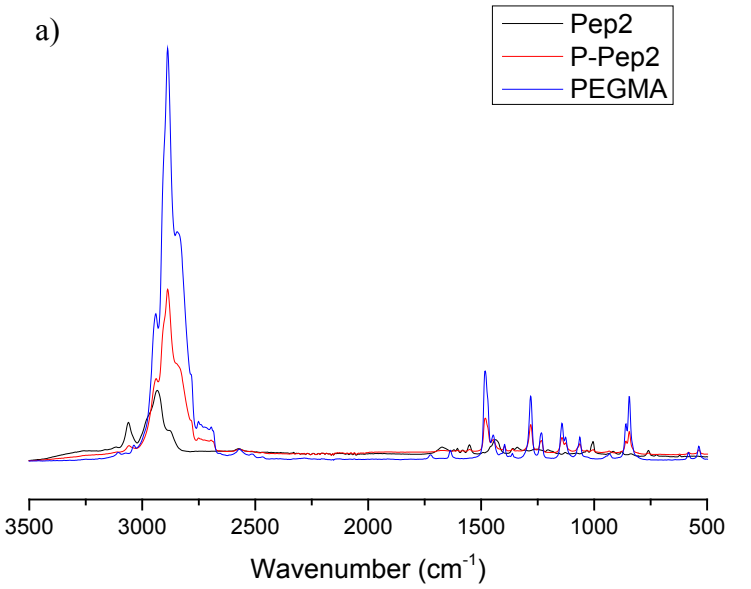
a)
Pep2
P-Pep2
PEGMA
3500
3000
2500
2000
1500
1000
500
Wavenumber (cm-1)

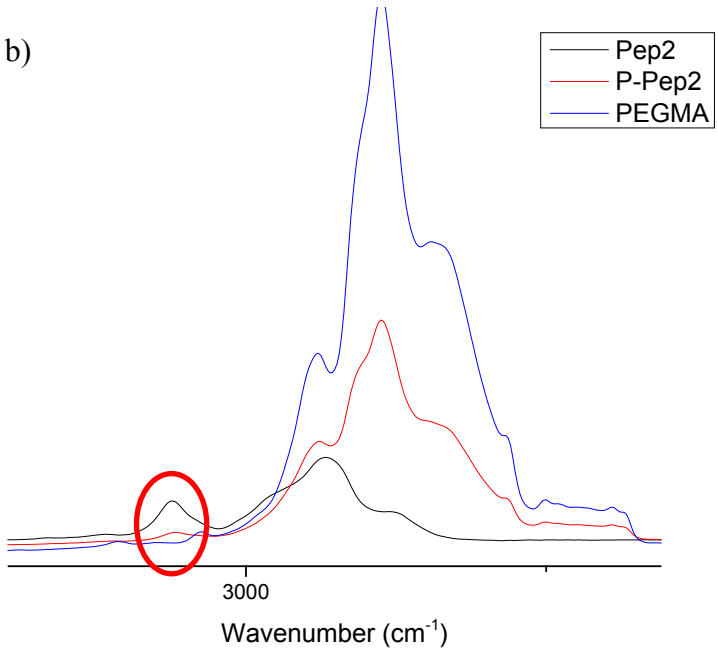
b)
Pep2
P-Pep2
PEGMA
3000
Wavenumber (cm-1)

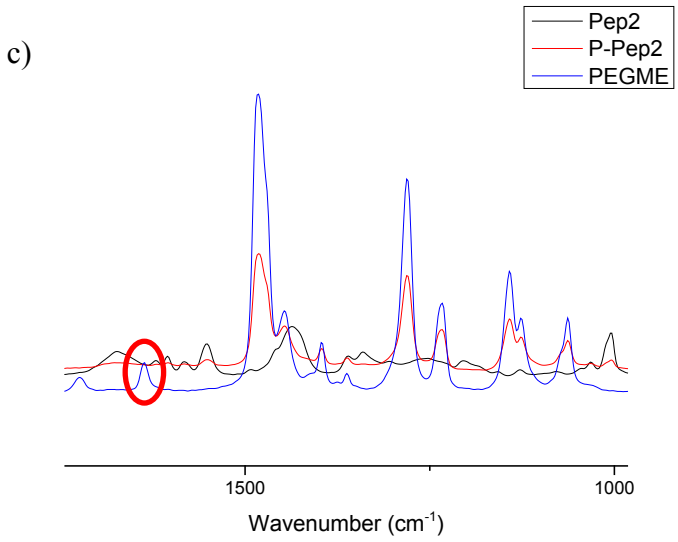

Fig 3.18 Raman spectra of PEGMA (blue), peptide 2 (black) and their reaction product (red), (b) and (c) show the spectra after zooming in the high (around 3000 cm^{-1}) and middle wavenumber region (around 1500 cm^{-1}), respectively.

The NMR spectrum after modification of PEGMA with peptide 2 shows singlet signals at 2.0 and 3.3 ppm that correspond to both the polymer and the peptide which supports a successful linkage (Fig 3.19). All proton signals from the $CH{=}CH_2$ group whose signals are at 4.25 ppm and 5.5-6.5 ppm also disappear. Above all, judging from the results of the NMR spectroscopy, the modification is successful.

Due to the high cost of the long peptide chain, a shorter peptide chain 3 (H-Gly-Gly-Gly-Gly-Gly-Trp-Phe-Trp-Cys-OH, molecular weight is 926 g/mol), which has the same terminal ends Cys and GGGGG but a short spacer, was applied to modify PEGMA instead of peptide 2. Since the free peptide reacts faster in sortagging as the one with polymer attached, excessive PEGMA was added to avoid the existence of free peptide 3. For this reason, excess free polymer is visible in the MALDI-ToF mass spectrum of PEGMA-peptide 3 (Fig 3.20).

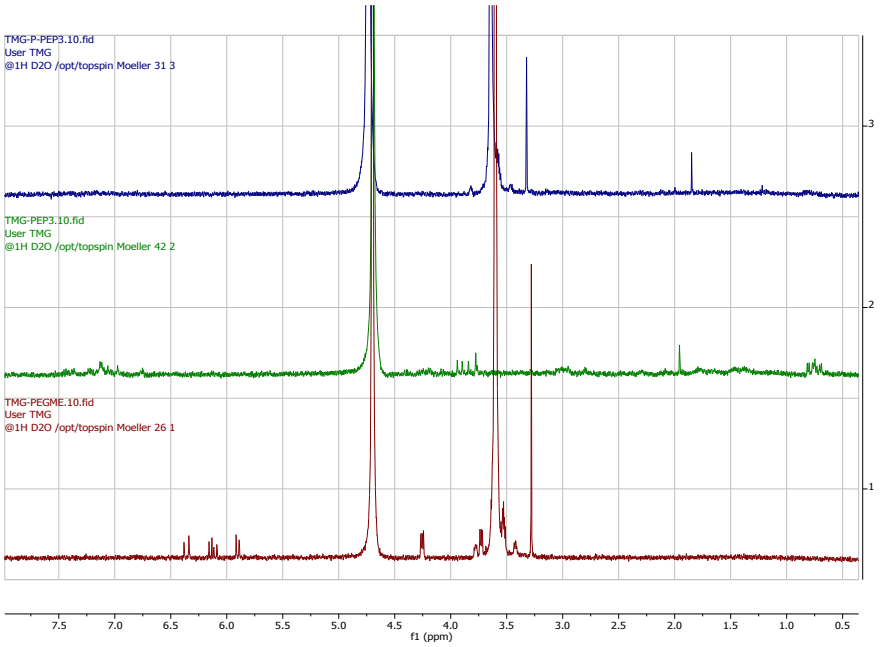

Fig 3.19 NMR spectra of peptide 2 (green) and PEGMA (red), in comparison with their reaction product (blue).

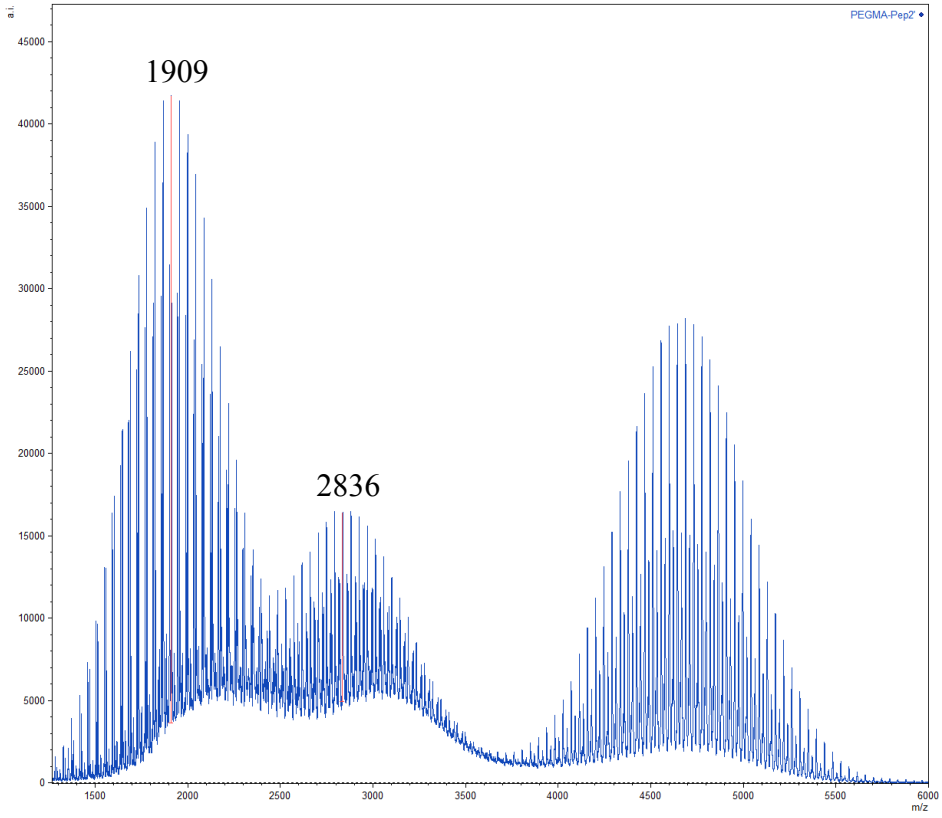

Fig 3.20 MALDI-ToF mass spectrum of PEGMA modified with peptide 3.

The MALDI-ToF mass spectrum of the product shows that the mass difference between PEGMA-peptide 3 and PEGMA is exactly the same as the molecular weight of peptide 3 (926 g/mol), which implies a successful modification. The higher m/z value in the spectrum was proved to be an impurity from the commercial PEGMA (see chapter 5). It corresponds to the

aforementioned NMR results that the PEGMA starting material could not be completely modified.

3.6 SrtA Reaction between two peptide sequences

Before performing SrtA reactions with artificial substrates, SML was conducted on two peptides and analyzed with MALDI-ToF mass spectrometry. Peptide 3 possesses GGG nucleophilic sequence and peptide 4 LPETG recognition sequence. The molecular weights of the two peptides are 926 Da and 1172 Da, respectively. The mass spectra of the two peptides show the 1-times charged peptide and a dimeric species, probably produced by disulfide bridge formation between the terminal cysteine units (Fig 3.21). In the spectrum of negative control (without SrtA), except the two single peptides, only dimeric species of peptides were detected, including a peak at m/z 2096 which belongs to peptide 3–peptide 4 probably linked by a disulfide bridge. In contrast, the spectrum of the product after SrtA reaction (red) shows a peak at m/z 2022. This is the product of successful SML between the two peptides as the terminal glycine (75 Da) of the recognition sequence LPETG was cleaved off in agreement with reported SrtA reaction mechanism. The theoretical molecular weight of the product should be 2023 Da (926 Da + 1172 Da – 75 Da), well in agreement with the observed molecular weight.

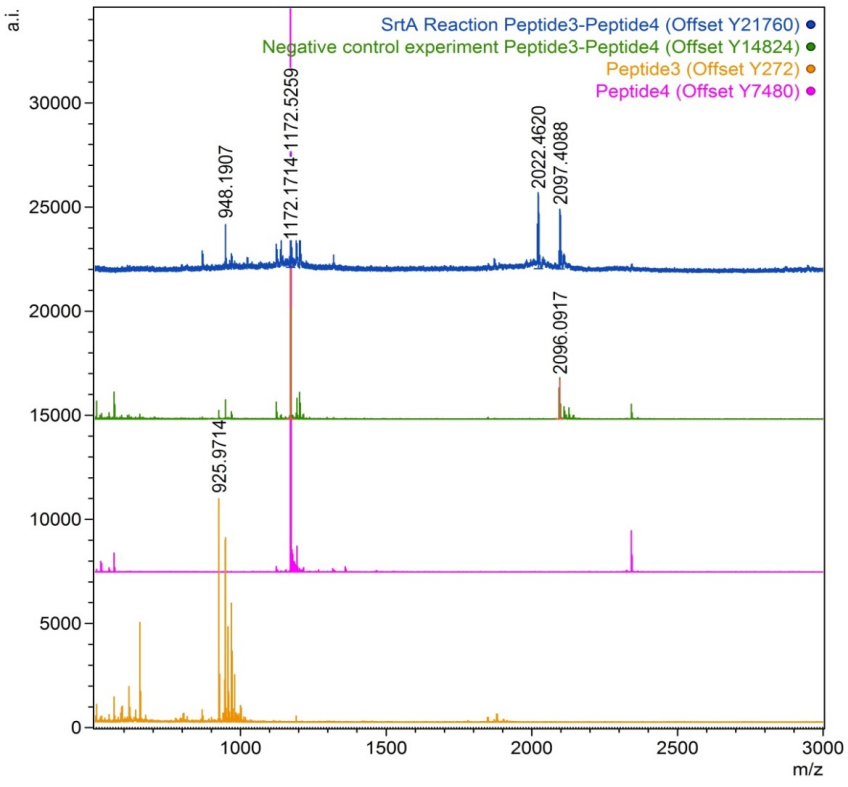

Fig 3.21 The MALDI-ToF mass spectra of peptide 3 (orange), peptide 4 (pink), SrtA reaction product (blue) and the negative control sample (green).

3.7 SrtA-mediated liagtion of peptide-functionalized nanoparticles and polymers

After silica NPs have been functionalized with LPETG recognition sequence and PEGMA with GGGGG nucleophilic sequence, SML was performed to link these two building blocks (Scheme 3.1).

3.7.1 Preparation of SrtA

Sortase A from *Staphylococcus aureus* was expressed in genetically modified form without its transmembrane domain to favor soluble expression after cell lysis (SrtA Δ59) and with a His-tag at the N-terminus to facilitate the purification of the enzyme. The corresponding gene was cloned into the pET28a vector between the restriction sites NdeI and XhoI and the construct was transformed in *Escherichia coli* BL21 (DE3) cells for sortase expression. The enzyme was purified to homogeneity by Ni^{2+}-affinity chromatography and the purity degree was checked by SDS-PAGE and MALDI-ToF mass spectrometry. As expected, the molecular mass of the protein was about 19 kDa, more specifically, 18 942 Da according to the MALDI-ToF mass spectrum (Fig 3.22).

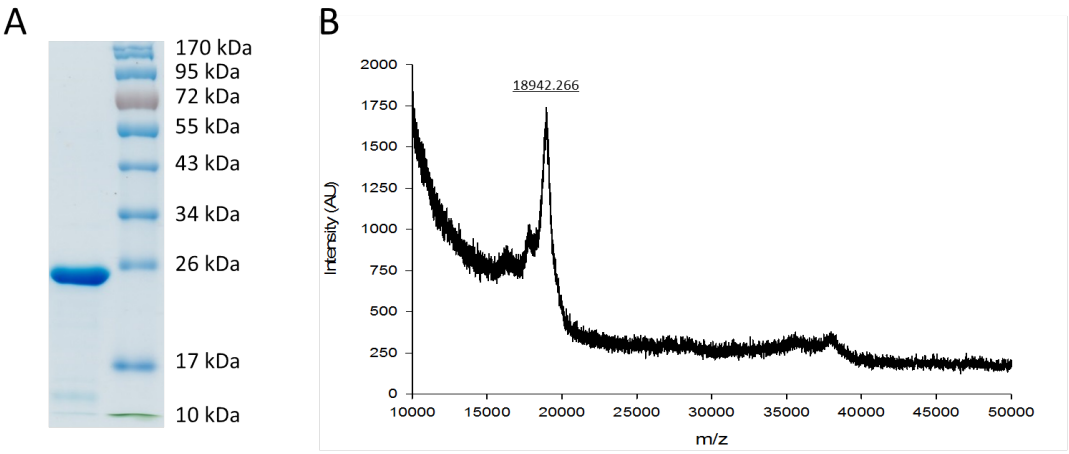

Fig 3.22 Characterization of SrtA. (A) SDS-PAGE after SrtA purification. (B) MALDI-ToF mass spectrum of SrtA.

3.7.2 SrtA reaction

After the modifications of the two substrates, the SrtA reaction was performed to link the two building blocks. The reaction was conducted at 37°C in thermomixer, under shaking at 600 r/min for 24 h. Negative control samples were prepared in the meanwhile, which are mixtures without functionalized PEG or without SrtA, respectively. After the reaction, the products were washed with water and centrifuged 3-times. After the SrtA reaction, the product was washed with water 6-times to remove remaining free polymer and eventually also peptide. The SDS-PAGE shows

that there was no free peptide left (Fig 3.23). For the characterization of the reaction products of SrtA reaction and negative controls, FESEM, TEM, STEM and MALDI-ToF mass spectrometry were used.

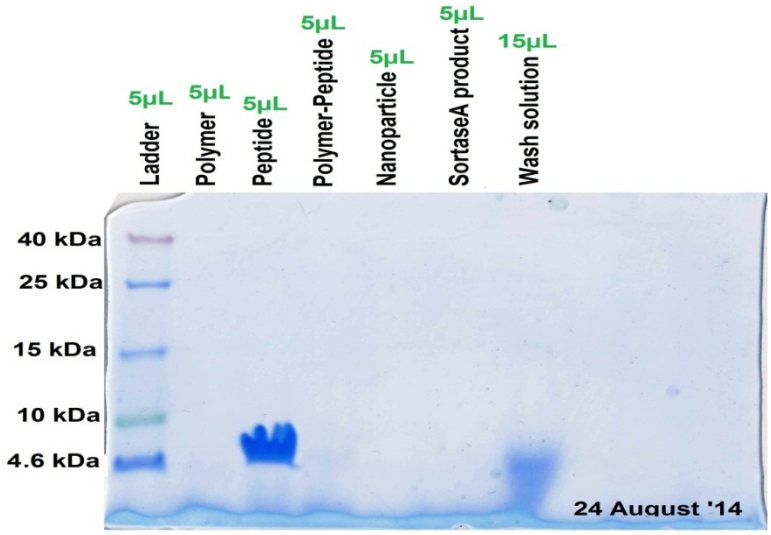

Fig 3.23 SDS-PAGE image demonstrating that free peptide was successfully removed by washing from the product after SML.

SiO_2 NPs of 200 nm in diameter, functionalized with the LPETG recognition motif, were reacted with an excess of GGGGG-functionalized PEG under the catalysis of SrtA. After the two peptides were linked by sortase, a thin polymer shell was formed around the NPs. As PEG is very well water soluble, the NP–polymer hybrids dispersed much better in water than the NPs without polymer shell. Negative control samples were prepared in the meanwhile, which are mixtures without functionalized PEG or without SrtA, respectively. The dispersion of the NP–polymer structures is more transparent than the negative control samples of the same concentration, indirectly showing the successful linkage (Fig 3.24). A quantitative UV/vis measurement confirmed the optical impression and verified that the sample of sortase reaction product is the most transparent one (Fig 3.25). Next, the supernatants after centrifugation from SrtA reaction and negative control samples were analyzed by MALDI-ToF mass spectrometry. The polymer–peptide conjugate (m/z ≈ 2800) can be detected in the solution of the negative control sample without SrtA (Fig 3.26, black spectrum), but not in the SrtA reaction (Fig 3.26, red spectrum). This implies that a high amount of polymer-peptide conjugate was linked to the NPs by SrtA. The polymer PEGMA (m/z ≈ 2000) was used in slight excess for the linkage with the peptide and is hence visible in the spectra of both the reaction and the negative control. The MALDI-ToF mass spectrum of the other negative control sample of NPs with SrtA but without polymer-peptide conjugate (Fig 3.26, blue line) does not show anything in the low m/z range.

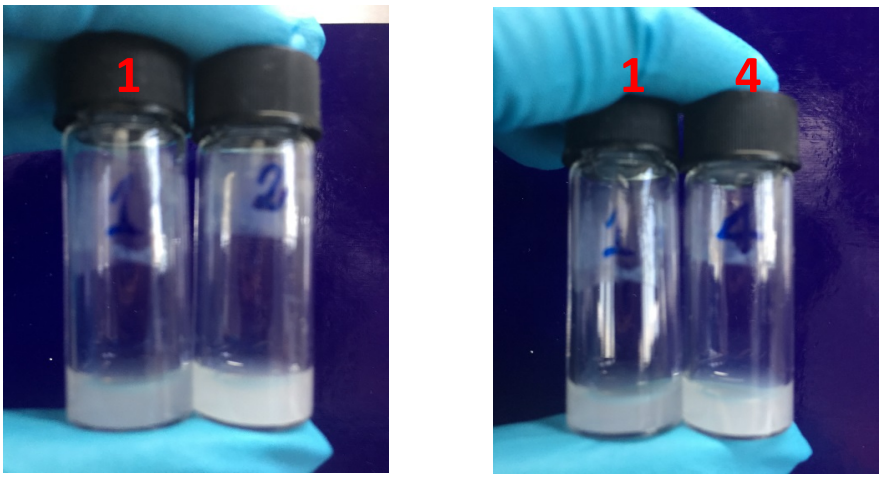

Fig 3.24 Dispersability comparison between 1: NP-polymer after SrtA reaction; 2: mixture of functionalized NPs and SrtA without polymer; 4: mixture of functionalized NPs and PEG without SrtA.

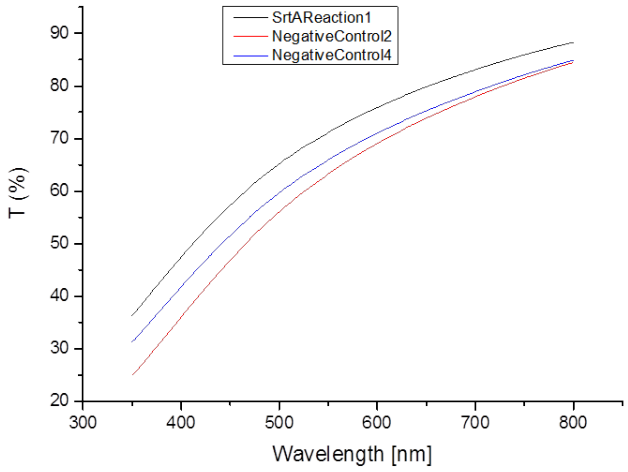

Fig 3.25 Transmittance curves of the samples shown in Fig 3.24: product from SrtA reaction 1 (black), negative control 2 (red, without polymer) and negative control 4 (blue, without SrtA). The concentration of all samples was 0.5 mg/mL. The wavelength was in the normal visible light range, 350-800 nm. The average transmittance of the samples was calculated through integration: SrtA reaction (1) 69.9 %, negative control (2) 62.2 %, negative control (4) 65.0 %.

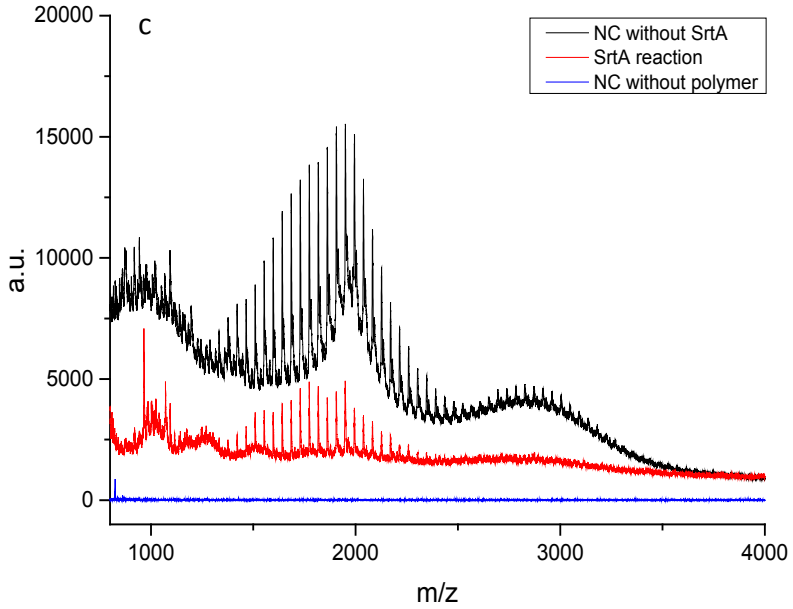

Fig 3.26 MALDI-ToF mass spectra of NP-polymer sample after SrtA reaction showing only unmodified free polymer (red), negative control solution without SrtA showing both unmodified free polymer as well as peptide-polymer (black), and negative control with SrtA but without peptide-polymer (blue).

Confocal microscopy images show the fluorescence of the tryptophan units in the peptides around the NPs (Fig 3.27). As both peptide 1 and peptide 2 contain tryptophan, these images cannot prove a successful reaction. However, the fluorescence appears brighter compared with Fig 3.11 indicating the higher content of both peptides around the NPs.

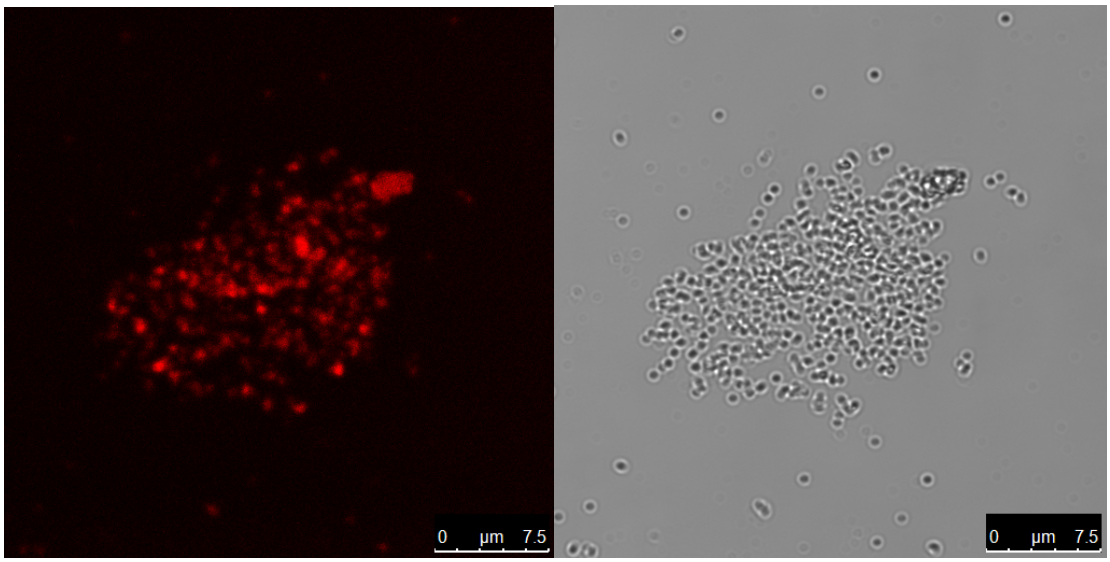

Fig 3.27 Confocal microscopy images after SML.

Moreover, TEM images of NP-polymer particles show a big difference in comparison to the negative control samples (Fig 3.28 a-g). The surface of the NPs is covered with a polymer film

after linkage of the polymer while the negative control samples show a sharp edge of the NPs. Hence, the polymer shell surrounding the NPs was only observed after SrtA reaction, but not formed around the NPs for the negative control samples under the same experimental conditions. The observed film is too thick to be caused by polymer-peptide of approximately 4000 g/mol. Therefore, it can be assumed that free polymer is adsorbed to the covalently linked polymer. Interestingly, the thick polymer film stayed after 3-times washing of the NPs. In contrast, no free polymer can be observed around the NPs in the negative control without sortase after 3-times washing. Hence, it is expected that free polymer can only adsorb to NPs which are surface-modified with the polymer, but does not adsorb to non-functionalized or peptide-modified NPs. The same conclusion was taken from field emission scanning electron microscopy (Fig 3.29) which showed a pronounced soft layer around the NPs after SrtA reaction.

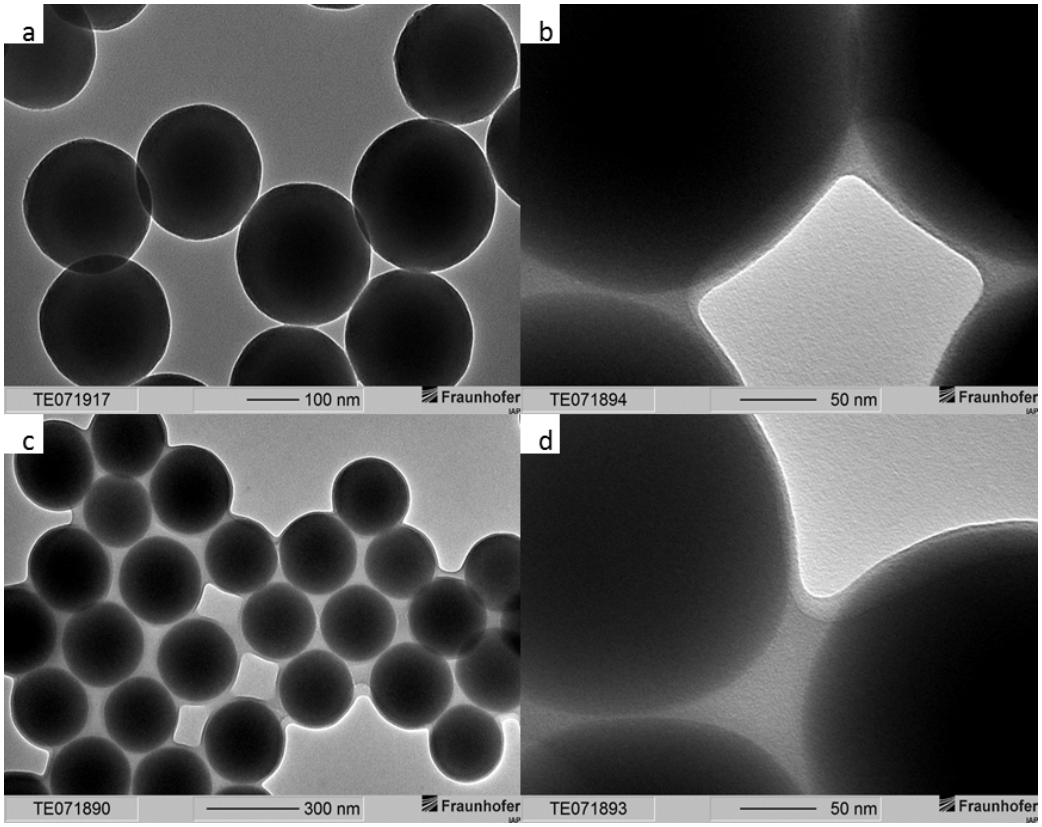

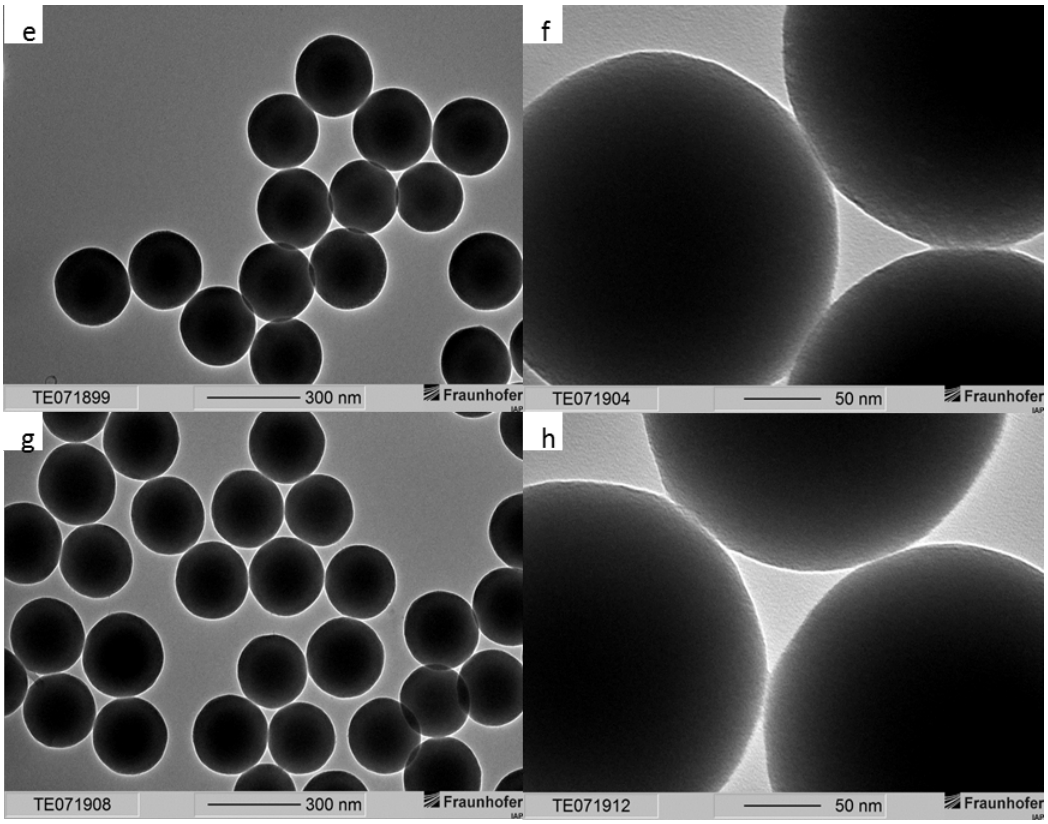

Fig 3.28 TEM images before and after the Srt A reaction. a) before reaction, NP-peptide 2; b), c) and d) after SrtA reaction; e) and f) are negative control without polymer; g) and h) are negative control without SrtA.

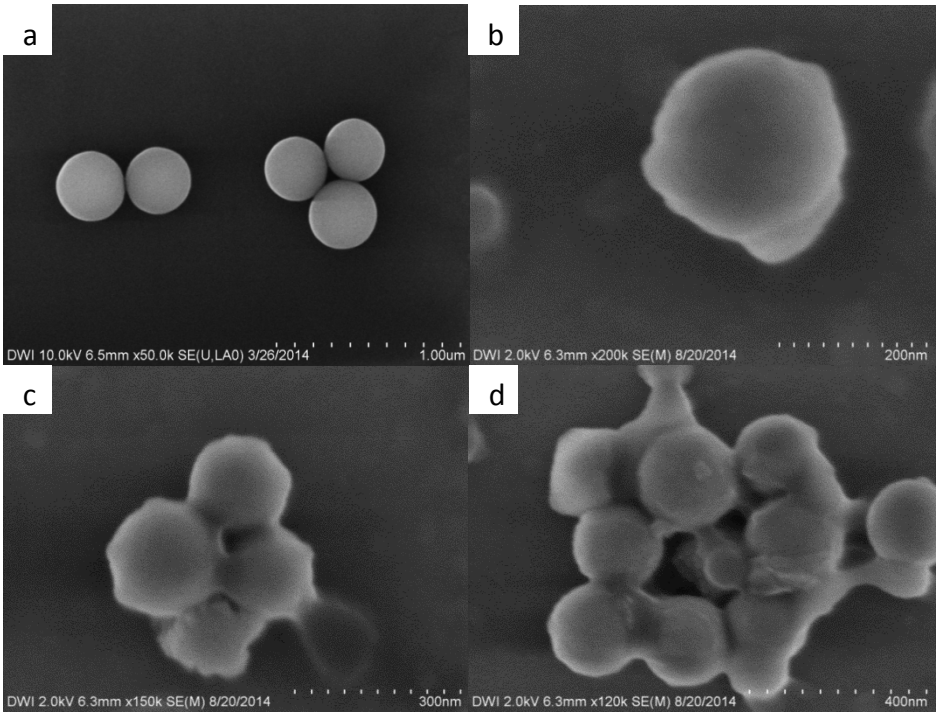

Fig 3.29 FESEM images before (a) and after (b, c, d) SrtA reaction.

STEM images before the SrtA reaction show a smooth and sharp surface of the NPs (Fig 3.30 a and b), which is covered by a polymer film after the reaction (c and d).

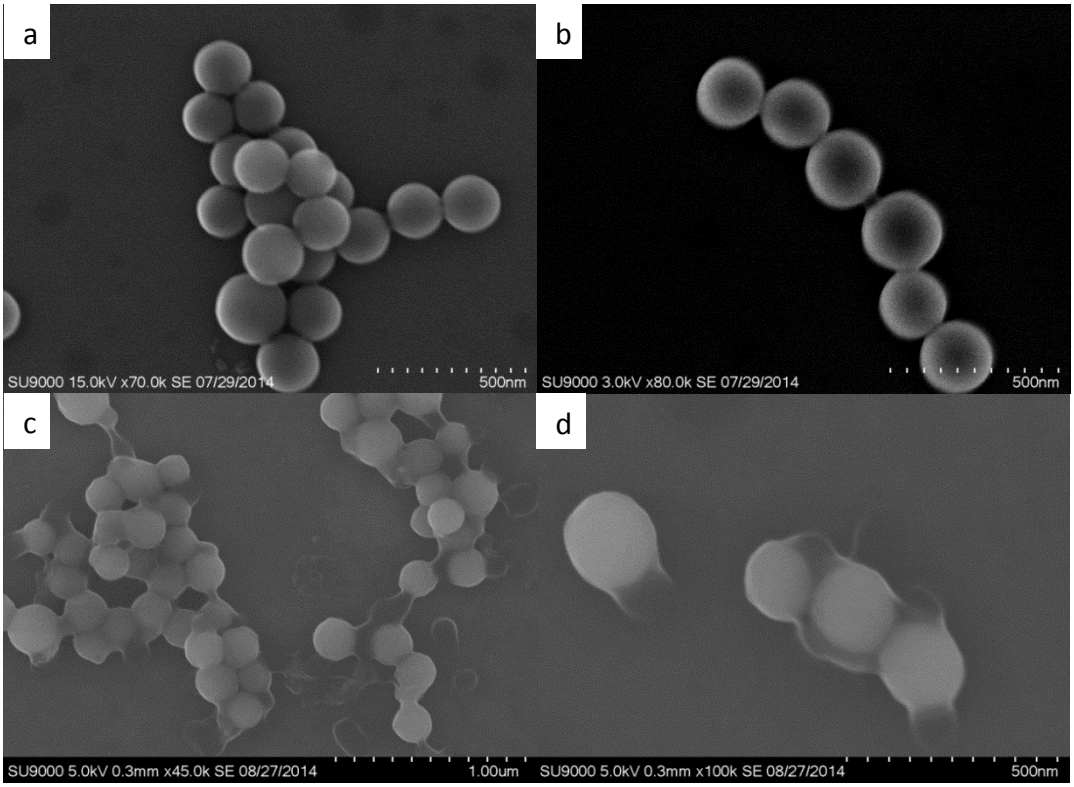

Fig 3.30 STEM images after SrtA reaction.

3.8 Summary

The aim of this chapter is to prove the concept, that nanoparticles and polymers can be linked via the catalysis of the enzyme sortase A. SrtA can ligate the peptide motifs LPXTG- and G_x, which were equipped on the two chosen substrates, namely SiO_2 NPs and PEG as polymer.

The silica NPs were synthesized via sol-gel method and then functionalized with MPS in order to obtain a C=C coating. PEGMA was commercially received from Sigma-Aldrich. Both the NPs and PEGMA were equipped with the peptide motifs through 'thiol-ene' reactions between -SH group of cysteine and C=C groups of the substrates. Due to the high cost of peptides, *N*-acetyl-L-cysteine (NAC) was taken to analyze optimum reaction conditions between a cysteine compound and the C=C coating on the functionalized SiO_2 NPs as well as the C=C end group of PEGMA.

The results showed that NAC reacted with the functionalized SiO_2 NPs under UV light and the photoinitiator ABCVA in N_2 atmosphere for 24 hours. The successful modification was proven via Raman spectroscopy and Zetasizer measurements. The process was consequently applied

onto the reaction between peptide 1 and C=C-functionalized SiO_2 NPs. For the polymer part, it turned out that a higher degree of modification of PEGMA was reached under N_2 atmosphere and the catalysis of triethylamine for 24 hours, as demonstrated by Raman and NMR spectroscopy as well as MALDI-ToF mass spectrometry. Under the same conditions, PEGMA was successfully modified with peptide 2 and later on with peptide 3.

The SrtA reaction between the two substrates was consequently performed. MALDI-ToF mass spectrometry showed that no Peptide 3-PEGMA was detectable in the washing solution after the reaction, indicating that a high amount of the conjugate was consumed during the SrtA reaction. After 3-times washing with MilliQ water, the SiO_2 NPs showed better dispersity in water after SrtA reaction compared with the NPs in negative control samples, due to the hydrophilic thin polymer layer on the surface of the nanoparticles. This observation indirectly proved the successful linkage between the two substrates via SrtA. In addition, FESEM, TEM and STEM images showed the morphology of the nanoparticles, again with a thin polymer layer on the surface of the nanoparticles only after SrtA reaction.

In conclusion, the SrtA catalyzed linkage between nanoparticles and polymers could be demonstrated. The study with these two substrates is amongst the first incorporating only artificial building blocks and therefore transferring SML to materials science and enlarging the scope of sortagging. It opens the door of the concept that two purely artificial building blocks can be linked under the catalysis of the enzyme SrtA. More applications of SrtA will be demonstrated in the next chapters.

3.9 References

[1] H. Namazi, *BioImpacts* **2017**, *7*, 73–74.

[2] R. Singh, L. J. W., *Exp. Mol .Pathol.* **2009**, *86*, 215–223.

[3] A. Liberman, N. Mendez, W. C. Trogler, A. C. Kummel, *Surf. Sci. Rep.* **2014**, *69*, 132–158.

[4] L. Wu, U. Glebe, A. Böker, *Polym. Chem.* **2015**, *6*, 5143–5184.

[5] X. Y. Liu, J. M. Nothias, A. Scavone, M. Garfinkel, J. M. Millis, *ASAIO J.* **2010**, *56*, 241–245.

[6] E. Bourgeat-Lami, J. Lang, *J. Colloid Interface Sci.* **1998**, *197*, 293–308.

[7] M. Karg, I. Pastoriza-Santos, L. M. Liz-Marzán, T. Hellweg, *ChemPhysChem* **2006**, *7*, 2298–2301.

[8] G. H. Bogush, C. F. Zukoski IV, *J. Colloid Interface Sci.* **1991**, *142*, 19–34.

[9] A. G. Kalampounias, *Bull. Mater. Sci. Indian Acad. Sci.* **2011**, *34*, 299–303.

[10] A. B. Lowe, *Polym. Chem.* **2010**, *1*, 17–36.

[11] S. Kimoto, W. D. Dick, B. Hunt, W. W. Szymanski, P. H. McMurry, D. L. Roberts, D. Y. H. Pui, *Aerosol Sci. Technol.* **2017**, *51*, 936–945.

[12] L. Wu, U. Glebe, A. Böker, *Adv. Mater. Interfaces* **2017**, *4*, 1–10.

[13] L. Wu, U. Glebe, A. Böker, *Macromol. Rapid Commun.* **2017**, *38*, 1–7.

[14] C. E. Hoyle, C. N. Bowman, *Angew. Chemie - Int. Ed.* **2010**, *49*, 1540–1573.

[15] H. Chen, H. Zou, H. Paholak, M. Ito, W. Qian, Y. Che, D. Sun, *Polym. Chem.* **2014**, *50*, 2768–2773.

[16] A. Rhiannon K. Iha, K. L. Wooley, A. M. Nyström, D. J. Burke, M. J. Kade, C. J. Hawker, *Chem. Rev.* **2009**, *109*, 5620–5686.

[17] C. Weber, S. Reiss, K. Langer, *Int. J. Pharm.* **2000**, *211*, 67–78.

[18] A. B. Lowe, *Polym. Chem.* **2014**, *5*, 4820–4870.

4 Sortase-catalyzed cluster formation with silica NPs of different size

4.1 Introduction

Nanoparticle cluster structures attract more and more interest in the last decades, especially on the aspect of the electrostatic adherence and assembly of silica nanoparticles[1-2]. Most of the systems are built on the basis of electrostatic interaction. However, the linkage via SrtA has the advantage that it forms a covalent bond between the two substrates.

In this chapter, the synthesis of silica nanoparticles of two different sizes by sol-gel method is described. They were formed with diameters of approximately 200 nm and 60 nm, respectively, similar to published procedures. Subsequently, the NPs were functionalized by reaction with 3-(trimethoxysilyl) propyl methacrylate (MPS) which provides accessible C=C-double bonds on the surface of the nanoparticles. Peptide 1 with LPETG recognition sequence was linked to the 200 nm NPs and peptide 3 with GGGGG to 60 nm NPs. The successful functionalization was shown by Raman spectroscopy (Chapter 3). The two modified building blocks were then linked by SrtA (Scheme 4.1). TEM images and DLS experiments imply indirectly that the two NPs of different size were linked forming bigger clusters.

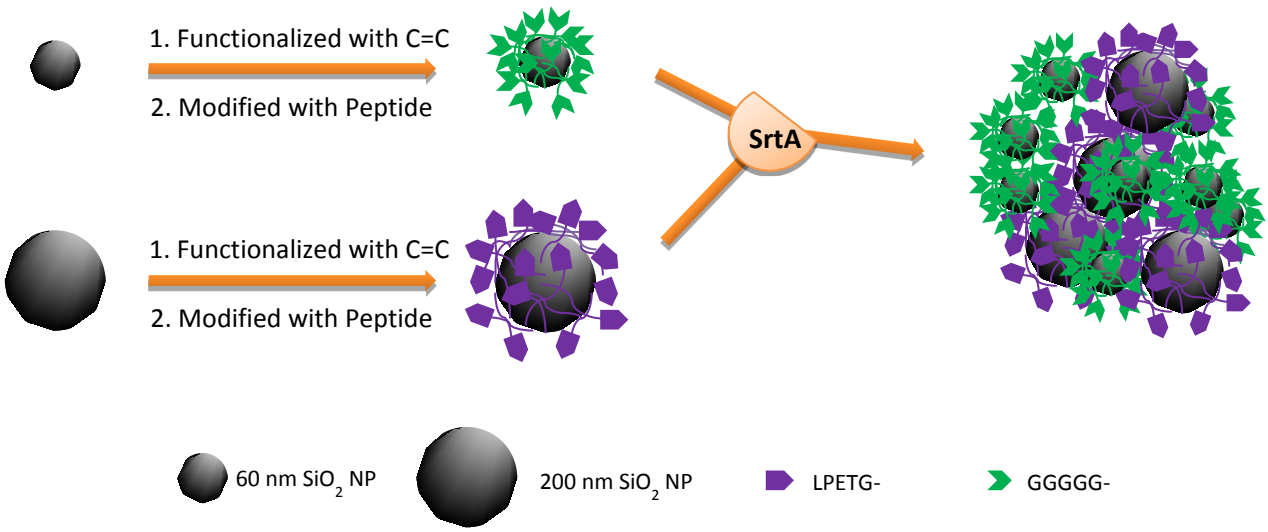

Scheme 4.1 Scheme of SrtA catalyzed linkage between silica NPs of approximately 60 nm and 200 nm diameter. Each building block is functionalized with a peptide motif needed for SrtA catalysis.

4.2 Preparation and characterization techniques

4.2.1 Materials

Chemicals: Tetraethyl orthosilicate (TEOS), ammonia solution 28-30%, 4,4′-azobis(4-cyanovaleric acid) (ABCVA), 3-(trimethoxysilyl) propyl methacrylate (MPS), and triethylamine were purchased from Sigma-Aldrich. SrtA was provided from our cooperation partner, Dr. Diana Mate in Prof. Schwaneberg's group at RWTH Aachen. Peptide 1 and peptide 2 were bought from Biotrend. MilliQ grade water was used.

4.2.2 Characterization methods

Dynamic Light Scattering. DLS measurements were performed on a Malvern (Worcestershire, England) Zetasizer Nano ZS device at 20 °C. Assuming Mark-Houwink parameters to be A = 0.428 and B = $7.67 \cdot 10^{-5}$, 173° backscattering was analyzed with equilibration time of 120 s. Multi-parameter analysis was performed on an average of three runs for every data point.

Transmission Electron Microscopy. TEM was performed on a Philips CM-200 device operating at 120 kV. The samples were deposited on nitrogen glow discharged carbon film coated grids, which were subsequently washed 3-times with Millipore water.

4.2.3 Preparation

Synthesis of silica NPs: In order to synthesize silica NPs of around 200 nm diameter, concentrations of water (5 mol/L), ammonia (0.2 mol/L), and TEOS (0.2 mol/L) were used, and the reaction mixture in a batch of 50 mL was stirred at room temperature for 48 h. For the preparation of silica NPs of 60 nm diameter, the concentration of water was changed to 1 mol/L.

Functionalization of silica NPs: After silica NPs were formed, in the presence of ammonia, MPS (12:1, mass ratio) was directly added in the system. The NPs were stirred at room temperature for another 24 h followed by 1 h reflux.

Functionalization of NPs with peptides: 200 nm NPs were reacted with peptide 1 (H-Cys-Ile-Arg-His-Met-Gly-Phe-Pro-Leu-Arg-Glu-Phe-Leu-Pro-Glu-Thr-Gly-OH), while 60 nm NPs were functionalized with peptide 2 (H-Gly-Gly-Gly-Gly-Gly-Phe-Glu-Arg-Leu-Pro-Trp-Phe-Trp-Gly-Met-His-Arg-Ile-Cys-OH). C=C-functionalized NPs and peptide were mixed in 1.1:1 molar ratio (peptide : C=C group) with 3 mol % 4,4′ -azobis(4-cyanovaleric acid) (ABCVA) in water. The

mixture was stirred in N_2 atmosphere for 24 h under exposure to UV light (365 nm). Afterwards, the NPs were washed with Millipore water by centrifugation and ultrasonication.

SrtA reaction: A typical reaction mixture of 100 µL consisted of 30 µL aqueous solution of the two substrates with approximately 50-times excess of GGG substrate with respect to LPETG substrate, 20 µL SrtA (7.95 mg/mL), 20 µL 250 mM Tris-HCl and 750 mM NaCl (pH 7.5), 20 µL 25 mM $CaCl_2$, 10 µL Millipore water, and was conducted at 37 °C in a thermomixer for 24 h.

4.3 Synthesis and functionalization of silica NPs of different size

SiO_2 nanoparticles of different size can be easily synthesized via sol-gel method and slight variation of the composition of the reaction mixture[3-7]. The details of synthesis and subsequent functionalization with MPS and peptide sequences are explained in chapter 3. Fig 4.1 shows TEM images demonstrating the different size of the unmodified NPs, more precise approximately 60 nm and 200 nm in diameter.

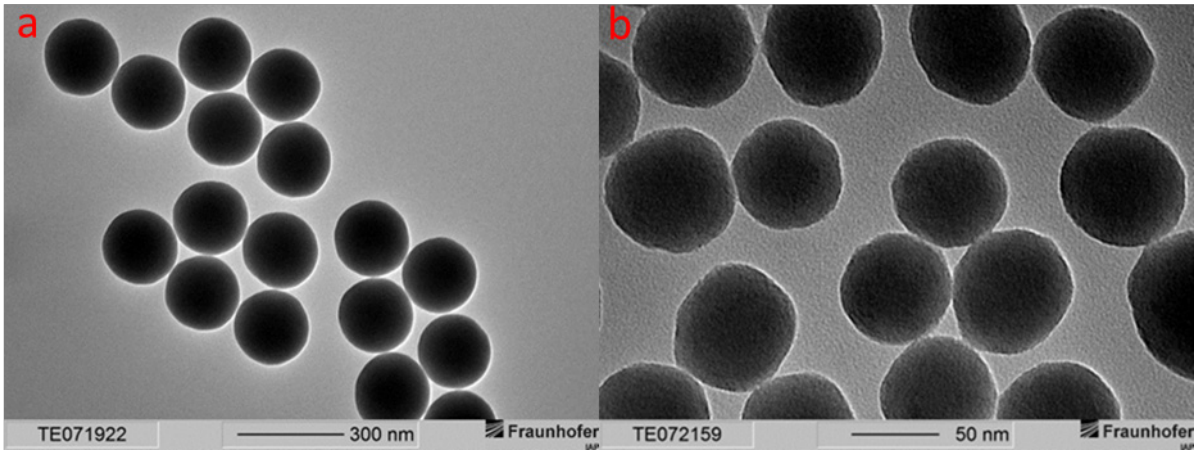

Fig 4.1 TEM images of unmodified 200 nm SiO_2 NPs (a) and 60 nm NPs (b).

4.4 Sortase A reaction between peptide-functionalized silica NPs of different size

After the functionalization and the modification of NPs of the two different sizes, the SrtA reaction was applied to link these NPs and form a cluster structure (Scheme 4.2). A negative control experiment was done consisting of the same reaction mixture, but without SrtA.

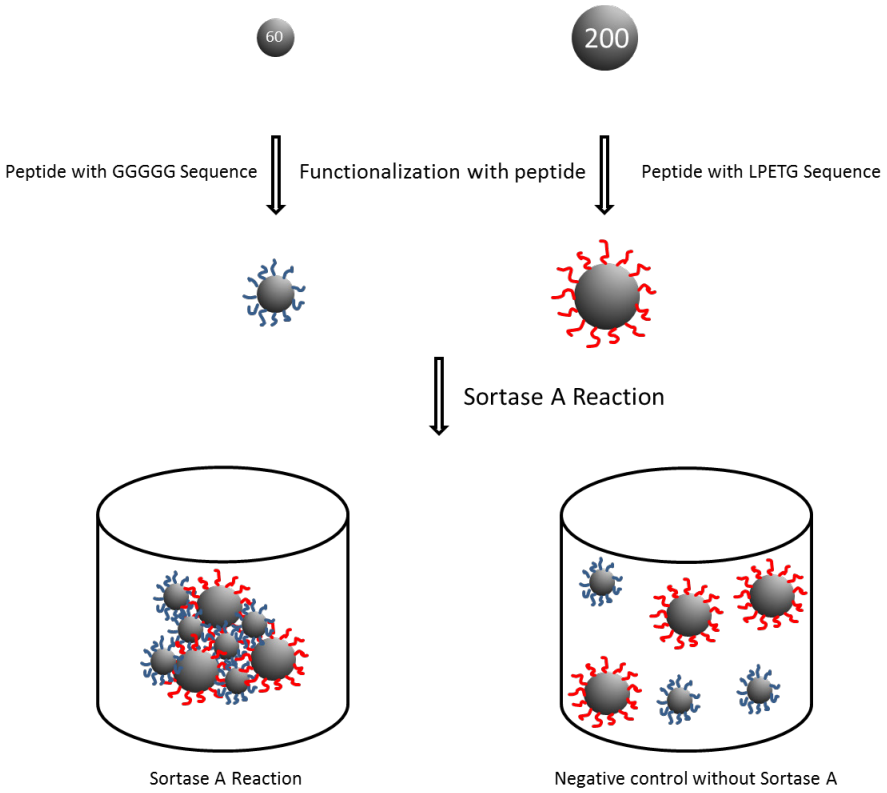

Scheme 4.2 The scheme of SrtA reaction between NPs of different size.

From the dispersity of the NP-NP SrtA reaction mixture (Fig 4.2, right) and negative control experiment (Fig 4.2, left), it can be seen that the dispersion after SrtA reaction is much more turbid than the negative control sample. This indirectly suggests the successful formation of the larger cluster structure and therefore the linkage between the NPs.

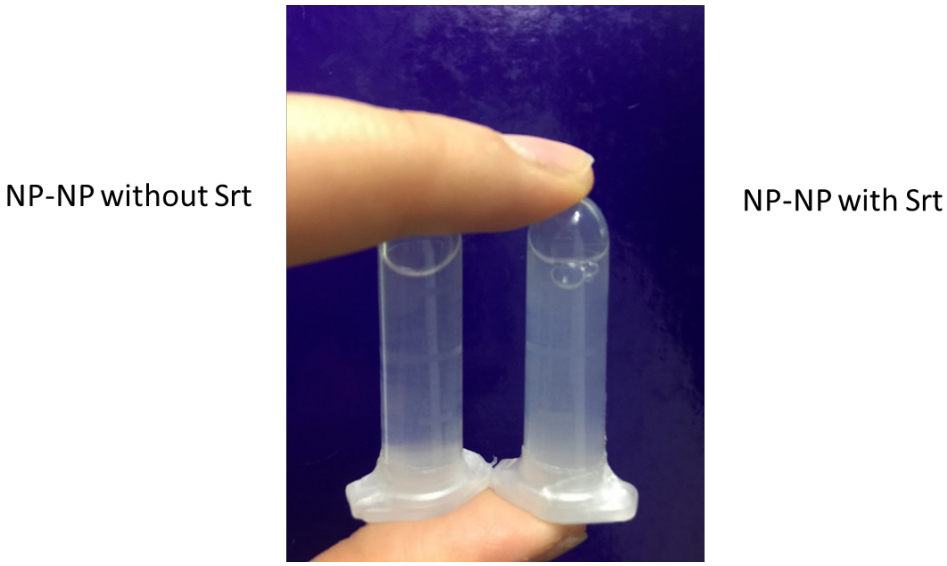

Fig 4.2 Dispersability comparison between left: NP-NP mixture without SrtA; right: Cluster of NP-NP after SrtA reaction.

DLS measurements were performed on the samples (Fig 4.3). The unmodified small and large NPs were detected in DLS measurements with diameters in agreement to their size observed with TEM (Fig 4.1). The negative control sample with peptide-functionalized NPs showed a simple mixture of these two sizes of nanoparticles. In contrast, after SrtA reaction, no single nanoparticles were detected anymore. Instead, larger aggregates of different sizes were detected due to the linkages between large and small NPs. Therefore, the DLS measurements verify the optical impression from the dispersability comparison.

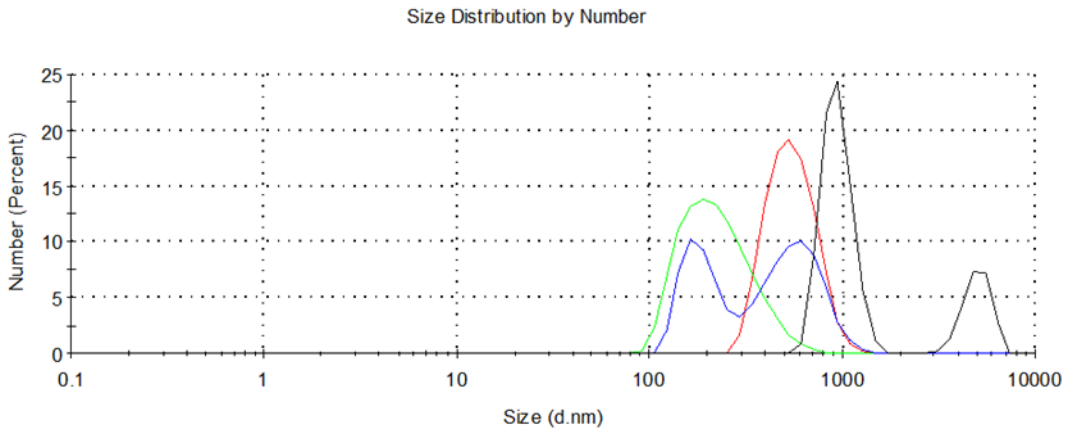

Fig 4.3 DLS measurements of small NPs (green), large NPs (red), negative control (mixture without SrtA, blue) and SrtA reaction product (black).

TEM images of the products of SrtA reaction and the negative control experiment are shown in Fig 4.4. Unsurprisingly, the image of the product after SrtA reaction (Fig. 4.4, left) shows more or less the state of aggregation or cluster formation between the large and small NPs, while the

other image (Fig 4.4, right) shows a status of a normal mixture between the NPs of different size without pronounced aggregation. The smaller aggregates visible in the image are probably from sample preparation which involves evaporation of the solvent from the TEM grid and often leads to aggregation. The TEM images imply the morphology change between the products of negative control and SrtA reaction, and therefore also the successful linkage between the NPs via SrtA[8].

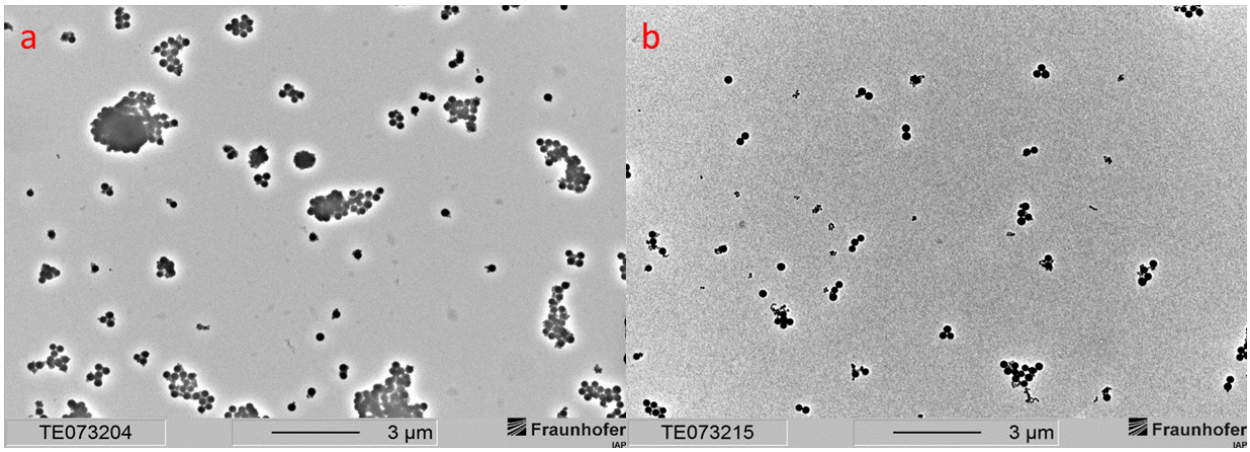

Fig 4.4 TEM images for NP-NP aggregates after SrtA reaction (a) and negative control without sortase (b).

4.5 Summary

This chapter demonstrated the cluster formation via covalent linkage of peptide-functionalized SiO_2 nanoparticles of different sizes through SrtA-mediated ligation. The two substrates were first functionalized with C=C groups, modified with the SrtA recognition sequence (peptide 1; 200 nm NPs) and nucleophilic sequence (peptide 2, 60 nm NPs), respectively, and then the clusters formed under the catalysis of SrtA. The successful linkage between the NPs was indirectly proven by water dispersability, DLS measurements and TEM images.

However, due to unavoidable aggregation of NPs during sample preparation, a fully convincing conclusion is not possible with TEM. As the NP surfaces contain numerous peptides, the stoichiometry of the formed aggregates is not controllable and these structures were therefore not studied in more detail. Further studies of such systems could be done by static light scattering (SLS), analytical ultracentrifugation (AUC) or field flow fractionation (FFF). However, because the cluster formation leads to strongly polydisperse products, no more effort was put into these systems using elaborate and in part expensive measurement techniques. Nonetheless, SML proofed its potential for the covalent linkage between nanoparticles.

The studied NPs contain many peptide sequences uniformly distributed around them. The synthesis of Janus NPs with peptides in small patches could be a means to control the cluster formation. However, such Janus NPs are complicated to form and therefore out of the scope of this thesis.

4.6 References

[1] R. Brüx, S. Hiltl, V. Schröder, C. Von Essen, A. Böker, *Part. Part. Syst. Charact.* **2014**, *31*, 871–878.

[2] L. Wu, U. Glebe, A. Böker, *Polym. Chem.* **2015**, *6*, 5143–5184.

[3] E. Bourgeat-Lami, J. Lang, *J. Colloid Interface Sci.* **1998**, *197*, 293–308.

[4] M. Karg, I. Pastoriza-Santos, L. M. Liz-Marzán, T. Hellweg, *ChemPhysChem* **2006**, *7*, 2298–2301.

[5] A. G. Kalampounias, *Bull. Mater. Sci. Indian Acad. Sci.* **2011**, *34*, 299–303.

[6] A. B. Lowe, *Polym. Chem.* **2010**, *1*, 17–36.

[7] S. Kimoto, W. D. Dick, B. Hunt, W. W. Szymanski, P. H. McMurry, D. L. Roberts, D. Y. H. Pui, *Aerosol Sci. Technol.* **2017**, *51*, 936–945.

[8] X. Dai, D. Mate, U. Glebe, T. Mirzaei Garakani, A. Körner, U. Schwaneberg, A. Böker, *Polymers (Basel).* **2018**, *10*, 151.

5 The formation of PEG-PNIPAM block copolymer via SML

5.1 Introduction

Block copolymers have received a lot of attention due to their special diverse properties and wide range of applications[1]. In this substance class, multiple polymer blocks are attached to each other in defined order. Still, their potential function in many fields is researched as well as fine-tuning for special applications. For instance, block copolymers can be used as surfactants[2], drug delivery vehicles[3] and so on. Hence, the preparation of block copolymers has been seen a very interesting topic in the research field, but also full of challenges.

A lot of research works have addressed the synthesis of block copolymers during the last decades. Block copolymers can be synthesized either through subsequent polymerization of different monomers or post-polymerization linkage of blocks with suitable reactive end groups. However, the synthesis of multiblock copolymers is challenging in general, especially for three or more polymer blocks with different physical and chemical properties[4-5]. Copolymers with typically up to six polymer blocks can be synthesized by stepwise polymerization of different monomers. However, due to different reactivities in some combinations of monomers, it is not possible to synthesize any kind of block copolymer through sequential polymerization techniques[6]. As an alternative, the polymer blocks can also be synthesized individually and afterwards linked by a click chemical reaction, e.g. CuAAC and Diels-Alder cycloaddition. End-functionalized blocks can either be synthesized from a functional initiator or RAFT CTA, or the clickable group can be introduced in a post-polymerization step[7]. As click reactions are unspecific, every type of reaction can only be used to introduce one new block into a copolymer.

In this chapter, a new approach for the preparation of block copolymers via SML is introduced. The aim of this chapter is to prove the concept, that SrtA can also catalyze the linkage reaction between two polymer blocks, which provides the opportunity for the preparation of block copolymers via an enzymatic strategy in addition to the traditional chemical way. Although the demonstrated diblock copolymer could be easily synthesized by established chemical techniques, this example can serve as a starting point for the future synthesis of multiblock copolymers aided by SML.

Two commercially available polymers (PEG and PNIPAM) with a C=C terminal group were first modified with SrtA recognition or nucleophilic sequence, respectively, as already reported for PEG in chapter 3. The linkage between the two parts was then conducted via catalysis of SrtA (Scheme 5.1), and a negative control experiment without SrtA also performed. The successful modifications of the two polymers and their subsequent linkage were characterized by MALDI-ToF mass spectrometry.

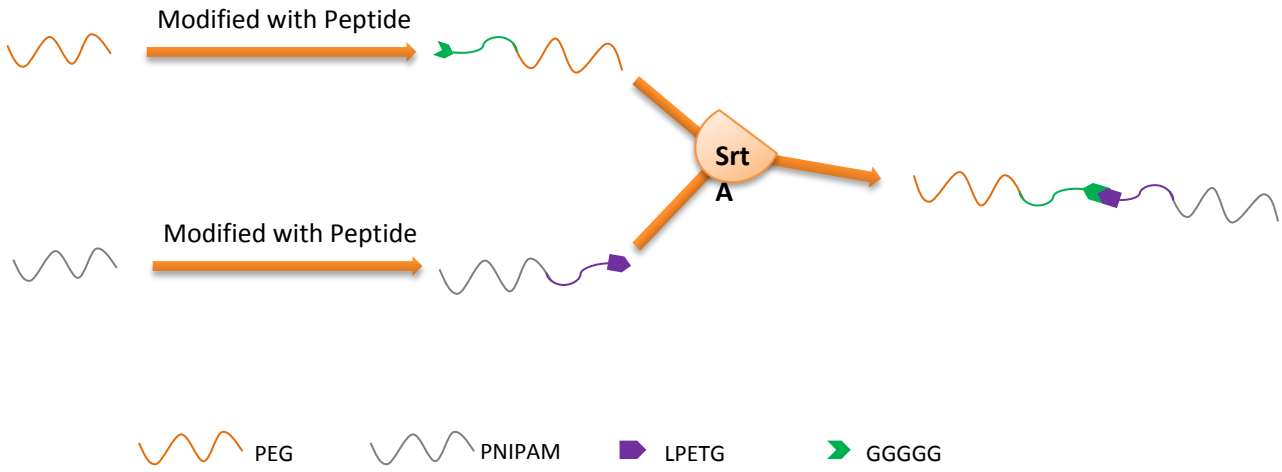

Scheme 5.1 Scheme of SrtA catalyzed linkage between two peptide-functionalized polymer blocks.

5.2 Preparation and characterization methods

5.2.1 Materials

Poly(ethyleneglycol) methyl ether acrylate (PEGMA), maleimide terminated poly(*N*-isopropylacrylamide) (PNIPAM), triethylamine and matrix as well as salt used for MALDI (CCA, NaTFA) were purchased from Sigma-Aldrich. Peptide 3 and peptide 4 were purchased from Biotrend company. MilliQ grade water was used.

5.2.2 Preparation

Modification of PEGMA with peptide 3: PEGMA and peptide 3 (1.2: 1, eq) were added into a Schlenk flask, NEt_3 (1 eq) in PI buffer (pH=7.5) was added under N_2 atmosphere. The reaction was performed in N_2 atmosphere at 22 °C for 24 h. The product was dialyzed against a membrane with 1 kDa MWCO and then lyophilized. The same conditions were also applied for the modification of PNIPAM with peptide 4.

SrtA reaction between the two peptide-functionalized polymer blocks: A typical reaction mixture of 100 µl consisted of 30 µl aqueous solution of the two substrates with approximately 50-times excess of GGG substrate with respect to LPETG substrate, 20 µl SrtA (7.95 mg/ml), 20 µl

250 mM Tris-HCl and 750 mM NaCl (pH 7.5), 20 µl 25 mM $CaCl_2$, 10 µl Millipore water, and was conducted at 28 °C in thermomixer for 24 h.

The negative control experiment was performed the same, only water was added instead of SrtA.

5.2.3 Characterization methods

MALDI-ToF mass spectrometry: Spectra were acquired using a 337 nm laser Bruker microflex MALDI-ToF mass spectrometer (Bruker, Bremen, Germany) with pulsed ion extraction. The masses were determined in positive ion linear mode. The sample solutions were applied on a ground steel target using the dried droplet technique. Mass calibration was performed with external calibration. Polymer samples were prepared as follows: α-cyano-4-hydroxycinnamic acid (CCA) was used as matrix substance in a 10 mg/ml solution in Millipore water:acetonitrile 7:3 with 0.1 % trifluoroacetic acid. Sodium trifluoroacetate was used as salt in 0.1 mol/l solution in the same solvent mixture. Sample (5 mg/ml), matrix and salt solutions were mixed in 5:20:1 ratio and 2 µl of the mixture applied on the target.

5.3 Modification of PEGMA with peptide 3

Characterization of the reaction product was already reported in chapter 3. Here, the MALDI-ToF mass spectra of unmodified and peptide-functionalized polymer were analyzed in detail. This analysis was done by Dr. Andrea Körner (DWI – Leibniz-Institute for Interactive Materials e.V., Aachen) with the software Polymerix. The mass spectrum of PEGMA shows a bimodal distribution with a total/average M_n of 2713.8 Da, an average M_n of 1927.3 Da for the partial series with the lower and an average M_n of 3973.7 Da for the one with the higher masses (Fig 5.2 and Table 5-1).

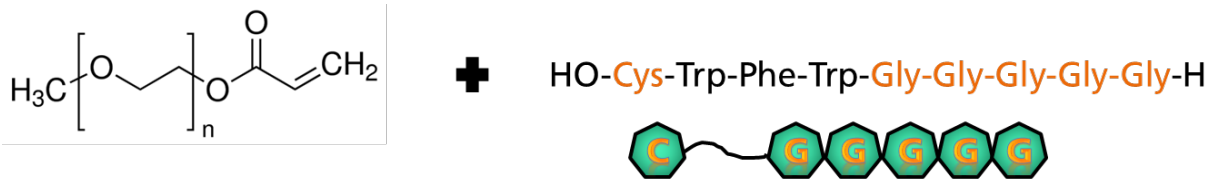

Fig 5.1 Overview of the modification of PEGMA with peptide 3.

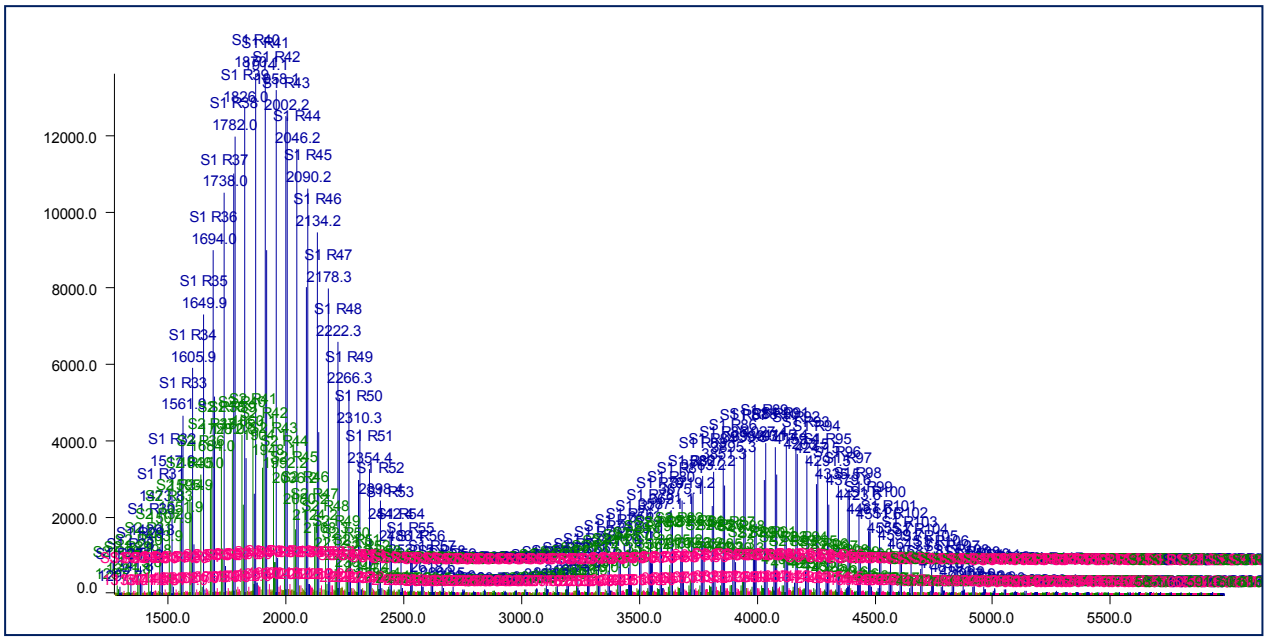

Fig 5.2 Assignment of PEGMA spectral features to the homopolymer series S1-S3 specified in Table 5.1 (Polymerix Software, Sierra Analytics).

Table 5-1 Assignment of PEGMA spectral features to homopolymer series S1-S3 (Polymerix Software, Sierra Analytics)

Series	M_n	M_w	M_z	PD	DP_n	DP_w	DP_z	Percent Series	Percent Spectrum
Total/Average	2667.218	3069.459	3471.892	1.151	58.825	67.962	77.103	100	95.67
S1	2713.812	3117.959	3500.632	1.149	59.687	68.866	77.558	80.61	77.12
S2	2309.982	2687.705	3181.627	1.164	51.741	60.32	71.539	16.06	15.37
S3	3263.082	3737.526	4176.951	1.145	72.163	82.939	92.92	3.33	3.18

Series Label	Alpha End Group	Repeat	Omega End Group	Charge State	Adduct	Adduct Charge	Formula
S1	CH_3	C_2H_4O	$C_3H_3O_2$	1	Na	1	CH_3 $[C_2H_4O]n$ $C_3H_3O_2$ + Na
S2	CH_3	C_2H_4O	OH	1	Na	1	CH_3 $[C_2H_4O]n$ OH + Na
S3	CH_3	C_2H_4O	$C_3H_3O_2$	1	K	1	CH_3 $[C_2H_4O]n$ $C_3H_3O_2$+ K

For the PEG-peptide 3 conjugate, four series S3-S6 (MH^+, MNa^+, MK^+, and MNH_4^+ species), colored in blue, were obtained (Fig 5.3). The bimodal distribution observed for the PEGMA starting material is maintained but accompanied with a mass shift to higher values due to the linkage of the peptide (MW = 926 g/mol). Residual PEGMA and PEG were detected as well (Table 5-2). The polymer PEGMA was used in slight excess for the linkage with the peptide and is hence still present in the sample after modification. Furthermore, the PEGMA starting material contains a series without methyl ether acrylate end group (Table 5-1) which therefore can't be modified with peptide.

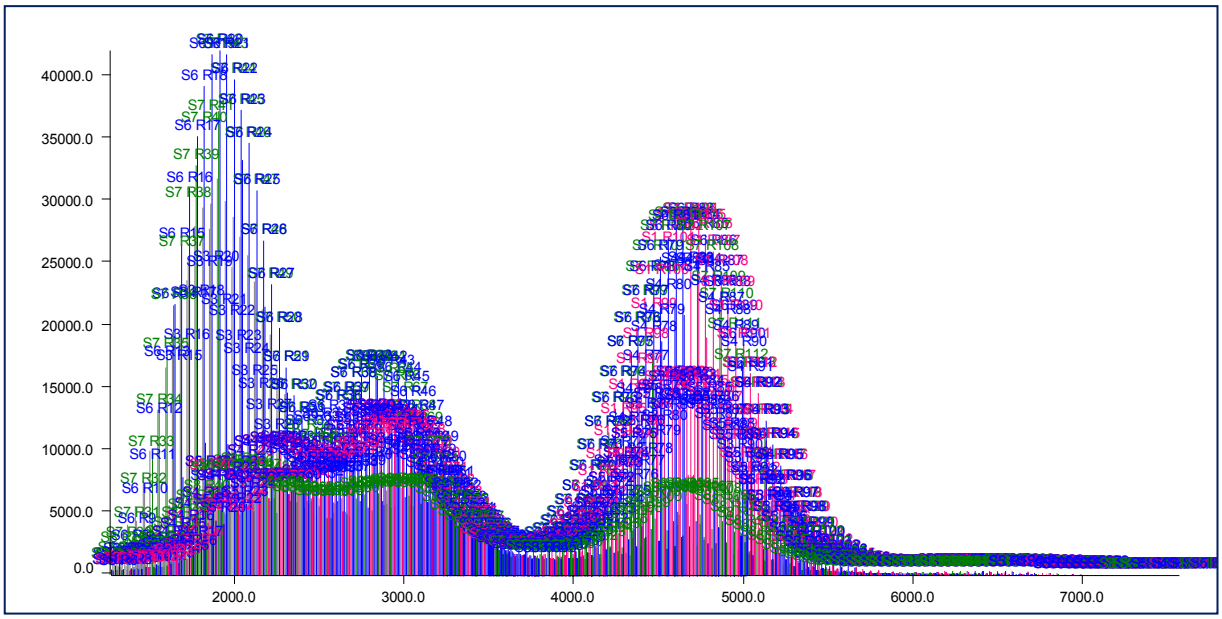

Fig 5.3 Assignment of PEG-peptide 3 conjugate spectral features to the homopolymer series S1-S8 specified in Table 5.2 (Polymerix Software, Sierra Analytics).

Table 5-2 Assignment of PEG-peptide 3 conjugate spectral features to homopolymer series S1-S8 (Polymerix Software, Sierra Analytics)

Series Label	M_n	M_w	M_z	PD	DP_n	DP_w	DP_z	Percent Series	Percent Spectrum
Total/Average	3106.419	3485.768	3847.545	1.123	59.173	67.789	76.007	100	90.51
S1	3194.554	3560.673	3917.722	1.115	70.606	78.922	87.032	6.05	5.47
S2	3398.037	3731.395	4028.177	1.098	75.228	82.8	89.541	10.4	9.41
S3	2686.168	3019.729	3400.209	1.124	38.04	45.617	54.259	16.27	14.72
S4	3127.648	3478.705	3831.261	1.112	48.068	56.042	64.05	5.83	5.27
S5	3390.837	3729.981	4031.661	1.1	54.046	61.749	68.602	9.96	9.01
S6	3299.075	3703.732	4060.022	1.123	51.962	61.153	69.246	14.96	13.54
S7	3029.715	3479.199	3892.599	1.148	68.089	78.298	87.688	24.57	22.23
S8	3049.471	3409.363	3759.979	1.118	68.537	76.712	84.676	11.98	10.84

Label	Alpha End Group	Repeat	Omega End Group	Charge State	Adduct	Formula
S1	CH_3	C_2H_4O	$C_3H_3O_2$	1	Na	CH_3 $[C_2H_4O]_n$ $C_3H_3O_2$+ Na
S2	CH_3	C_2H_4O	$C_3H_3O_2$	1	K	CH_3 $[C_2H_4O]_n$ $C_3H_3O_2$+ K
S3	CH_3	C_2H_4O	OOC-CH_2-CH_2-S-$C_{44}H_{50}N_{11}O_{10}$	1	H	CH_3 $[C_2H_4O]_n$ OOC-CH_2-CH_2-S-$C_{44}H_{50}N_{11}O_{10}$ + H
S4	CH_3	C_2H_4O	OOC-CH_2-CH_2-S-$C_{44}H_{50}N_{11}O_{10}$	1	Na	CH_3 $[C_2H_4O]_n$ OOC-CH_2-CH_2-S-$C_{44}H_{50}N_{11}O_{10}$ + Na
S5	CH_3	C_2H_4O	OOC-CH_2-CH_2-S-$C_{44}H_{50}N_{11}O_{10}$	1	K	CH_3 $[C_2H_4O]_n$ OOC-CH_2-CH_2-S-$C_{44}H_{50}N_{11}O_{10}$ + K
S6	CH_3	C_2H_4O	OOC-CH_2-CH_2-S-	1	NH_4	CH_3 $[C_2H_4O]_n$ OOC-CH_2-CH_2-S-$C_{44}H_{50}N_{11}O_{10}$

			$C_{44}H_{50}N_{11}O_{10}$			+ NH_4
S7	CH_3	C_2H_4O	OH	1	Na	CH_3 $[C_2H_4O]_n$ OH + Na
S8	CH_3	C_2H_4O	OH	1	K	CH_3 $[C_2H_4O]_n$ OH + K

5.4 Modification of PNIPAM with peptide

Poly(*N*-isopropylacrylamide) (PNIPAM) with maleimide chain-end functionalization was functionalized with peptide 4 bearing the LPETG recognition sequence in the same manner like PEGMA using a thiol-ene reaction between C=C polymer functional end group and thiol group of cysteine (Fig 5.4).

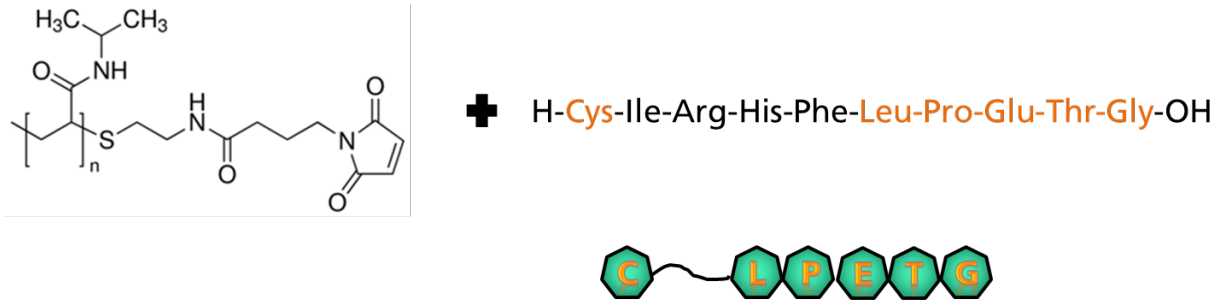

Fig 5.4 Overview of the modification of PNIPAM with peptide 4.

The assignment of distinct ion series to the mass spectrum of the PNIPAM chain-end functionalized with maleimide groups (Fig 5.5) was made difficult by the lack of information on the alpha-end group by the polymer provider. Common initiators for the synthesis of PNIPAM via ATRP are α-bromoisobutyric acid (BIBA, $C_4H_7O_2$) or azobisisobutyronitrile (AIBN, C_4H_6N); the homolytical cleavage of AIBN, e.g., produces two 2-cyanoprop-2-yl radicals which form the corresponding alpha-end group. The optimal assignment to the spectral features of the maleimide chain-end functionalized PNIPAM was in this case, however, obtained with a simple hydrogen atom forming the alpha-end group (Table 5-3).

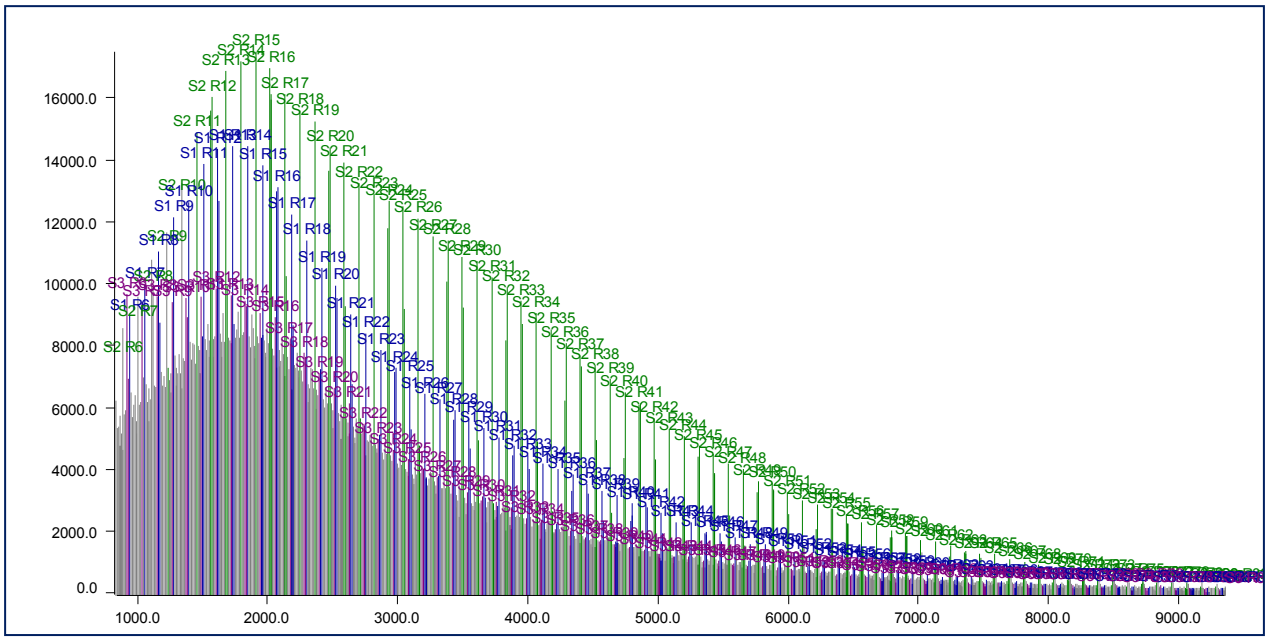

Fig 5.5 Assignment of PNIPAM spectral features to the homopolymer series S1-S3 specified in Table 5.3 (Polymerix Software, Sierra Analytics).

Table 5-3 Assignment of PNIPAM spectral features to homopolymer series S1-S3 (Polymerix Software, Sierra Analytics)

Series Label	M_n	M_w	M_z	PD	DP_n	DP_w	DP_z	Percent Series	Percent Spectrum
Total/Average	2940.566	3799.202	4713.751	1.294	24.048	31.641	39.729	100	29.18
S1	2806.555	3636.466	4550.281	1.296	22.678	30.017	38.097	31.31	9.13
S2	3233.803	4104.834	4935.246	1.269	26.898	34.601	41.944	41.95	12.24
S3	2637.568	3510.388	4557.735	1.331	21.183	28.902	38.163	26.75	7.8

Series Label	Alpha-End Group	Repeat	Omega-End Group	Charge	Adduct	Formula
S1	H	$C_6H_{11}ON$	$SCH_2CH_2NH(CO)CH_2CH_2CH_2(C_4H_2NO_2)$	1	Na	H $[C_6H_{11}ON]_n$ $SCH_2CH_2NH(CO)CH_2CH_2CH_2(C_4H_2NO_2)$ + Na
S2	$C_4H_7O_2$	$C_6H_{11}ON$	SCH_2CH_2COOH	1	Na	$C_4H_7O_2$ [$C_6H_{11}ON$]n SCH_2CH_2COOH + Na
S3	H	$C_6H_{11}ON$	$SCH_2CH_2NH(CO)CH_2CH_2CH_2(C_4H_2NO_2)$	1	Li	H [C6H11ON]n SCH2CH2NH(CO)CH2CH2CH2(C4H2NO2) + Li

Four different series were detected in the MALDI-ToF mass spectrum of PNIPAM-peptide 4 (Fig 5.6). While the PNIPAM oligomers were detected as sodium ions (Table 5-3), the charge of the peptide conjugate is mainly provided by protonation, presumably of the peptide part, and to a lower extent by sodium adducts (S1, S2 in Table 5-4). The successful linkage of the peptide causing a shift of 1150 Da (peptide 4 with a MW = 1172 g/mol) is proven. Like for the PNIPAM

starting material (Table 5-3) the optimal assignment to the spectral features is again obtained with a hydrogen atom forming the alpha-end group of the PNIPAM-peptide conjugate. To a lesser extent series were also assigned PNIPAM with BIBA and AIBN alpha-end groups.

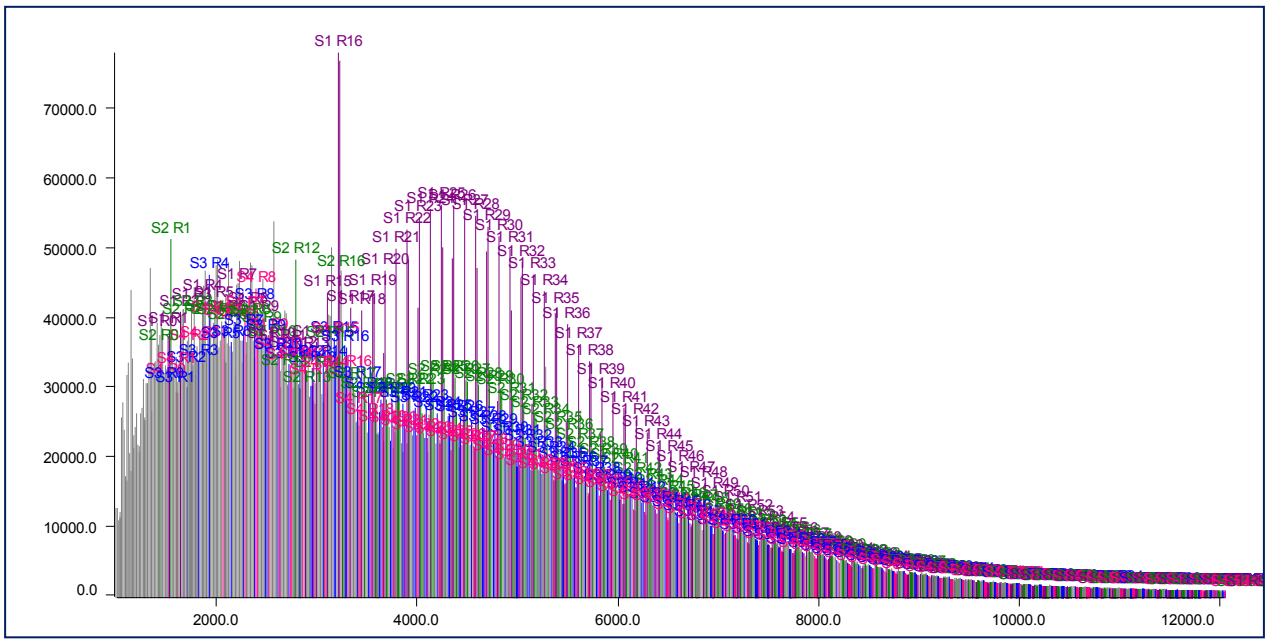

Fig 5.6 Assignment of PNIPAM-peptide 4 spectral features to homopolymer series S1-S4 as specified in Table 5.4 (Polymerix Software, Sierra Analytics).

Table 5-4 Assignment of PNIPAM-peptide 4 conjugate spectral features to homopolymer series S1-S4 (Polymerix Software, Sierra Analytics)

Series Label	M_n	M_w	M_z	PD	DP_n	DP_w	DP_z	Percent Series	Percent Spectrum
Total/Average	4363.871	5519.961	6820.906	1.265	25.79	36.014	47.518	100	37.11
S1	4394.992	5390.436	6533.843	1.226	26.364	35.167	45.278	30.38	11.27
S2	4351.796	5546.481	6855.732	1.275	25.982	36.547	48.124	25.37	9.41
S3	4359.861	5591.238	6977.653	1.282	25.46	36.349	48.609	22.74	8.44
S4	4338.396	5596.272	7019.565	1.29	25.103	36.226	48.812	21.51	7.98

Series Label	Alpha End Group	Repeat	Omega End Group	Charge State	Adduct	Formula
S1	H	$C_6H_{11}ON$	$SCH_2CH_2NH(CO)CH_2CH_2$ $CH_2(C_4H_2NO_2)C_{52}H_{81}N_{15}O_{14}S$	1	H	$H[C_6H_{11}ON]_nSCH_2CH_2NH(CO)CH_2CH_2CH_2$ $(C_4H_2NO_2)$ $C_{52}H_{81}N_{15}O_{14}S$
S2	H	$C_6H_{11}ON$	$SCH_2CH_2NH(CO)CH_2CH_2$ $CH_2(C_4H_2NO_2)C_{52}H_{81}N_{15}O_{14}S$	1	Na	$H[C_6H_{11}ON]_nSCH_2CH_2NH(CO)CH_2CH_2CH_2$ $(C_4H_2NO_2)$ $C_{52}H_{81}N_{15}O_{14}S$ + Na
S3	C_4H_6N	$C_6H_{11}ON$	$SCH_2CH_2NH(CO)CH_2CH_2$ $CH_2(C_4H_2NO_2)C_{52}H_{81}N_{15}O_{14}S$	1	H	$C_4H_6N[C_6H_{11}ON]_nSCH_2CH_2NH(CO)CH_2CH_2CH_2$ $(C_4H_2NO_2)$ $C_{52}H_{81}N_{15}O_{14}S$ + H
S4	$C_4H_7O_2$	$C_6H_{11}ON$	$SCH_2CH_2NH(CO)CH_2CH_2$ $CH_2(C_4H_2NO_2)C_{52}H_{81}N_{15}O_{14}S$	1	H	$C_4H_7O_2[C_6H_{11}ON]_nSCH_2CH_2NH(CO)CH_2CH_2CH_2$ $(C_4H_2NO_2)$ $C_{52}H_{81}N_{15}O_{14}S$ + H

5.5 SrtA reaction between peptide-PEG and PNIPAM-peptide building blocks

Finally, GGG-functionalized PEG and LPETG-functionalized PNIPAM were linked by means of SML. The expected reaction product of sortase-linked PNIPAM-peptide-PEG is shown in Fig 5.7 and with detailed peptide structure in Fig 5.8. The SrtA reaction was performed similar to the description for NP-Polymer and NP-NP linkage with the only difference in the reaction temperature. The optimal reaction temperature is usually reported to be around 37 °C, however, PNIPAM is water insoluble at this temperature because of its LCST behavior. Therefore, the temperature of the SrtA reaction was set to 28 °C, a temperature at which SrtA still has high activity (as proven by our collaboration partner Dr. Diana Mate, data not shown here).

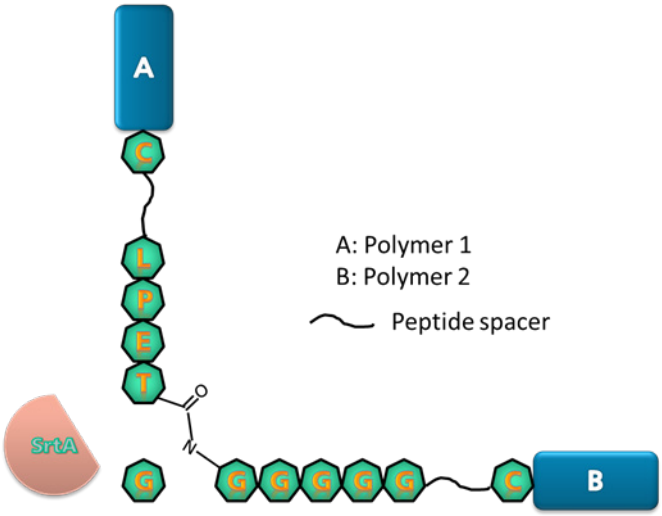

Fig 5.7 The linkage of PNIPAM (A) and PEG (B) via SrtA.

MALDI-ToF mass spectrometry proved successful to analyze the reaction product. It is remarkable that a MALDI mass spectrum of the triblock copolymer could be obtained as the characterization of block copolymers is difficult in general. After the SrtA reaction, there is not only a shift to higher m/z values but also a much broader molecular weight distribution as expected for a block copolymer (Fig 5.9, green spectrum). The mass spectrum reveals two main ion series with an unambiguous shift to higher molecular weights when compared to the PEG-peptide 3 and PNIPAM-peptide 4 conjugate precursors. Apart from the shift to higher molecular weight, the presence of the repeating units of both PEG and PNIPAM clearly confirms the linkage of the two polymer blocks. Fig 5.10 shows an excerpt of the mass spectrum of the block copolymer reaction product. The difference corresponding to the molecular weights of the repeating units could be found multiple times for both PEG and PNIPAM. Due to the downright complex nature of the sortase A linked reaction product (Fig 5.8), the high number of possible

polymer conjugates and resulting mass conflicts, an unambiguous assignment of m/z values to defined ion species with the Polymerix software tools is not possible.

Negative control experiment under same conditions but without SrtA was done as well. Fig 5.9 shows a comparison of the MALDI-ToF mass spectra of precursors, product and negative control. Analysis of single peaks of the polymer-peptide spectra, which both contain unmodified polymer, show exactly the MW of the linked peptides, well in agreement with the analysis presented in chapter 5.3 and 5.4. The molecular weight of the formed product after SML should be the sum of the two precursors minus 75, because one glycine should be cut off. Fortunately, I could identify such mass relationships in the spectra that suggest a successful product formation. For example, one m/z value from the peptide-modified PEGMA is 2887, and one m/z value from the modified PNIPAM is 4406. The sum of them minus 75 is 7218, exactly 21 more than 7197, which can be explained by a Na^+ ion for ionization. Hence, the mass values of reactors and product match very well in agreement with the mechanism of SrtA reaction and are therefore a sign for the successful linkage of the two functionalized polymer blocks. In contrast, the MALDI-ToF mass spectrum of the negative control experiment shows only the modified and unmodified polymers, but no sign for the linkage of the two substrates.

Although the unambiguous assignment of m/z values to defined ion species was not possible with Polymerix software tools, the successful linkage by sortase A is undoubtedly proven by the analysis of the mass spectra.

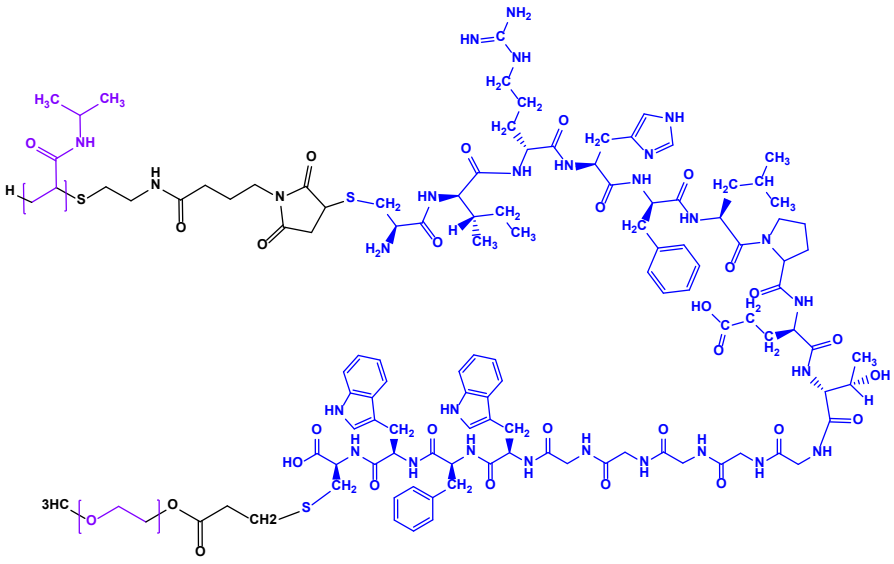

Fig 5.8 Structure of sortase A linked PNIPAM-peptide-PEG conjugate.

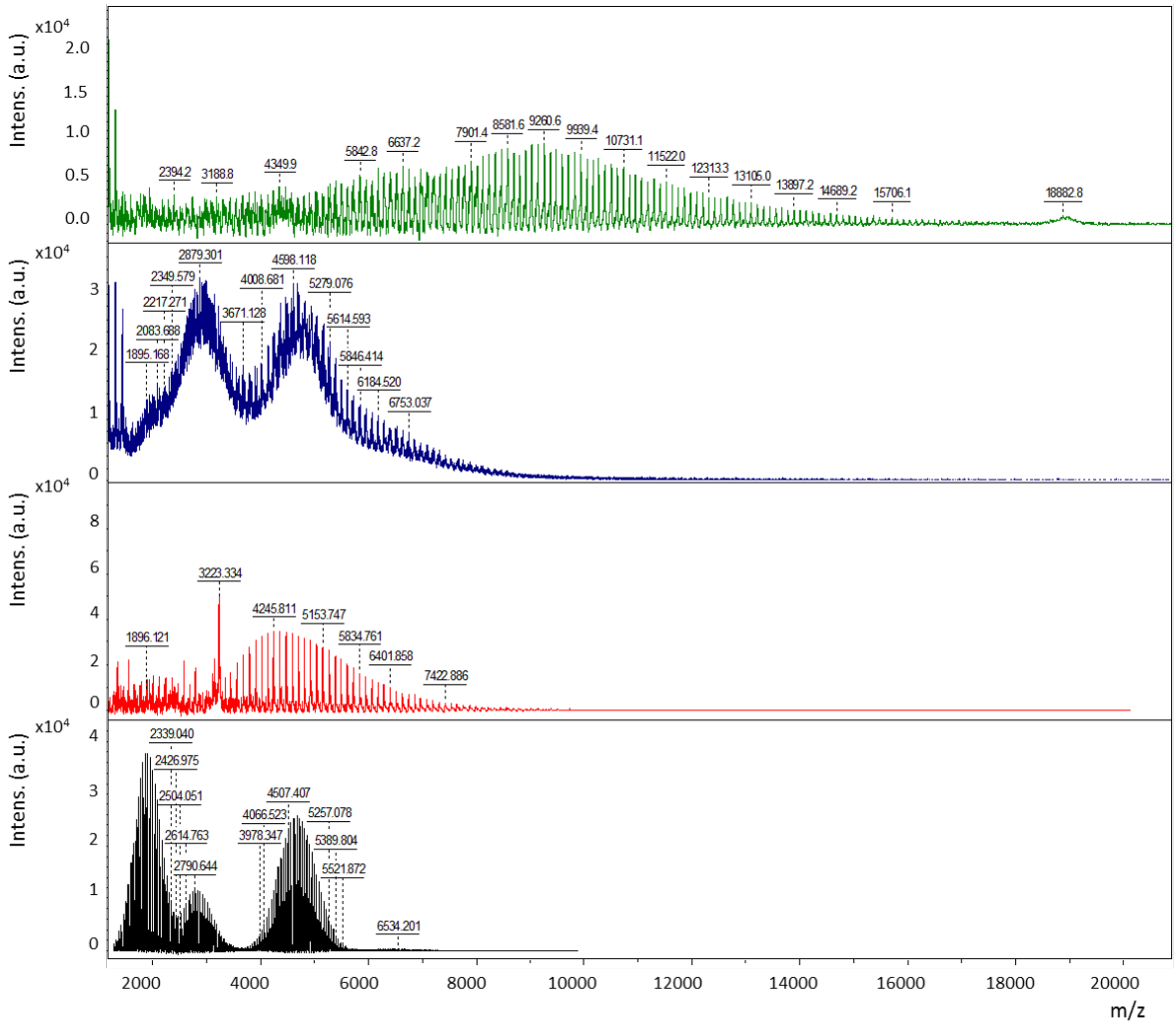

Fig 5.9 MALDI-ToF mass spectra of the sortase A linked polymer-peptide-polymer conjugate (green), negative control without SrtA and their PEG-peptide 3 (black) and PNIPAM-peptide 4 (red) precursors.

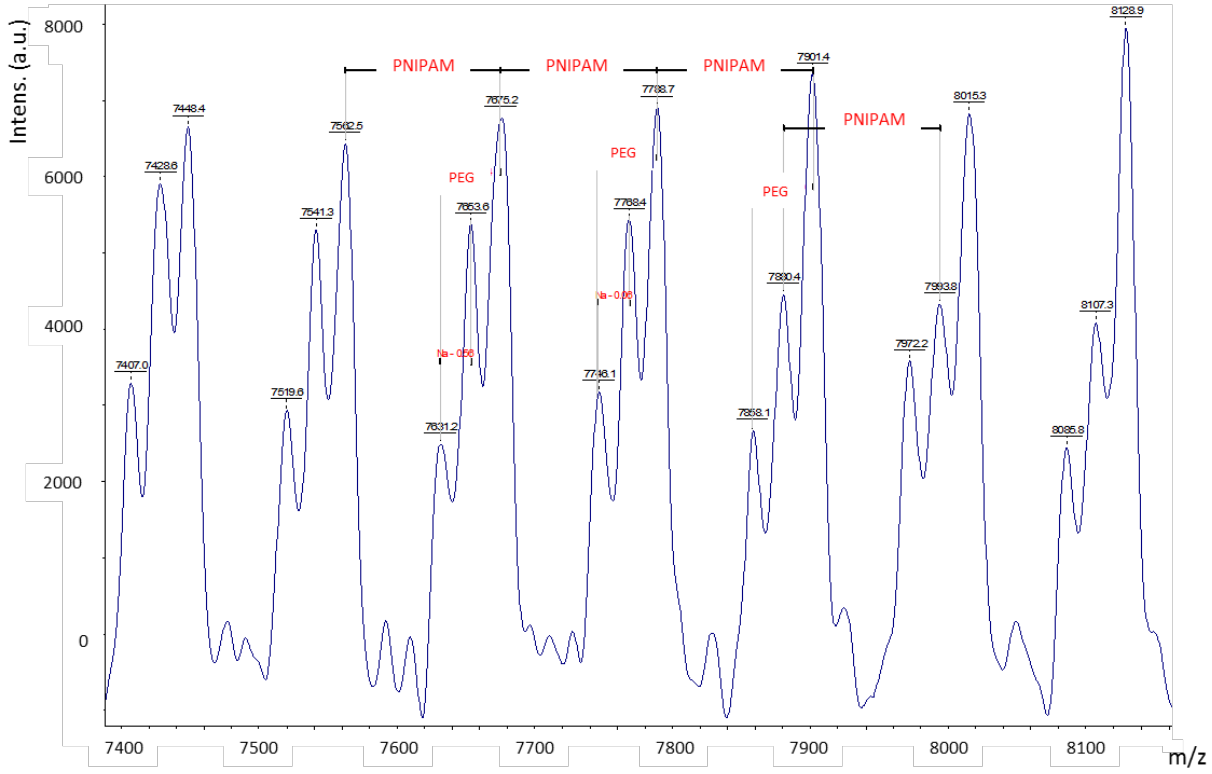

Fig 5.10 Section of the MALDI-ToF mass spectrum of the sortase A linked reaction product showing the presence of both PEG and PNIPAM repeating units in the molecular ion series.

5.6 Summary

This chapter demonstrates the linkage between the two polymer blocks PEG and PNIPAM catalyzed by the enzyme SrtA. The successful modification of PEGMA with peptide 3 and PNIPAM with peptide 4 were proven through analysis with MALDI-ToF mass spectrometry. SrtA reaction was performed below the phase transition temperature of PNIPAM to avoid the solution getting turbid. The molecular weight of the SrtA reaction product shifted significantly to a higher m/z value, while no change was observed for the negative control experiment without SrtA.

The MALDI-ToF mass spectra show undoubtedly that the linkage was successful, and hence that SML can also be applied for the linkage of sterically demanding polymer blocks. However, the presented approach has also distinct challenges. For example, the purification of the product has not been done because of the small scale of the performed reaction. To separate the product from unreacted polymer and polymer-peptide is quite difficult. For the characterization, gel permeation chromatography (GPC) was not possible because of the limited amount of the product. The costs of the commercial peptides are also quite high.

Nevertheless, the successful linkage between PEG and PNIPAM provides a variety of possibilities for the synthesis of block copolymers mediated by sortase A. This work reports for the first time, that a block copolymer can be synthesized via an enzymatic strategy, thus completing the classical chemical synthetic procedures, which could have a significant impact for the future developments. Although this proof of concept only shows examples that can be also synthesized by exclusively chemical techniques, a toolbox of such building blocks will enable the future formation of new materials and pave the way for the application of enzymes in materials science. The next chapter presents a newly developed approach for the synthesis of polymer-peptide building blocks suitable for SML that avoids a mixture of starting materials as well as using commercial peptides and polymers.

5.7 References

[1] D. J. Keddie, *Chem. Soc. Rev.* **2014**, *43*, 496–505.

[2] A. Muóz-Bonilla, S. I. Ali, A. Del Campo, M. Fernández-Garc??a, A. M. Van Herk, J. P. A. Heuts, *Macromolecules* **2011**, *44*, 4282–4290.

[3] R. Savić, A. Eisenberg, D. Maysinger, *J. Drug Target.* **2006**, *14*, 343–355.

[4] F. S. Bates, M. a. Hillmyer, T. P. Lodge, C. M. Bates, K. T. Delaney, G. H. Fredrickson, *Science* **2012**, *336*, 434–440.

[5] J. F. Lutz, *ACS Macro Lett.* **2014**, *3*, 1020–1023.

[6] K. Sugiyama, T. Oie, A. A. Ei-Magd, A. Hirao, *Macromolecules* **2010**, *43*, 1403–1410.

[7] P. L. Golas, K. Matyjaszewski, *Chem. Soc. Rev.* **2010**, *39*, 1338–1354.

6 Synthesis of polymer-peptide and peptide-polymer building blocks for sortase-mediated ligation

6.1 Introduction

In the last chapters, a new enzymatic strategy for linking different chemical building blocks was developed and applied to several systems. However, the polymer building blocks were synthesized using commercial polymers and peptides via 'click reaction', which was accompanied by a limited quantity of products and a mixture with starting material that could not be purified[1]. The main aim of this chapter is to present the synthesis of pure polymer building blocks that are amenable for sortagging. Therefore, strategies for the synthesis of polymer-peptide and peptide-polymer conjugates need to be developed, hence with the polymer unit attached to the N- or C-terminus, respectively, of the peptide.

The desired conjugates lay the foundation for the synthesis of any polymer building blocks for sortagging, therefore not limited by the use of commercial polymers with suitable end groups and only restricted to polymers that can be synthesized by the specific polymerization technique (see below). The polymer building blocks presented in this chapter are capable of being linked to diblock copolymers (diblock when the peptide spacer is not taken into account). However, these copolymers are not relevant for the polymer community as they can be synthesized much easier by exclusively chemical techniques. Nevertheless, they are the important step for future development of polymer building blocks with peptide sequences on both ends. In several years, such building blocks could be used for the sortase-catalyzed synthesis of multiblock copolymers with multiple different polymer blocks. The synthesis of such defined block copolymers is still an important issue in polymer synthesis.

Currently, the synthesis of protein-polymer conjugates with the polymer building blocks presented in this chapter is much more interesting. The conjugates available nowadays are often polydisperse with different number of attached polymer chains (see chapter 2.3.5). In contrast, sortase-mediated ligation allows the synthesis of defined conjugates with predefined position of the one attached polymer chain. Most studies of synthesizing protein-polymer conjugates directly by sortagging use commercially available PEG polymers with defined end group [2-6].The polymer building blocks presented in this chapter enlarge the portfolio considerably with different types of polymers and adjustable molecular weight. The syntheses of polymer building blocks were explored and developed herein by using reversible addition fragmentation chain

transfer (RAFT) polymerization due to several reasons. RAFT polymerization is performed without transition metal catalyst that could interact with peptides; and a broad variety of monomers can be used with this polymerization technique[7]. It allows the synthesis of polymer chains with defined end groups, more precisely, the chain transfer agent is usually not decomposed during the reaction[8]. Moreover, the RAFT group can be modified in a post-polymerization step for further functionalization of the polymer[8-10]. In general, CTAs can be synthesized with various functional groups which facilitate the linkage to peptides among others. Two different strategies are described in this chapter to enable polymer chains linked to C- and N-terminus of a peptide.

The design of the two polymer building blocks for sortagging is shown in Fig 6.1. For the nucleophilic sequence, G_n, the polymer needs to be attached to the C-terminus of the peptide. Peptides are synthesized from C- to N-terminus during solid phase peptide synthesis (SPPS).[11] Therefore, G_n-CTA can only be formed in two steps. First, the peptide is synthesized by SPPS, and second, after cleavage from the support, reacted with a suitable functional group from a CTA. Subsequently, the polymerization can be realized. Scheme 6.1 gives an overview of the strategy for the synthesis of peptide-polymer conjugates of this type. The nucleophilic sequence for sortase catalysis was composed of five glycines in the previous chapters. However, as the number of glycines within the nucleophile is not pivotal[12,13], we used a diglycine nucleophile in the framework of this chapter.

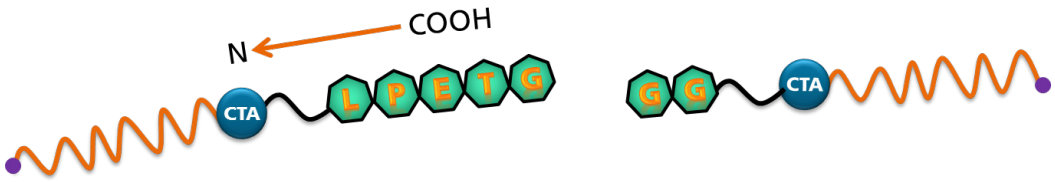

Fig 6.1 Design of polymer-peptide (left) and peptide-polymer (right) building blocks for sortagging. The arrow emphasizes the direction of peptide synthesis via SPPS.

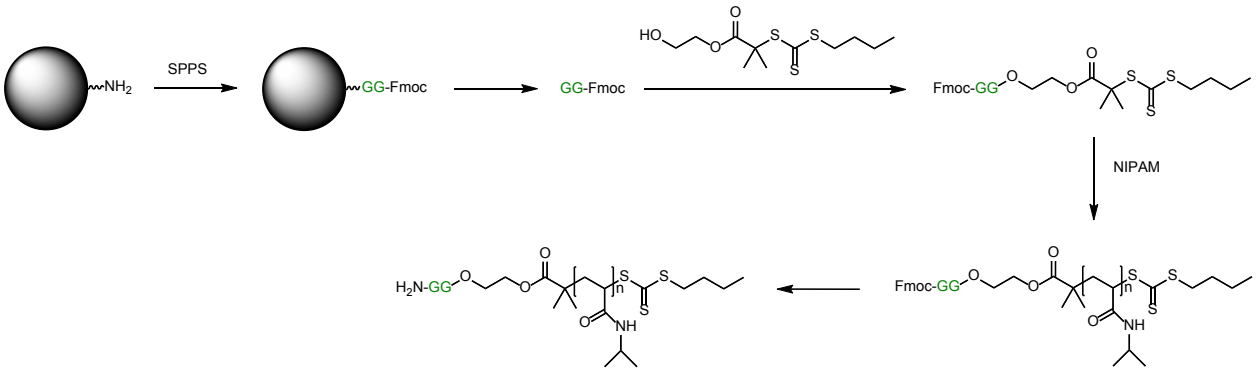

Scheme 6.1 Strategy for the synthesis of peptide-polymer building blocks. The grey sphere represents the resin from SPPS.

For polymer-peptide building blocks with the recognition sequence LPETG, the polymer has to appear on the N-terminal side of the peptide. Hence, a very elegant synthesis is to conduct the linkage of the CTA in a peptide synthesizer as the last ligation to the peptide chains before cleavage of the peptides from the resin. The groups of Börner and Wooley already demonstrated this strategy for the formation of conjugates via different polymerization techniques, namely ATRP[14,15], NMP[15] and RAFT polymerization[16-18]. At first, peptides with N-terminal attached dithiobenzoate CTAs were synthesized either by transformation of a linked ATRP initiator or by ligation of a CTA with carboxylic acid group[16]. However, a byproduct was formed by nucleophilic attack of the peptide amine terminus to the dithioester group. Upon ligating a trithiocarbonate – exhibiting a higher tolerance against nucleophiles – formation of significant amount of side products could be avoided[17]. RAFT polymerization of *n*-butyl acrylate could be performed from all described macrotransfer agents in a controlled manner[16,17]. Therefore, the CTAs used in the framework of this thesis are based on trithiocarbonates. Principally, the leucine N-terminus of the sortase recognition sequence LPETG should be reacted with a CTA bearing a COOH group. This can be performed in an automated step in a peptide synthesizer with the CTA instead of the last Fmoc-proteced amino acid. The strategy used in the framework of this thesis is illustrated in Scheme 6.2.

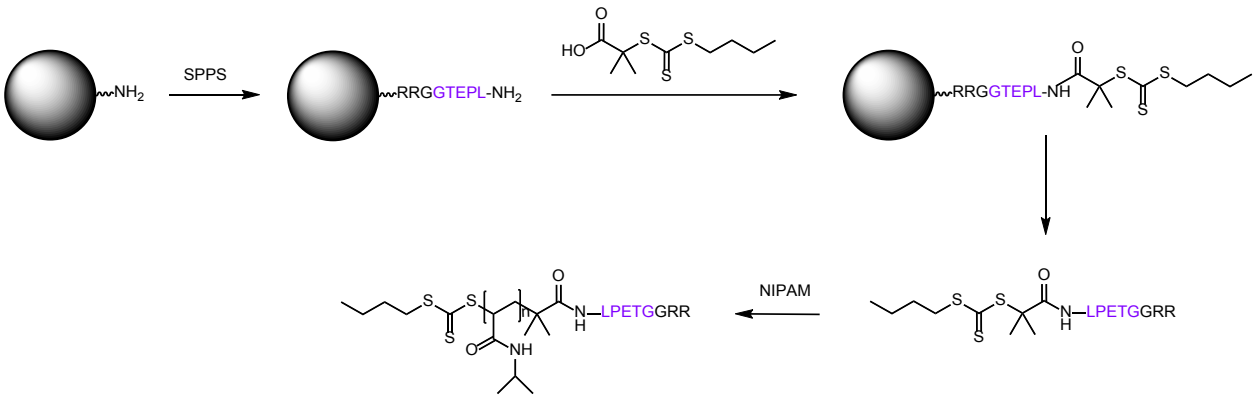

Scheme 6.2 Strategy of the synthesis of polymer-peptide building blocks. The grey sphere represents the resin from SPPS.

This chapter is organized as follows. After the Experimental Section, the synthesis of relevant CTAs is presented. Next, the synthesis of GG-PNIPAM building blocks is demonstrated. Finally, SPPS of important peptide sequences for sortase studies is discussed.

6.2 Preparation and characterization methods

6.2.1 Materials

The following chemicals were used as received from commercial suppliers: *n*-butanethiol, sodium hydroxide, carbon disulfide, 2-methyl 2-bromopropanoic acid, HCl (aq), dichloromethane (DCM), tetrahydrofuran (THF), magnesium sulfate, , maleimide, formaldehyde solution (37 wt.% in water), ethyl acetate, *n*-hexane, 1,4-dioxane, ethyleneglycol. *N*-isopropylacrylamide was purified by two successive recrystallizations from a mixture of *n*-hexane and benzene (4:1 v:v). 4,4‘-azobis(4-cyanovaleric acid) (ABCVA), N-Fmoc-L-glycylglycine, (97%, Alfa Aesar), *N,N’*-dicyclohexylcarbodiimide (DCC), and 4-(dimethylamino)pyridine (DMAP) were used as received. Millipore pure water with an electrical resistance of 18.2 MΩ·cm was used.

Several solvents and reagents were used with high purity for peptide synthesis: Dimethylformamide (DMF), N,N,N’,N’-tetramethyl-O-(1H-benzotriazol-1-yl)uronium hexafluorophosphate (HBTU), methylpyrrolidone (NMP), 4-methylmorpholine (NMM), triisopropylsilane (Tiips), trifluoroacetic acid (TFA), N,N’-diisopropylcarbodiimide (DIC), N-methylimidazole (NMI), piperidine. Fmoc-Rink-Amide-(aminomethyl)-Resin, Fmoc-Gly-TCP-Resin, Fmoc- and possibly side chain-protected amino acids were purchased from INTAVIS Bioanalytical Instruments AG (Köln).

6.2.2 Preparation

The syntheses of 2-(((butylthio)carbonothioyl)thio)-2-methylpropanoic acid (CTA 1), and 2-hydroxyethyl 2-(((butylthio)carbonothioyl)thio)-2-methylpropanoate (CTA 2) was performed according to the reference[19].

Synthesis of CTA 3: N-Fmoc-L-glycylglycine (720 mg, 2.04 mmol) and CTA 2 (60 mg, 0.20 mmol) were added into a flask with DCC (618 mg, 3.0 mmol), and dissolved in 6 mL THF. The mixture was then stirred while being cooled with an ice bath 5 minutes prior to the addition of DMAP (72 mg, 0.6 mmol). The flask was kept in the ice bath for 1 h and the reaction mixture was subsequently stirred overnight at room temperature. The resulting solution was added into approximately 20 mL diethyl ether, filtered and washed with 5% sodium hydrogen carbonate solution (3-times, 20 mL) and water (2-times, 20 mL). Next, the organic phase was dried over anhydrous magnesium sulfate, filtered and the solvent was removed under vacuum. The product was isolated by column chromatography using silica gel and ethyl acetate : pentane (1:1, v/v) as

eluent. The product (56 mg) was obtained in 43 % yield. ^{1}H-NMR (500 MHz, $CDCl_3$, 298 K) δ: 7.75 (d, J = 7.1 Hz, 2H, Ar-H), 7.59 (d, J = 6.3 Hz, 2H, Ar-H), 7.39 (m, 2H, Ar-H), 7.29 (m, 2H, Ar-H), 4.42 (m, 2H, -CH_2-), 4.32 (m, 2H, -CH_2-), 4.21 (m, 2H, -CH_2-), 4.09 (m, 1H, -CH-), 4.05 (m, 2H,-CH_2-), 3.92 (s, 2H, -CH_2-), 3.26 (t, J = 7.6 Hz, 2H, -CH_2-), 1.68 (s, 6H, -CH_3), 1.59 (m, 2H, -CH_2-), 1.40 (m, 2H, -CH_2-), 0.91 (t, 3H, -CH_3).

Polymerization of NIPAM from CTA 3 (with a targeted polymerization degree of 130): 174.5 mg NIPAM (1.54 mmol), 7.5 mg CTA 3 (0.012 mmol), 5 mL dioxane and 0.6 mg ABCVA (2.14 µmol) were introduced in a Schlenk flask with a magnetic stirring bar. The degassing process was performed via five freeze-evacuate-thaw cycles. The polymerization mixture was heated to 90 °C using an oil bath and kept stirring under nitrogen atmosphere for 6 h. Afterwards, the flask was immersed in liquid nitrogen to cool down the system and stop the polymerization. The mixture was transferred into a centrifuge tube and excess diethyl ether added to precipitate the PNIPAM. The precipitated PNIPAM was then washed 2-times with diethyl ether and dried under vacuum. Samples for NMR spectroscopic analysis were taken immediately after polymerization and after isolation of pure polymer.

Deprotection of N-terminus: Fmoc-GG-PNIPAM was dissolved in 2 mL piperidine : DCM (1:1, v: v) and stirred for 12 h. Diethyl ether was added to precipitate the polymer. The precipitate was then washed with diethyl ether and collected through centrifugation.

Solid phase peptide synthesis: SPPS was performed on an automated MultiPep RS peptide synthesizer from INTAVIS Bioanalytical Instruments AG (Köln) using a column module and a synthesis scale of 25 µmol. Respective amount of Fmoc-Rink-Amide-(aminomethyl)-Resin or Fmoc-Gly-TCP-Resin was weighed and placed in 2 mL reaction vessels. 0.5 M solutions of amino acids and HBTU in DMF were prepared. During SPPS, amino acids were activated by preparing a mixture of 200 µL HBTU in DMF, 50 µL NMM, 5 µL NMP and 210 µL of respective amino acid derivative solution. Coupling was performed with 4-fold derivative excess compared to peptide for 2-times 20 min. Cleavage of Fmoc groups was realized by 2-times addition of 450 µL 20 % piperidine in DMF for 3 and 8 min, respectively, and after the final coupling for 5 and 12 min, respectively. In case the Fmoc protection group should be preserved, the reaction vessel was removed from the synthesizer prior to this step. Washing during SPPS was performed with DMF and after the final step additionally with DCM.

The coupling product was liberated from the resin (ca. 1 g) by treatment with ca. 2 ml of a mixture of TFA : Tiips : MilliQ water (92.5 : 5 : 2.5) under shaking for 3 h. After precipitation in

ca. 50 mL ice-cold diethyl ether, the precipitate was centrifuged (4000 rpm, 10 min, 2 °C). The supernatant was decanted, the pellet resuspended in cold diethyl ether and the centrifugation process repeated (1- or 2-times). The product was then dissolved in water, lyophilized and stored at -20 °C until, if needed, purification, characterization or use in sortagging experiments.

Purification of peptides was performed by preparative liquid chromatography-mass spectrometry (LC-MS) systems from Waters GmbH (Eschborn, Germany). The instrument was equipped with Waters high performance liquid chromatography (HPLC) 2454 Binary Gradient Module, Waters XSelect CSH C18 prep 5 µm (10 x 150 mm), Waters SingleQuad (SQ) Detector, Waters UV/Vis Detector 2489 and Waters Sample Manager 2767. Solvent A consisted of H_2O + 0.05 % TFA and solvent B of acetonitrile + 0.05 % TFA. The sample was usually solved in H_2O / acetonitrile 95:5 with a concentration of 1 mg/ml. 1 ml of the sample was injected and a flow rate of 6 ml/min at 22 °C used. The following solvent gradient (A % : B %) was used: 0 min 95 : 5, 3 min 95 : 5, 18 min 60 : 40, 27 min 5 : 95, 28 min 95 : 5, 40 min 95 : 5. UV detection at 214 nm and electrospray ionization (ESI) mass detection (m/z 150-3000, 0.5 s scan time, positive mode, 30 V cone voltage) was used to trigger fraction sampling.

Synthesis approach to CTA 1-YLPETGG via SPPS: CTA 1 (455 mg, in 3.33 mL DMF) was used for the last coupling step instead of an amino acid derivative to be coupled to the amine group of peptides XLPETG. Different approaches were tested for the coupling of the CTA 1: prolonged coupling times (90 min), higher excess of 5-fold of the CTA 1 compared to the peptide, activation with DIC + NMP, DIC + NMI and DCC + NMP. The cycle “Final” was performed without the “Deprotection” step, hence without addition of piperidine in DMF.

6.2.3 Characterization methods

Analytical LC-MS: Characterization of peptides was performed with instruments from Waters GmbH (Eschborn, Germany). The system was equipped with Waters HPLC 2454 Binary Gradient Module, Waters XSelect CSH C18 5 µm (4.6 x 250 mm), Waters SingleQuad (SQ) Detector, Waters UV/Vis Detector 2489 and Waters Sample Manager 2767. Solvent A consisted of H_2O + 0.05 % TFA and solvent B of acetonitrile + 0.05 % TFA. The sample was usually solved in H_2O / acetonitrile 95:5 with a concentration of 1 mg/ml. 20 µl of the sample was injected and a flow rate of 1 ml/min at 22 °C used. The following solvent gradient (A % : B %) was used: 0 min 95 : 5, 5 min 95 : 5, 30 min 60 : 40, 45 min 5 : 95, 46 min 95 : 5, 60 min 95 : 5. UV detection at 214 nm and ESI mass detection (m/z 150-3000, 0.5 s scan time, positive mode, 30 V cone voltage) was used.

NMR spectroscopy: Proton nuclear magnetic resonance (^{1}H-NMR) spectra were recorded on an INOVA 500 spectrometer from Varian Inc. at 500 MHz. $CDCl_3$, dimethylsulfoxide (DMSO)-d_6 and D_2O were used as solvents. Measurements were performed at room temperature. The signal of non-deuterated solvent was used as internal standard.

Gel permeation chromatography: Polymer number-average molecular weight (M_n,GPC), weight-average molecular weight (M_w,GPC), and molecular weight distribution (also polydispersity index, PDI) were determined by GPC using DMF with LiBr (1 mg/mL) as eluent, a flow rate of 1.0 mL/min, a high pressure liquid chromatography pump (Spectra Systems P 1000), and a refractometer SEC-3010 (WGE Dr. Bures) detector. Calibration was achieved using polystyrene standards. Results were evaluated using Parsec 5.62 (Brookhaven Instruments) software.

ESI -MS: The products were analyzed by LC-MS using a Flexar SQ300 MS detector from PerkinElmer run in ESI set-up. The samples were diluted in MeCN : H_2O : Formic acid (50 : 50 : 0.1) and applied with a flow rate of 15 µL/min. We used positive ion mode at a drying gas temperature of 300 °C with all voltages automatically set by calibration with the used mass range. The measurements were averaged over 1 min and the dominating m/z signals were evaluated.

MALDI-ToF mass spectrometry: Spectra were acquired using a 337 nm laser Bruker microflex MALDI-ToF mass spectrometer (Bruker, Bremen, Germany) with pulsed ion extraction. The masses were determined in positive ion linear mode. The sample solutions were applied on a ground steel target using the dried droplet technique. Mass calibration was performed with external calibration. Polymer samples were prepared as follows: α-cyano-4-hydroxycinnamic acid (CCA) was used as matrix substance in a 10 mg/ml solution in Millipore water : acetonitrile 7:3 with 0.1 % trifluoroacetic acid. Sodium trifluoroacetate was used as salt in 0.1 mol/L solution in the same solvent mixture. Sample (5 mg/mL), matrix and salt solutions were mixed in 5:20:1 ratio and 2 µL of the mixture applied on the target.

UV/Vis spectroscopy: The measurements were performed using SPECORD 210 UV-Vis spectrometer from Analytik Jena.

6.3 Synthesis of CTA 1

CTA 1, namely 2-(((butylthio)carbonothioyl)thio)-2-methylpropanoic, was chosen due to the higher stability of the trithiocarbonate group against nucleophiles compared with dithioesters on

the one side, and the variety of possibilities for modification of the carboxylic acid group on the other side. This CTA can be directly used to link a peptide via its N-terminus. Furthermore, different functional groups can be easily introduced via modification of CTA's carboxylic acid group. Synthesis of CTA 1 was performed according to a literature procedure[17] (Scheme 6.3) and the ^{1}H-NMR spectrum of the obtained product (Fig 6.2) is well in agreement with the literature report[17]. CTA 1 was subsequently used for experiments to link a peptide via its N-terminus (see subchapter 6.7) and in parallel as precursor to synthesize CTA 2 (see 6.4).

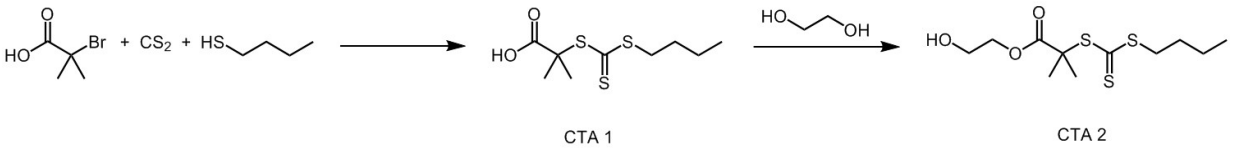

CTA 1 CTA 2

Scheme 6.3 Synthesis route of CTA 1 and CTA 2.

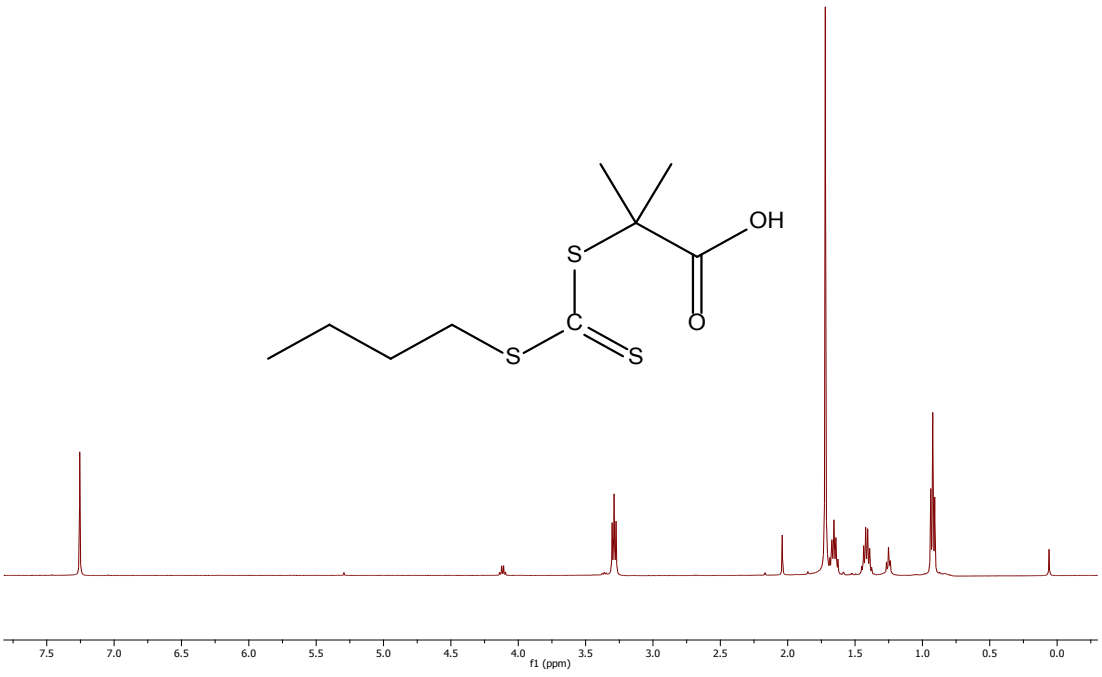

Fig 6.2 ^{1}H NMR spectrum of CTA 1 measured in $CDCl_3$.

6.4 Synthesis of CTA 2

CTA 2 was designed to meet the needs of a functional group that can be reacted with the C-terminus of a peptide. For instance, the oligo glycine nucleophilic sequence for the SrtA reaction requires a free N-terminus while the C-terminus can be linked with a CTA. Therefore, CTA 2 contains a hydroxy function that can be reacted with the carboxylic acid group of the peptide in an esterification reaction which is easy to perform in high yield. CTA 2 was successfully

prepared following a published procedure[19]. The ^{1}H-NMR spectrum of CTA 2 (Fig 6.3) is in agreement with literature data.

Fig 6.3 ^{1}H-NMR spectrum of CTA 2 measured in $CDCl_3$.

6.5 Synthesis of CTA 3

In order to synthesize an oligoglycine motif with a CTA attached to the C-terminus (Scheme 6.1), different oligoglycine containing peptides were formed with the peptide synthesizer. It is important that the Fmoc protection group is preserved so that no kind of polymerization of the oligoglycine occurs during reaction with a functional CTA. This could be easily achieved by omitting the last deprotection during SPPS as verified by ESI MS. However, two inherent problems of solid phase peptide synthesis appeared to complicate the process. First, SPPS with multiple repetition of the same amino acid is inefficient and leads to low yields. Second, very short peptide sequences often do not precipitate in diethyl ether or methyl-isopropyl ether during workup and are consequently difficult to isolate after cleavage from the resin. In our lab, Fmoc-triglycine could not be isolated by precipitation in one of the two used ethers. In contrast, a pentaglycine precipitated in diethyl ether, although the amount was comparably low (not exactly determined as a mixture was obtained). However, the crude material contained 66 % Fmoc-G_5,

25 % Fmoc-G_4 and 3 % Fmoc-G_3. No effort was put in the workup of this mixture by HPLC as the yield of isolated pure product would be too low to represent an efficient approach for the synthesis of peptide-polymer conjugates. An option could be to add several more amino acids on the C-terminal side of the peptide in order to enable both efficient synthesis and isolation of for example a diglycine derivative. However, previous chapters indicated that longer spacers are not needed during sortagging with sterically demanding building blocks. Addition of amino acids that are not needed is not economically preferable as solvents and reagents for SPPS are expensive. Therefore, a different option was realized to obtain the product described in Scheme 6.1. Fmoc-L-glycylglycine (Fmoc-G_2) was commercially available and obtained from Alfa Aesar for a low price – probably less than the cost for own SPPS of such a peptide in lab scale.

Fmoc-G_2 (see Fig 6.4 for ^{1}H-NMR spectrum) was reacted with CTA 2 in a typical esterification reaction using DCC and DMAP. The resulting CTA 3 was isolated by column chromatography and characterized via ^{1}H-NMR spectroscopy (Fig 6.5) and ESI MS (Fig 6.6).

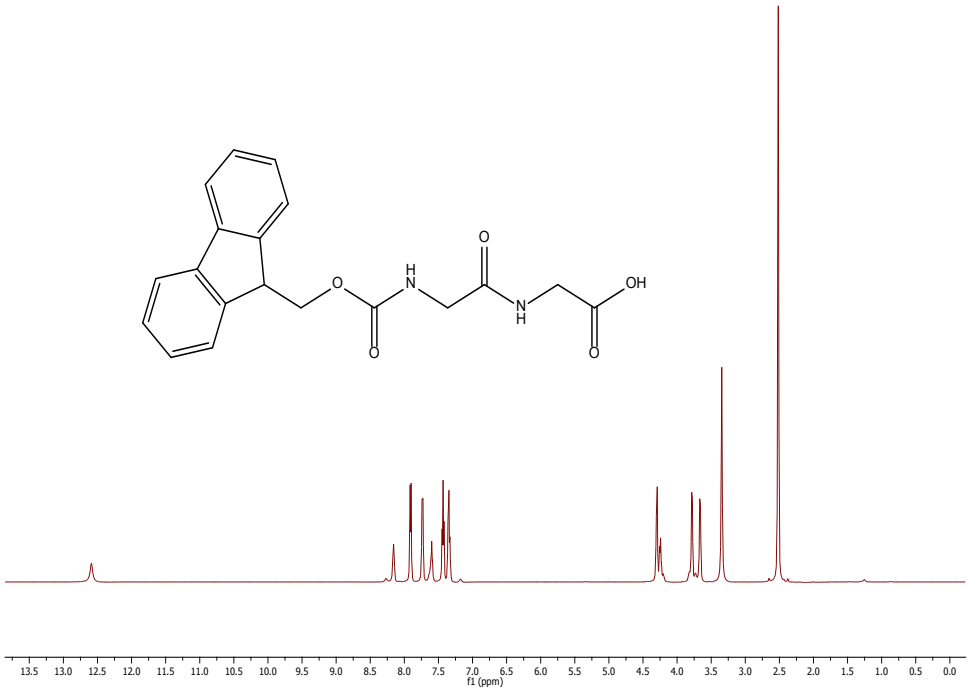

Fig 6.4 ^{1}H-NMR spectrum of Fmoc-L-glycylglycine measured in DMSO-d_6.

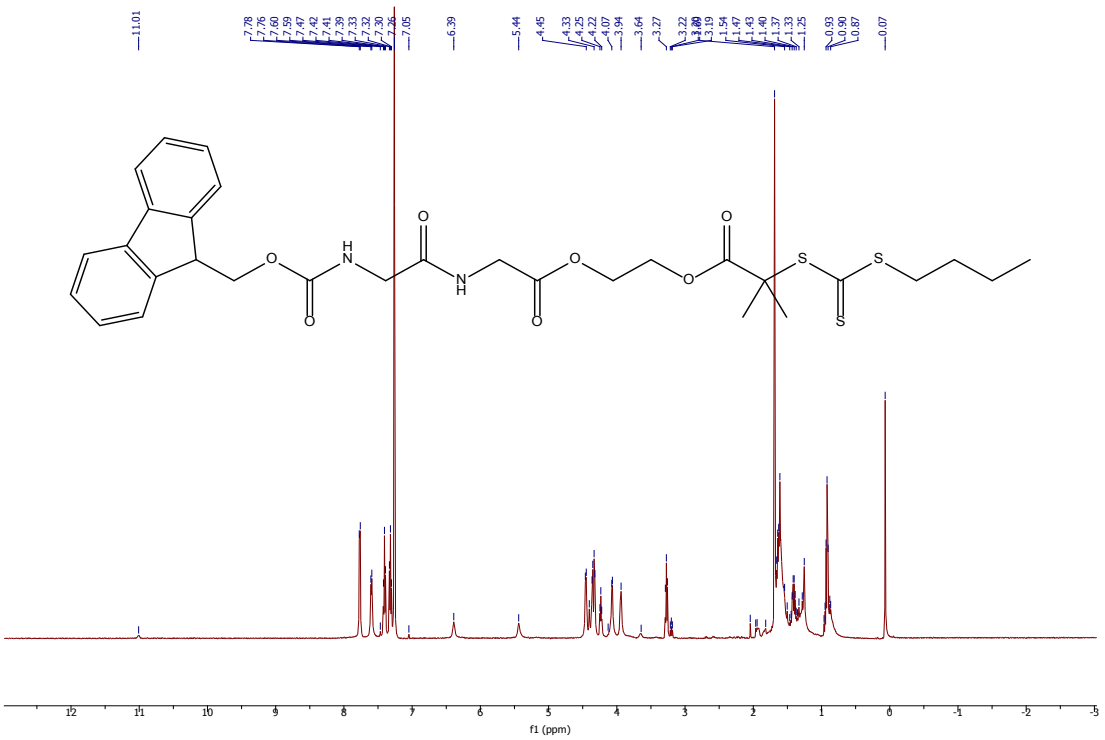

Fig 6.5 ^{1}H-NMR spectrum of CTA 3 measured in $CDCl_3$.

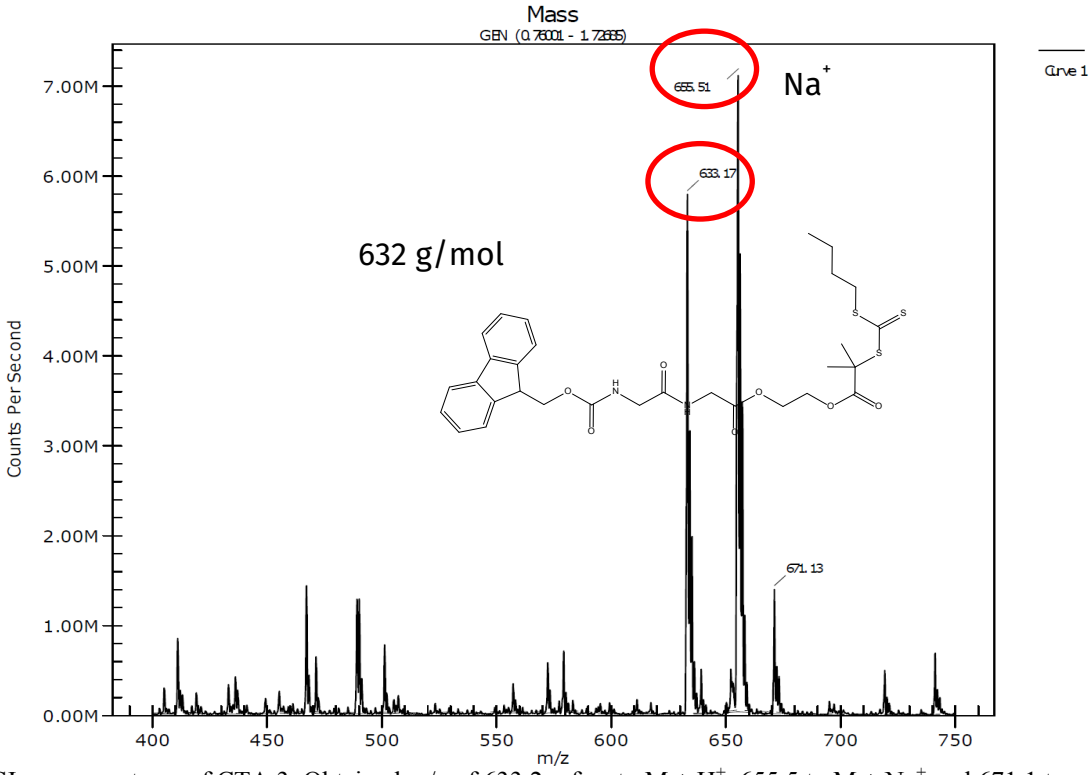

Fig 6.6 ESI mass spectrum of CTA 3. Obtained m/z of 633.2 refers to M + H^+, 655.5 to M + Na^+ and 671.1 to M + K^+.

The ^{1}H-NMR spectrum of the product matches the structure of CTA 3 and all signals belonging to the compound could be found. According to the ^{1}H-NMR spectrum of CTA 2 and Fmoc-L-glycylglycine, the chemical shift of some -CH_2- groups slightly changed.

The ESI mass spectrum of CTA 3 shows the following main signals: M+1 (H^+), M+23 (Na^+) and M+39 (K^+), which likewise verifies the successful synthesis of CTA 3.

Hence, CTA 3 can be applied as chain transfer agent to the polymerization via RAFT to form a peptide-polymer conjugate.

6.6 Preparation of GG-PNIPAM

After synthesis of Fmoc-GG-CTA, the next step is to synthesize a corresponding peptide-polymer conjugate (Scheme 6.4). For the polymerization from the peptide-CTA conjugate, NIPAM was chosen as monomer due to the outstanding thermo-stimuli property of PNIPAM, which has a lower critical solution temperature at 32 °C. This property enabled PNIPAM to be extensively studied in a variety of aspects such as functional materials and drug delivery carriers, among others.

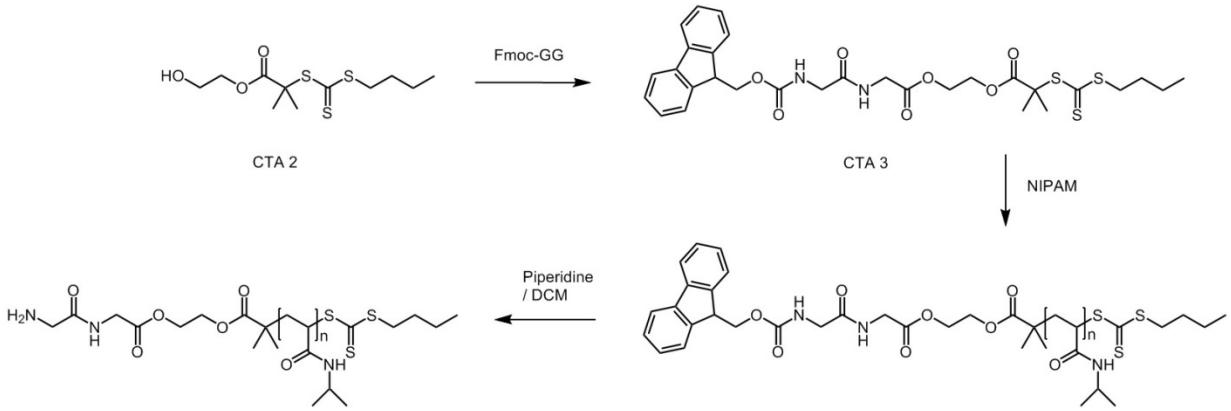

Scheme 6.4 Overview of the synthesis of Fmoc-GG-CTA, followed by polymerization of NIPAM and cleavage of Fmoc group to yield peptide-polymer conjugates.

Polymerization of NIPAM was conducted in dioxane for 6 h at 90 °C with ABCVA as photoinitiator and a targeted polymerization degree of 130. After polymerization, a sample was taken for NMR spectroscopic analysis before isolation of the polymer. The NMR spectrum of the mixture shows both signals of PNIPAM and residual monomer (Fig 6.7). A conversion of 84 % was reached as calculated through integration of signals belonging to monomer or polymer, respectively. The appearance of signals from aromatic groups confirms the preservation of Fmoc group from CTA 3. The peptide-polymer conjugate was isolated by precipitation in diethyl ether before being further characterized by NMR spectroscopy and GPC. The polydispersity index (PDI) turned out to be 1.6 (Fig 6.8a), which is slightly higher than expected for a controlled polymerization process and should be later improved by optimization of polymerization conditions.

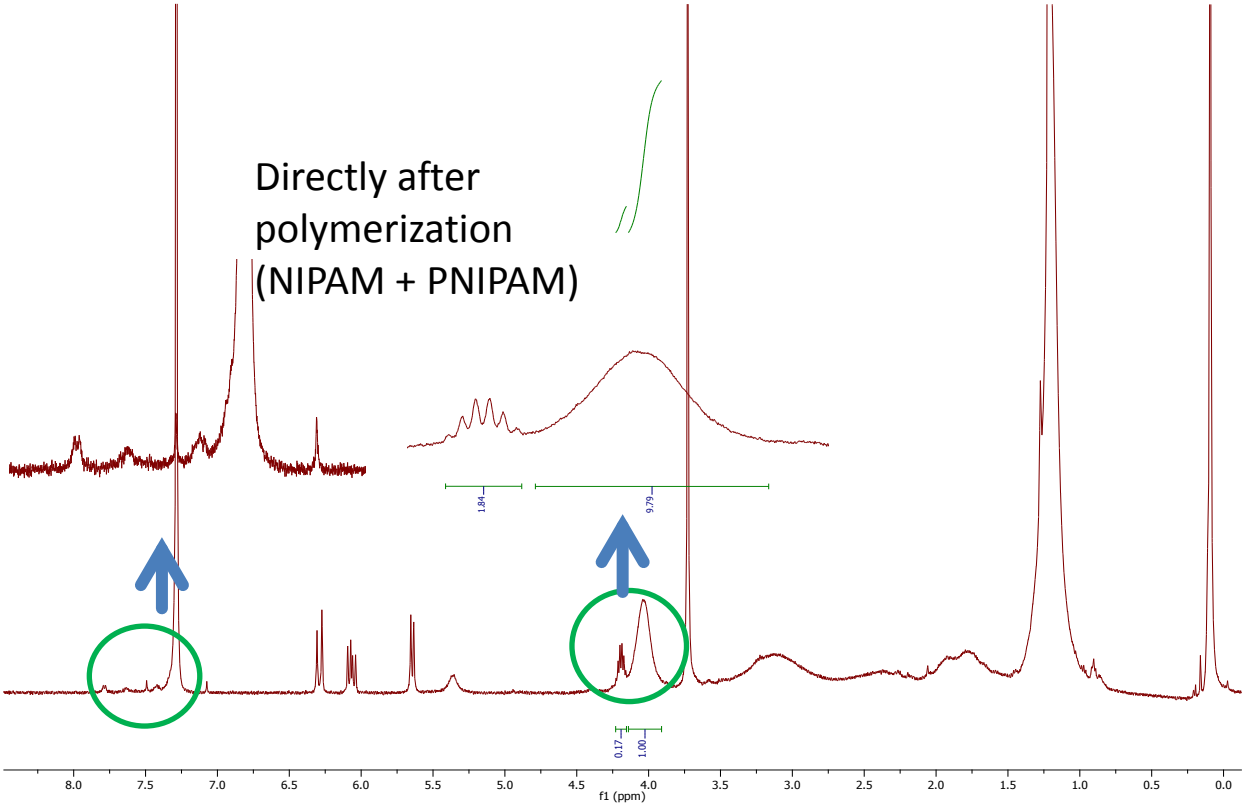

Fig 6.7 ^{1}H-NMR spectrum of the NIPAM polymerization solution after 6 h before workup, measured in $CDCl_3$.

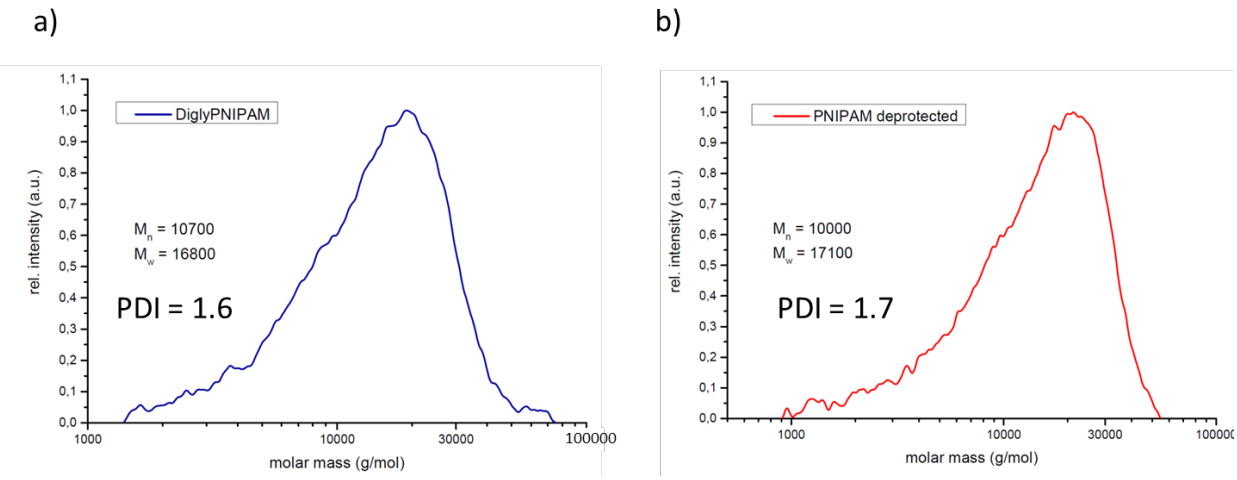

Fig 6.8 Gel permeation chromatographs of Fmoc-GG-PNIPAM (a) and GG-PNIPAM (b), measured in DMF.

As last step to liberate the nucleophilic diglycine unit, cleavage of Fmoc group was performed according to literature procedures. Usually, Fmoc is cleaved by piperidine in DCM with typical reaction times of 10-30 min[20]. In order to ensure cleavage at the end of a synthetic polymer chain, the reaction time was increased to 12 h. The product was again isolated by precipitation in diethyl ether and GG-PNIPAM characterized via NMR and UV/Vis spectroscopy as well as MALDI-ToF mass spectrometry and GPC. The disappearance of signals corresponding to aromatic groups in the NMR spectrum (Fig 6.9) and disappearance of the aromatic absorption band in the UV spectrum between 250-280 nm (Fig 6.10) imply the successful deprotection. As expected, molecular weight and PDI obtained by GPC analysis changed only slightly upon cleavage of Fmoc (Fig 6.8b).

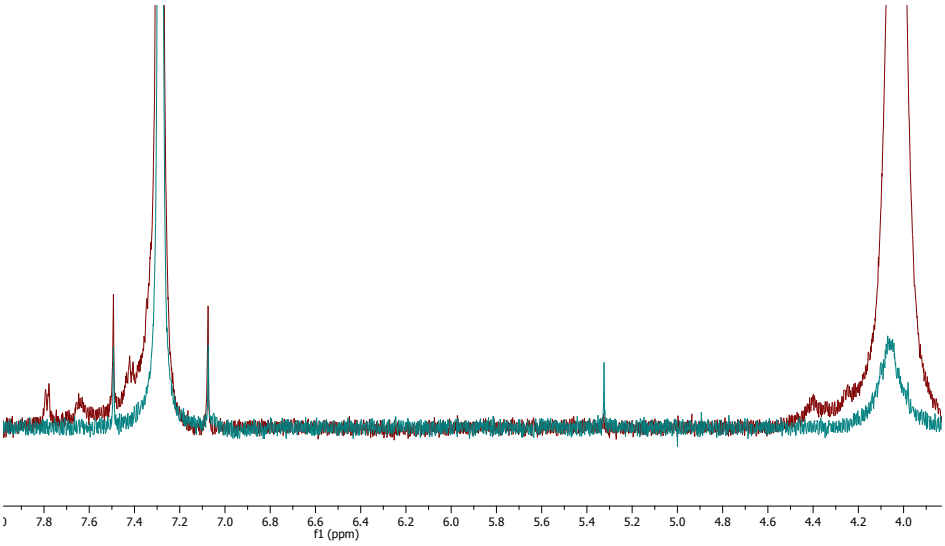

Fig 6.9 ^{1}H-NMR spectra of Fmoc-GG-PNIPAM (red) and GG-PNIPAM (green), both measured in $CDCl_3$.

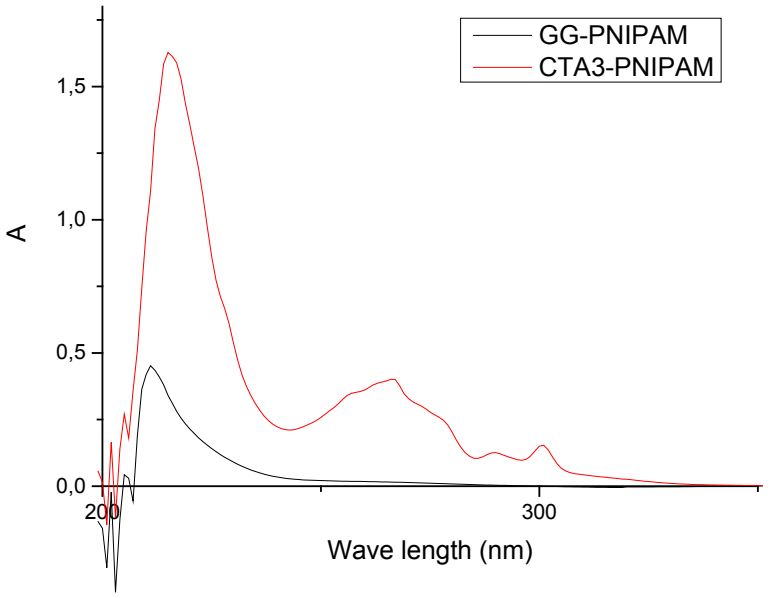

Fig 6.10 UV spectra of Fmoc-GG-PNIPAM (red) and GG-PNIPAM (black), measured in ethanol.

MALDI-ToF mass spectra were compared for PNIPAM synthesized from CTA 2 (CTA without linkage of Fmoc-GG), CTA 3 (Fmoc-GG-PNIPAM) and after deprotection (GG-PNIPAM). However, the theoretical difference of the molecular weight between the CTA 2 and CTA 3 is 337, which nearly equals to three times NIPAM repeat units and results in the difficulty to distinguish the two polymers. Similarly, the difference of the molecular weight between Fmoc-GG-PNIPAM and GG-PNIPAM is 224, which is almost the same as two times NIPAM repeat units. Hence, in this case, MALDI-ToF MS was not suitable to demonstrate the successful cleavage of the Fmoc group. However, absence of signals belonging to the Fmoc group in the NMR spectrum clearly verified the deprotection.

To conclude, peptide-polymer conjugates with nucleophilic sequence for sortagging could be successfully synthesized. There are several advantages of this strategy. First a composite peptide-CTA was formed via an esterification, which was easy to perform and reached a high yield. Polymerization was carried out on the basis of the peptide-CTA, purification was easily performed by precipitation, followed by a standard deprotection procedure. Thus, an N-terminal-free peptide-polymer conjugate could be obtained.

6.7 Peptide synthesis for polymer-peptide conjugates

In addition to peptide-polymer conjugates, similar conjugates with opposite orientation of the peptide are desired to have the complete portfolio for sortase-mediated ligation. As indicated in

the Introduction of this chapter, such conjugates can be synthesized via the linkage of a CTA as last step during peptide synthesis prior to polymerization (Scheme 6.2). At first, several peptides containing the sortase A recognition sequence were synthesized in order to evaluate the conditions for successful peptide synthesis with the newly installed peptide synthesizer in Fraunhofer IAP (Fig 6.11). Subsequently, experiments were performed in order to link CTA 1 to the N-terminus of the peptide XLPETGG. As previous studies showed that addition of at least one amino acid to the LPXTG recognition sequence improves the efficiency of sortagging[21], LPETGG was used within this chapter. One spacer amino acid was placed between recognition sequence and CTA (see below).

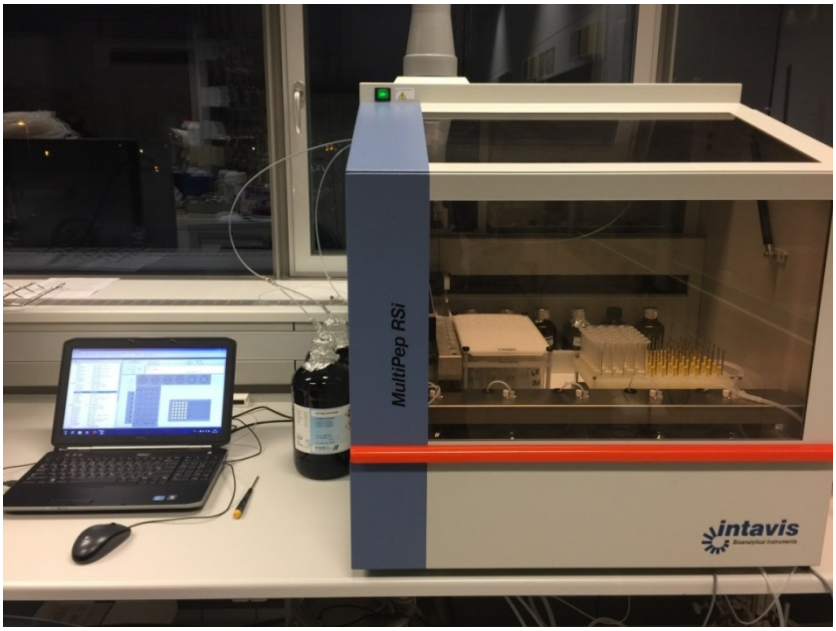

Fig 6.11 Picture of peptide synthesizer in Fraunhofer IAP.

At first, the peptides LPETGG and LPETGGRR were synthesized. Usually, a glycine is added after the recognition sequence and often peptides with additional -GRR used for SML. The peptides were synthesized using standard coupling conditions for Fmoc-protected amino acids. Two different resins were used: a standard Fmoc-Rink-Amide-(aminomethyl)-Resin giving an amide at the C-terminus after cleavage of the peptide from the resin and an Fmoc-Gly-TCP-Resin which is preloaded with a glycine and its cleavage results in a carboxylic acid group at the C-terminus. The amino acid derivatives were activated by HBTU in DMF and NMM and coupling performed using a 4-fold excess of the derivative compared to the peptide. Cleavage of Fmoc was conducted with 20 % piperidine in DMF. The peptides were liberated from the resin utilizing TFA, isolated by precipitation in diethyl ether, centrifugation, lyophilization, and finally subjected to purification by HPLC and analysis by ESI mass spectrometry. Several peptides

could be successfully synthesized using this procedure. Exemplarily, the peptide LPETGGRR could be isolated in 97 % purity. The ESI mass spectrum shows the 1- and 2-times charged species (Fig 6.12).

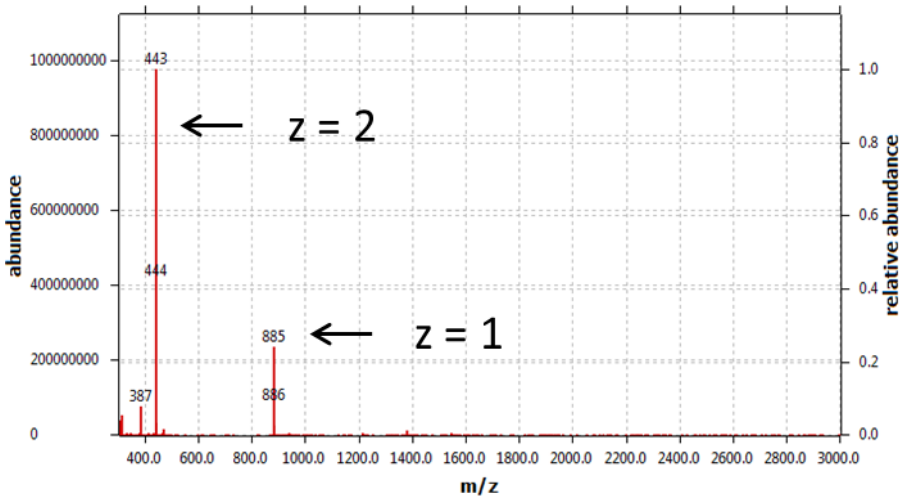

Fig 6.12 ESI mass spectrum of the peptide LPETGGRR.

The process described so far was subsequently extended to the linkage of CTA 1, hence synthesis of CTA 1-XLPETGG. After the desired peptide sequence XLPETGG (in opposite direction from C- to N-terminus) was formed, coupling between the last amino acid (free -NH_2 group after deprotection) and the carboxylic acid group from CTA 1 can be achieved in an automated fashion in the peptide synthesizer before cleavage of the CTA-peptide conjugate from the resin. The first attempt was to use the same coupling conditions like for an amino acid derivative. Afterwards, the reaction conditions were varied according to lessons learnt from first attempts and literature reports.

Fig 6.13 shows the ESI mass spectrum of the product from the first attempt for synthesis of CTA 1-YLPETGG. No peak of the desired product could be found (although the range of the spectrum shown in Fig. 6.13 is too small). Instead, m/z values appear that can be assigned to pure peptide and a cleaved species of the product (Fig 6.14). The m/z value of the main product shown in Fig 6.12 is 836.4. It is assumed that the trithiocarbonate group was cleaved which results in a product consisting of the peptide and only a part of the CTA 1 structure.

Thiocarbonylthio groups are known to react with nucleophiles and ionic reduction agents like amines, thiols, hydroxides and boron hydrids[8,9]. Such a cleavage by a nucleophile (like indicated with the dotted line in Fig 6.14) would lead to a –SH functional group and explain the observed m/z value. Possible nucleophiles are bases used for activation of amino acids or for

cleavage of Fmoc protecting group.

In this regard, it should be noted that the cycle "Final" of a standard peptide synthesis consists of the cleavage of the Fmoc group after the last coupling of an Fmoc-protected amino acid. This deprotection step is not needed when a CTA is linked instead of an Fmoc-amino acid. However, I was not aware of this deprotection in the "Final" cycle during first SPPS. Although this step was deleted for following CTA-peptide syntheses, the cleaved species could be still observed during synthesis of CTA 1-XLPETGG structures (Table 6-1). The m/z value of the CTA-peptide could be detected neither in ESI nor in MALDI mass spectra. Instead, m/z values in agreement with the assumed cleavage product could be observed amongst other peaks. Therefore, the cleavage takes place also in absence of piperidine. The activation of coupling derivatives with HBTU is performed in presence of the bases NMM and NMP. One of them could also lead to the cleavage of the CTA which could already occur during activation.

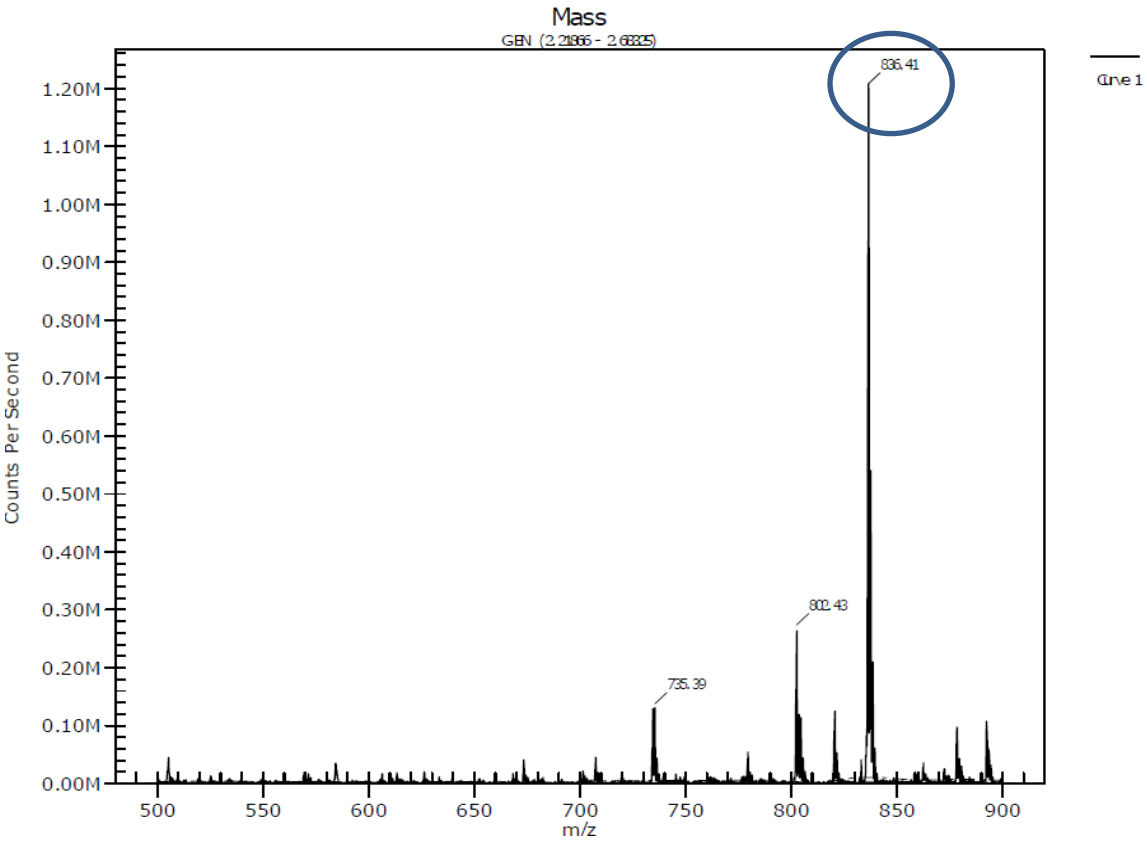

Fig 6.13 ESI mass spectrum after first synthesis attempt of CTA 1-YLPETGG.

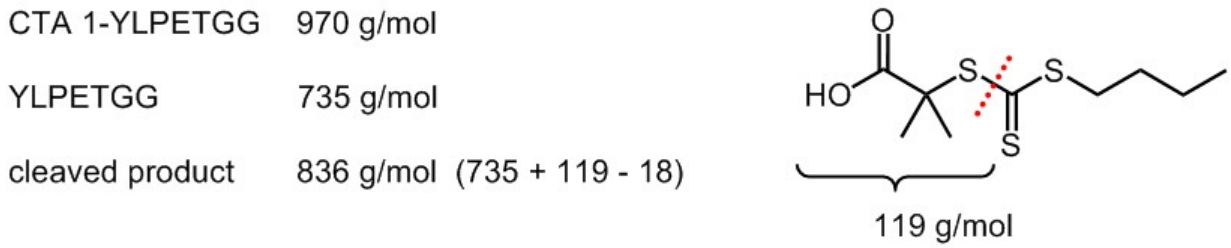

Fig 6.14 Molecular weight of CTA 1-YLPETGG, pure peptide and cleaved product together with possible cleavage site in the CTA.

Table 6-1 Formula of different CTA 1-XLPETGG structures, their molecular weight, theoretical molecular weight of the assumed cleavage product and the observed m/z value by ESI mass spectrometry

Formula	Molecular weight / (g/mol)	Molecular weight of assumed cleavage product / (g/mol)	Observed m/z by ESI MS
CTA 1-YLPETGG	970	837	838
CTA 1-QLPETGG	935	802	803
CTA 1-SLPETGG	894	761	769
CTA 1-NLPETGG	920	787	789

It should be noted that the CTA 1-XLPETGG conjugates reported in Table 6-1 consist of a different spacer amino acid between CTA and recognition sequence. The synthesis was planned with X = Y, Q, S, and N; all of them being polar amino acids with low steric demand that could influence SML. No influence of the spacer amino acid on the binding of the CTA was observed between the four tested amino acids. However, other peptide sequences should be also considered in future because some of the used amino acids also contain nucleophilic groups in their side chains. Although protection groups are also used for the amino acid side chains, the latter are unprotected in the final peptides after liberation from the resin.

Although HBTU showed successful in ligating the derivatives in general, this kind of activator chemistry is probably not suitable for base-sensitive CTAs. Hence, other coupling procedures were tested next.

There are very few literature reports on the linkage of CTAs during SPPS. The group of Börner linked a dithiobenzoate CTA with carboxylic acid functional group to a peptide N-terminus with the help of DCC and NMP[16]. Later on, a trithiocarbonate based CTA was linked to a peptide by help of DIC and *N*-methylimidazole (NMI)[22].

Based on this, different reaction attempts were started with the combinations of DIC + NMP, DIC + NMI and DCC + NMP for the last coupling step. A typical synthesis approach for CTA 1-YLPETGG consisted of coupling conditions with 5 equivalents CTA, 5 equivalents DIC and 4 equivalents NMP for 90 min. However, their analysis showed that the CTA 1 was not linked to the peptide. An ESI mass spectrum is exemplarily shown in Fig 6.15. The reason why CTA 1 could not be linked is currently unclear and needs to be further investigated in future.

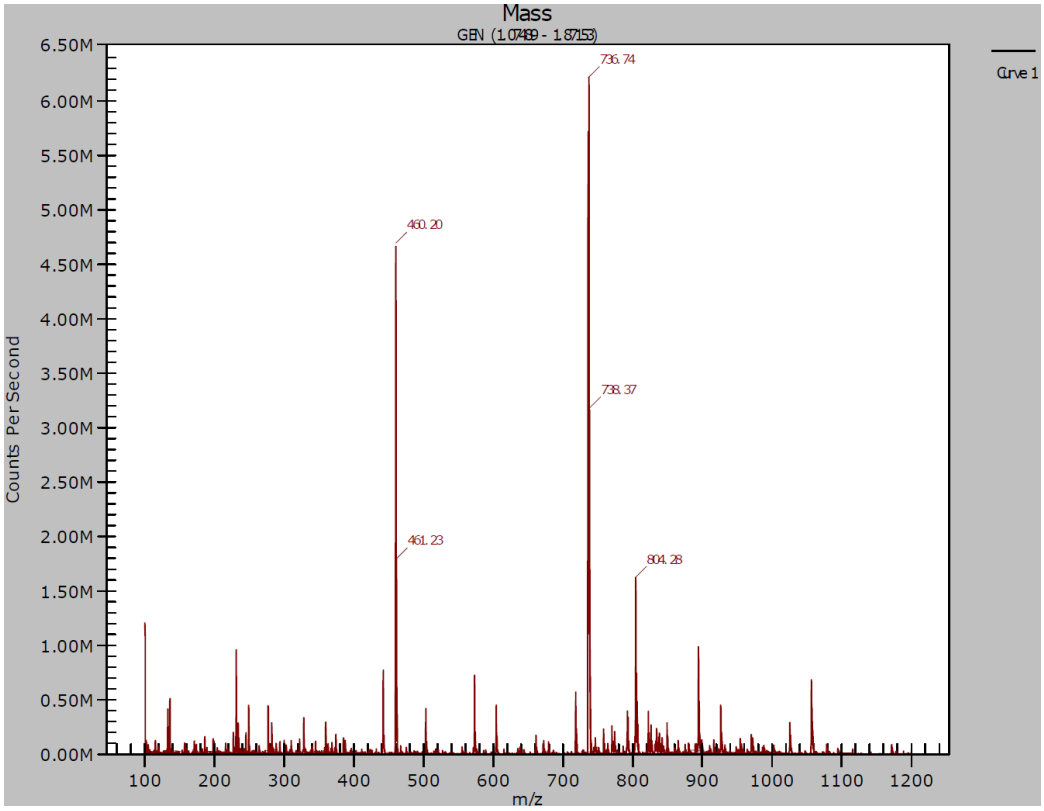

Fig 6.15 ESI mass spectrum after synthesis attempt for CTA 1-YLPETGG.

The RAFT technique was chosen for the ease of end group modification, among other things, as this could enable the synthesis of synthetic polymer blocks with two peptide motifs for SML. However, for the application in near future to synthesize protein-polymer conjugates by sortagging, only one peptide sequence per polymer block is required. Therefore, synthesis of these blocks can be also conducted via ATRP or NMP technique with the simplification that ATRP and NMP initiators are not base-labile like RAFT CTAs are[14,15]. Looking into future, the building blocks can be certainly synthesized exploiting RAFT polymerization regardless of first difficulties because resins and coupling agents would be also available for peptide synthesis that do not require basic conditions although these reagents are not the most common for standard peptide synthesis.

Although difficult to carry out when starting without experience in SPPS, the strategy itself is very nice, provides an excellent way to get a desired CTA-peptide conjugate. As similar structures were published before, a successful synthesis of these conjugates can be probably reached in future by variation of reaction conditions. In addition to the reports from the group of Prof. Börner, the group of Prof. Wooley also studied the synthesis of polymer-peptide conjugates via ATRP and NMP[15]. However, reference[15] was found late during writing of this thesis, the reported reaction conditions couldn't be applied to the synthesis of CTA-LPETGG conjugates and it is unclear if they could be transferred to CTAs instead of ATRP and NMP initiators. Anyway, it is remarkable that reference[15] reports the polymerization process while the peptide is still linked to the resin, prior to liberating the conjugate from the resin. Hence, a multitude of approaches can be tested in future for the synthesis of the desired polymer-LPETGG conjugates.

6.8 Summary

In this chapter, two different routes for the synthesis of peptide-CTA and CTA-peptide conjugates, respectively, were shown to form polymer building blocks for sortase-mediated ligation by RAFT polymerization. This represents a continuation of previous chapters in which peptide-polymer and polymer-peptide conjugates were formed by means of a 'click reaction' between commercially available polymers and peptides. To transfer this approach to a completely own formation of conjugates with much more synthetic possibilities for variation, a peptide synthesizer was exploited. Instead of realizing the conjugation through thiol-ene reaction between a cysteine residue and a certain CTA with double bond functionality, the CTAs were directly ligated to the termini of the peptides.

The first route for the synthesis of peptide-polymer conjugates with free N-terminus for sortagging was designed via an esterification reaction between CTA and peptide and carried out by reaction of Fmoc-protected diglycine and hydroxyl group functionalized CTA 2. The successfully formed CTA 3 generally provides a new approach to yield peptide-polymer conjugates via RAFT polymerization method. The polymerization of NIPAM was performed followed by a classical deprotection process to remove the Fmoc group. There are several benefits of this 'grafting-from' strategy: Any peptide with protected N-terminus can be used, the esterification reaction between the peptide and the CTA avoids the steric hindrance of a pre-synthesized polymer chain end, and any monomer polymerizable via RAFT technique can be used. In addition, the purification of all intermediate products (Fmoc-GG-CTA, Fmoc-GG-polymer) as well as the product (GG-polymer) can be easily realized via column chromatography

or precipitation of the polymer. Therefore, this work provides the possibility that N-terminal free GG-polymer conjugates can be obtained through the esterification reaction, which can be subsequently used as substrate for SrtA reaction.

The second concise route for C-terminal free CTA-peptide conjugates was designed to be performed in a peptide synthesizer via SPPS method. The CTA with carboxylic acid group can be ligated to the N-terminus of the peptide as last coupling step in the peptide synthesizer. Unfortunately, a CTA-LPETG structure could not be isolated yet probably because of the organic base employed during the SPPS process. Despite of this, the route itself is quite elegant and can be optimized in future to yield polymer-LPETG conjugates for SML after the subsequent RAFT polymerization or a similar reaction. Hence, it is worth trying other appropriate reaction conditions, e.g. coupling without organic base or coupling of ATRP or NMP initiators, in the future.

In the framework of this chapter, two strategies were developed that provide the possibility to obtain peptide-CTA and CTA-peptide conjugates that can be exploited to form pure polymer conjugates via RAFT polymerization. Therefore, both polymer building blocks with LPETG recognition sequence as well as G_x nucleophilic sequence for sortase-mediated ligation can be formed following the strategies of this chapter. As the successful synthesis could be shown with GG-PNIPAM, the approach can be transferred to many different types of polymers and it is expected that building blocks for sortagging can be formed with any kind of monomer that is polymerizable by RAFT technique.

In future, the polymer building blocks can be used for the formation of protein-polymer conjugates, among others. Polymer chains can be ligated to C- or N-terminus of proteins or both. A His-tag in the recognition sequence (for example LPETGGRRH$_6$, GRRH$_6$ is cleaved off during SML) can be exploited for the purification of the conjugates as the product is the only proteinic species without His-tag (SrtA also has a His-tag). However, the shift of the equilibrium of the sortase reaction is probably even more important for the ligation of two macromolecules compared to small functionalities linked to proteins. In case the protein-polymer conjugates cannot be efficiently formed just by using an excess of one compound, further possibilities for the shift of the equilibrium exist (see chapter 2.3). Especially when looking at more than one ligation, the only possibility acting on the formed bond is the formation of a β-hairpin. The β-hairpin prevents that the formed peptide sequence can be recognized by SrtA and thus can't be cleaved by the enzyme. Therefore, the formation of the β-hairpin is the only strategy that shifts

the equilibrium and, at the same time, prevents the cleavage of the formed bond. This strategy can be realized by addition of the amino acids WTWTW at both substrates for SML. The introduction of these further amino acids into the building blocks presented within this chapter can be easily realized using the peptide synthesizer.

6.9 References

[1] X. Dai, D. Mate, U. Glebe, T. Mirzaei Garakani, A. Körner, U. Schwaneberg, A. Böker, *Polymers (Basel)*. **2018**, *10*, 151.

[2] M. W. Popp, S. K. Dougan, T.-Y. Chuang, E. Spooner, H. L. Ploegh, *Proc. Natl. Acad. Sci. U. S. A.* **2011**, *108*, 3169–3174.

[3] R. Parthasarathy, S. Subramanian, E. T. Boder, *Bioconjug. Chem.* **2007**, *18*, 469–476.

[4] Z. Qu, V. Krishnamurthy, C. A. Haller, B. M. Dorr, U. M. Marzec, S. Hurst, M. T. Hinds, S. R. Hanson, D. R. Liu, E. L. Chaikof, *Adv. Healthc. Mater.* **2014**, *3*, 30–35.

[5] B. M. Dorr, H. O. Ham, C. An, E. L. Chaikof, D. R. Liu, *Proc. Natl. Acad. Sci. U. S. A.* **2014**, *111*, 13343–8.

[6] Y. Hou, J. Yuan, Y. Zhou, J. Yu, H. Lu, *J. Am. Chem. Soc.* **2016**, *138*, 10995–11000.

[7] J. Chiefari, Y. K. Chong, F. Ercole, J. Krstina, J. Jeffery, T. P. T. Le, R. T. A. Mayadunne, G. F. Meijs, C. L. Moad, G. Moad, et al., *Macromolecules* **1998**, *31*, 5559–5562.

[8] G. Moad, E. Rizzardo, S. H. Thang, *Polym. Int.* **2011**, *60*, 9–25.

[9] H. Willcock, R. K. O'Reilly, *Polym. Chem.* **2010**, *1*, 149–157.

[10] J. Chiefari, J. Krstina, G. Moad, A. Postma, S. H. Thang, *Macromolecules* **2000**, *33*, 243–245.

[11] R. Behrendt, P. White, J. Offer, *J. Pept. Sci.* **2016**, *22*, 4–27.

[12] H. Mao, S. A. Hart, A. Schink, B. A. Pollok, *J. Am. Chem. Soc.* **2004**, *126*, 2670–2671.

[13] K. Sarpong, R. Bose, *Anal. Biochem.* **2017**, *521*, 55–58.

[14] H. Rettig, E. Krause, H. G. Börner, *Macromol. Rapid Commun.* **2004**, *25*, 1251–1256.

[15] M. L. Becker, J. Liu, K. L. Wooley, *Biomacromolecules* **2005**, *6*, 220–228.

[16] M. G. J. Ten Cate, H. Rettig, K. Bernhardt, H. G. Börner, *Macromolecules* **2005**, *38*, 10643–10649.

[17] J. Hentschel, K. Bleek, O. Ernst, H. G. Bo, *Macromolecules* **2008**, *41*, 1073–1075.

[18] H. G. Börner, in *Controlled/Living Radical Polymerization: Progress in RAFT, DT, NMP & OMRP, Vol. 1024*, American Chemical Society, **2009**, 265–278.

[19] I. M. Heyns, R. Pfukwa, B. Klumperman, *Biomacromolecules* **2016**, *17*, 1795–1800.

[20] A. Meszynska, N. Badi, H. G. Börner, J.-F. Lutz, *Chem. Commun.* **2012**, *48*, 3887.

[21] C. P. Guimaraes, M. D. Witte, C. S. Theile, G. Bozkurt, L. Kundrat, A. E. M. Blom, H. L. Ploegh, *Nat. Protoc.* **2013**, *8*, 1787–99.

[22] J. Hentschel, K. Bleek, O. Ernst, H. G. Bo, *Macromolecules* **2008**, *41*, 1073–1075.

7 Summary and Outlook

The enzyme Sortase A catalyzes the formation of a peptide bond between the recognition sequence LPXTG and an oligoglycine. While manifold ligations between proteins and various biomolecules, proteins and small synthetic molecules as well as proteins and surfaces have been reported, the aim of this thesis was to investigate the sortase-catalyzed linkage between artificial building blocks. Hence, this could pave the way for the use of sortase A for tasks from a chemical point of view and maybe even materials science.

For the proof of concept, the studied systems were kept as simple as possible at first by choosing easily accessible silica NPs and commercially available polymers. These building blocks were functionalized with peptide motifs for sortase-mediated ligation. Silica nanoparticles were synthesized with diameters of 60 and 200 nm and surface modified with C=C functionalities. Then, peptides bearing a terminal cysteine were covalently linked by means of a thiol-ene reaction. 60 nm SiO_2 NPs were functionalized with pentaglycines, while peptides with LPETG motif were linked to 200 nm silica particles. Polyethyleneglycol (PEG) and poly(*N*-isopropylacrylamide) (PNIPAM) were likewise functionalized with peptides by thiol-ene reaction between cysteine residues and C=C units in the polymer end groups. Hence, G_5-PEG and PNIPAM-LPETG conjugates were obtained. With this set of building blocks, NP–polymer hybrids, NP–NP, and polymer–polymer structures were generated by sortase-mediated ligation and the product formation shown by transmission electron microscopy, MALDI-ToF mass spectrometry and dynamic light scatting, among others. Thus, the linkage of these artificial building blocks by the enzyme sortase A could be demonstrated.

It can be assumed that the validated linking principles can be transferred from these exemplarily chosen synthetic structures to all kinds of polymers and particles by attaching LPETG or G_x sequences. However, when using commercially available polymers, the purification of the polymer–peptide conjugates was impossible and resulted in a mixture containing unmodified polymer. Therefore, strategies were developed for the own synthesis of pure peptide-polymer and polymer-peptide conjugates as building blocks for sortase-mediated ligation. The designed routes are based on preparing polymer blocks via RAFT polymerization from CTAs that are attached to N- or C-terminus, respectively, of a peptide. GG-PNIPAM was synthesized through attachment of a suitable RAFT CTA to Fmoc-GG in an esterification reaction, followed by polymerization of NIPAM and cleavage of the Fmoc protection group. Furthermore, several peptides were synthesized by solid-phase peptide synthesis. The linkage of a RAFT CTA (or

polymerization initiator) to the N-terminus of a peptide can be conducted in an automated fashion as last step in a peptide synthesizer. The synthesis of such a conjugate couldn't be realized in the time frame of this thesis, but many promising strategies exist to continue this strategy using different coupling reagents. Such polymer building blocks can be used to synthesize protein-polymer conjugates catalyzed by sortase A and the approach can be carried on to the synthesis of block copolymers by using polymer blocks with peptide motifs on both ends.

Although the proof of concept demonstrated in this thesis only shows examples that can be also synthesized by exclusively chemical techniques, a toolbox of such building blocks will enable the future formation of new materials and pave the way for the application of enzymes in materials science. In addition to nanoparticle systems and block copolymers, this also includes combination with protein-based building blocks to form hybrid materials. Hence, sortase could become an enzymatic tool that complements established chemical linking technologies and provides specific peptide motifs that are orthogonal to all existing chemical functional groups.

The presented results therefore not only prove the concept but also provide the strategy that SrtA can catalyze the covalent linkage of purely artificial chemical structures to form hybrid materials. This could become a very powerful alternative method to the current established chemical ligation. It is obvious that the use of expensive peptides does not allow for the synthesis of products in large scale, but it is a promising strategy to reach compounds where traditional synthetic chemistry approaches are limited.

8 Zusammenfassung und Ausblick

Das Enzym Sortase A katalysiert die Bildung einer Peptidbindung zwischen der Erkennungssequenz LPXTG und einem Oligoglycin. Während vielfältige Ligationen zwischen Proteinen und verschiedenen Biomolekülen, Proteinen und kleinen synthetischen Molekülen, sowie Proteinen und Oberflächen durchgeführt wurden, besteht das Ziel dieser Arbeit darin, die Sortase-katalysierte Verlinkung von synthetischen Bausteinen zu untersuchen. Dies könnte den Weg bereiten für die Anwendung von Sortase A für chemische Aufgabenstellungen und eventuell sogar in den Materialwissenschaften.

Für diese grundsätzliche Untersuchung wurden die verwendeten Bausteine zunächst so einfach wie möglich gehalten und leicht zugängliche SiO_2 Nanopartikel und kommerziell erhältliche Polymerblöcke ausgewählt. Die Bausteine wurden als erstes mit den Peptidsequenzen für Sortase-vermittelte Ligationen funktionalisiert. SiO_2 Nanopartikel wurden mit Durchmessern von 60 und 200 nm hergestellt und mit C=C Doppelbindungen oberflächenmodifiziert. Dann wurden Peptide mit einem terminalen Cystein kovalent durch eine Thiol-en Reaktion angebunden. An die 60 nm NP wurden Peptide mit einem Pentaglycin und an die 200 nm Partikel Peptide mit LPETG Sequenz gebunden. Auf die gleiche Art und Weise wurden Peptide mit terminalem Cystein an die Polymere Polyethylenglykol (PEG) und Poly(*N*-Isopropylacrylamid) (PNIPAM), die beide über C=C Endgruppen verfügen, gebunden und G_5-PEG und PNIPAM-LPETG Konjugate erhalten. Mit den vier Bausteinen wurden nun durch Sortase-vermittelte Ligation NP–Polymer Hybride, NP–NP und Polymer–Polymer Strukturen hergestellt und die Produkte u. a. durch Transmissionselektronenmikroskopie, MALDI-ToF Massenspektrometrie sowie Dynamische Lichtstreuung charakterisiert. Die Verlinkung dieser synthetischen Bausteine konnte eindeutig gezeigt werden.

Auf den beispielhaft ausgewählten Bausteinen aufbauend kann davon ausgegangen werden, dass diese Art der Verknüpfung auf nahezu alle Polymere und Partikel, die mit LPETG oder G_x Sequenzen versehen werden, übertragen werden kann. Das Verwenden von kommerziell erhältlichen Polymeren hat jedoch zu einem Gemisch der Polymer-Peptid Konjugate mit unmodifiziertem Polymer geführt, welches nicht gereinigt werden konnte. Deswegen wurden anschließend Synthesestrategien für reine Peptid-Polymer und Polymer-Peptid Konjugate als Bausteine für Sortase-vermittelte Ligationen entwickelt. Diese basieren auf der RAFT Polymerisation mit CTAs, die entweder an N- oder C-Terminus eines Peptids gebunden sind. GG-PNIPAM wurde durch das Anbinden eines geeigneten RAFT CTAs an Fmoc-GG in einer

Veresterungsreaktion, Polymerisation von NIPAM und Abspalten der Fmoc Schutzgruppe synthetisiert. Weiterhin wurden mehrere Peptide durch Festphasen-Peptidsynthese erhalten. Die Anbindung eines RAFT CTAs (oder eines Polymerisationsinitiators) an den N-Terminus eines Peptids kann automatisiert als letzter Schritt in einem Peptid-Synthetisierer erfolgen. Die Synthese eines solchen Konjugats konnte in dem Zeithorizont dieser Arbeit noch nicht erreicht werden. Jedoch existieren mehrere vielversprechende Strategien, um diesen Ansatz mit verschiedenen Kopplungsreagenzien zur Anbindung des CTAs fortzusetzen. Solche Polymer Bausteine können in Zukunft für die Synthese von Protein-Polymer Konjugaten durch Sortase-Katalyse verwendet werden. Außerdem kann der Ansatz auch für die Synthese von Block-Copolymeren aus Polymerblöcken mit Peptidmotiven an beiden Enden ausgebaut werden.

Auch wenn bei der grundsätzlichen Untersuchung im Rahmen dieser Arbeit Hybridstrukturen hergestellt wurden, die auch durch traditionelle chemische Synthesen erhalten werden könnten, wird ein Bausatz solcher Bausteine in Zukunft die Synthese neuer Materialien ermöglichen und kann auch den Weg für die Anwendung von Enzymen in den Materialwissenschaften ebnen. In Ergänzung zu Nanopartikeln und Block-Copolymeren können dann auch Hybridmaterialien unter Einbezug von Protein-basierten Bausteinen hergestellt werden. Daher könnten Sortase Enzyme zu einem Werkzeug werden, welches etablierte chemische Verlinkungstechniken ergänzt und mit den hoch spezifischen Peptidmotiven über funktionale Einheiten verfügt, die orthogonal zu allen chemischen Gruppen sind.

Die erhaltenen Ergebnisse zeigen damit die Strategie auf, dass SrtA die kovalente Verknüpfung von synthetischen Strukturen bewerkstelligen und hybride Materialien herstellen kann. Dies könnte sich zu einer leistungsstarken Alternative zu derzeitig etablierten chemischen Techniken entwickeln. Zwar können mit vergleichsweise teuren Peptiden keine großtechnischen Synthesen durchgeführt werden, es handelt sich aber um eine vielversprechende Strategie gerade für die Fälle, bei denen chemische Ansätze nur eingeschränkt erfolgreich sind.